

**Epigenetic Regulation in Neural Crest Development:
Role of DNA Methyltransferases 3A and 3B**

Thesis by
Na Hu

In Partial Fulfillment of the Requirements for the
degree of
Doctor of Philosophy



CALIFORNIA INSTITUTE OF TECHNOLOGY

Pasadena, California

2013

(Defended April 16, 2013)

ACKNOWLEDGEMENTS

I owe my deepest gratitude to my thesis advisor Marianne Bronner. I truly thank her for providing me the opportunity and resources to develop as an independent scientist. I have learned a lot from her, and I could not thank her enough for her commitment. It has been her dedicated mentorship, stimulating discussions, strong support, and perpetual motivation that made everything possible to complete my degree.

I wish to express my sincere appreciation to my thesis committee members: Angelike Stathopoulos, Paul Sternberg and David Prober. I thank them for their guidance, valuable feedback on my research projects and their long-term support over the years. I am very fortunate to have them. They genuinely care about my success and always think in my best interest.

I am indebted to my postdoctoral mentor Pablo Strobl-Mazzulla for his scientific insight, constant support, and inspirations. I have benefitted tremendously from his mentorship and fruitful collaboration. I wish to thank Tatjana Sauka-Spengler for her intelligent advice, endless passion and successful collaboration. I would like to thank Celia Shiau for getting me settled in the lab, patiently training me with many useful lab skills and for our productive collaboration during my rotation. She is my role model in the lab. I wish to thank Meyer Barembaum and Marcos Simoes-Costa for sharing their technical expertise and insightful feedbacks to my research. I would like to thank Shuyi Nie, Benjamin Uy, Ankur Saxena, Elly Chow and Yun Kee for their companionship and encouragement. I thank them for making my daily life enjoyable and exciting. I would

like to thank Daniela Roellig for reading my thesis and giving me helpful feedbacks. I am grateful and honored to have worked with talented past and present members of the Bronner lab: Crystal Rogers, Tatiana Hochgreb, Max Ezin, Stephen Green, Hugo Parker, Saku Jayasena, Laura Kerosuo, Daniela Roellig, Rosa Uribe, Martha Henderson, Matthew Jones, Joanne Tan, Connie Gonzalez, David Mayorga, Daniela Haming, Paola Betancur, Kazumi Fukatsu, Katherine Fishwick, David Arce, Kathryn McCabe, and Mary Flowers.

I want to extend my thanks to my undergraduate advisor Richard Harland for his continued support and scientific discussions during my graduate studies. I thank my undergraduate mentors Timothy Grammer, Gabriela Loots, and Mustafa Khokha for their motivation, endless patience and for exposing me to research.

Last but not least, I owe many thanks to my parents and my fiancé Bin Zhang. I feel extremely blessed to have their unconditional love, understanding, and constant support.

The work presented in this thesis was supported by the Ruth L. Kirschstein National Research Service Award F31DE021643 and the National Institutes of Health.

ABSTRACT

The neural crest is a group of migratory, multipotent stem cells that play a crucial role in many aspects of embryonic development. This uniquely vertebrate cell population forms within the dorsal neural tube but then emigrates out and migrates long distances to different regions of the body. These cells contribute to formation of many structures such as the peripheral nervous system, craniofacial skeleton, and pigmentation of the skin. Why some neural tube cells undergo a change from neural to neural crest cell fate is unknown as is the timing of both onset and cessation of their emigration from the neural tube. In recent years, growing evidence supports an important role for epigenetic regulation as a new mechanism for controlling aspects of neural crest development. In this thesis, I dissect the roles of the de novo DNA methyltransferases (DNMTs) 3A and 3B in neural crest specification, migration and differentiation. First, I show that DNMT3A limits the spatial boundary between neural crest versus neural tube progenitors within the neuroepithelium. DNMT3A promotes neural crest specification by directly mediating repression of neural genes, like Sox2 and Sox3. Its knockdown causes ectopic Sox2 and Sox3 expression at the expense of neural crest territory. Thus, DNMT3A functions as a molecular switch, repressing neural to favor neural crest cell fate. Second, I find that DNMT3B restricts the temporal window during which the neural crest cells emigrate from the dorsal neural tube. Knockdown of DNMT3B causes an excess of neural crest emigration, by extending the time that the neural tube is competent to generate emigrating neural crest cells. In older embryos, this resulted in premature neuronal differentiation. Thus, DNMT3B regulates the duration of neural crest production by the neural tube and the timing of their differentiation.

My results in avian embryos suggest that de novo DNA methylation, exerted by both DNMT3A and DNMT3B, plays a dual role in neural crest development, with each individual paralogue apparently functioning during a distinct temporal window. The results suggest that de novo DNA methylation is a critical epigenetic mark used for cell fate restriction of progenitor cells during neural crest cell fate specification. Our discovery provides important insights into the mechanisms that determine whether a cell becomes part of the central nervous system or peripheral cell lineages.

TABLE OF CONTENTS

Acknowledgements	iii
Abstract	v
Table of Contents	vii
List of Figures and Tables.....	xii

Chapter 1:

Introduction: epigenetic regulation in neural crest development	1
Introduction.....	2
Neural crest induction.....	3
Neural crest specification	4
Neural crest EMT and migration.....	4
Developmental defects, diseases and syndromes.....	6
Epigenetic regulation	7
DNA methylation.....	8
Histone modifications.....	12
ATP-dependent chromatin remodelers.....	19
Other epigenetic regulators.....	20
Perspective and overview	21

Chapter 2:

DNA methyltransferase3A as a molecular switch mediating the neural tube to neural crest fate transition	31
Abstract	32
Introduction	32
Results and discussion	34
Expression pattern of DNMT3A in the early chick embryo.....	34
Knock-down of DNMT3A blocks neural crest specification, as assayed by FoxD3 expression, in a cell autonomous manner	34
Multiplex analysis reveals that loss of DNMT3A up-regulates neural genes, while down-regulating neural crest specifier genes.....	37
Neural specifier genes Sox2 & Sox3 are direct targets of DNMT3A .	40
Materials and methods.....	42
Embryos	42
In situ hybridization	42
Electroporation.....	42
NanoString nCounter	43
Chromatin immunoprecipitation	43
Acknowledgements.....	44

Chapter 3:

Loss of DNA methyltransferase3B prolongs neural crest EMT and causes premature neuronal differentiation	65
Abstract	66
Introduction	67
Results	70
DNMT3B is expressed in regions of neural crest formation and migration	70
Loss of function of DNMT3B causes prolonged production of neural crest cells from the neural tube, but does not affect induction	71
Multiplex analysis reveals that loss of DNMT3B up-regulates neural crest specifier genes, while down-regulating dorsal neural tube genes	73
Loss of DNMT3B results in extra migratory neural crest cells	74
Loss of DNMT3B results in premature differentiation of the trigeminal ganglia	75
Discussion	76
Materials and Methods	79
Embryos	79
In situ hybridization	79
Immunohistochemistry	80

In ovo electroporation..... 80

NanoString nCounter..... 80

Acknowledgements..... 81

Chapter 4:

Conclusions and future perspectives 94

 Summary and significance..... 95

 Future perspectives 97

Bibliography 106

Appendix A:

**Altering Glypican-1 levels modulates canonical Wnt signaling during
trigeminal placode development**..... 115

 Abstract..... 116

 Introduction..... 116

 Results..... 118

 Expression of Glypican-1 mRNA in the trigeminal placodes and other
 embryonic tissues during early chick development 118

 Overexpression of Glypican-1 in placodes causes loss of trigeminal

ganglia.....	121
GPC1 overexpression blocks proliferation and differentiation of the placodal ectoderm that leads to loss of ganglia	122
Altering GPC1 expression causes ganglion disorganization and both truncated and full-length forms require heparan sulfate modification	126
Manipulating levels of GPC1 alters endogenous activity of Wnt signaling	129
Activation of Wnt signaling reverses the effects of GPC1 overexpression but phenocopies effects of truncated GPC1	131
Discussion	133
Acknowledgements.....	137
Materials and Methods	138
References.....	156

LIST OF FIGURES AND TABLES

Chapter 1:	<i>Page</i>
Figure1	25
Figure2	27
Table1	29
Chapter 2:	
Figure1	45
Figure2	47
Figure3	49
Figure4	51
Figure5	53
Figure S1	55
Figure S2	57
Figure S3	59
Figure S4	61
Figure S5	63
Table1	64
Chapter 3:	
Figure1	82

Figure2 84

Figure3 87

Figure4 89

Figure5 91

Figure S1 93

Chapter 4:

Figure1 103

Figure2 103

Appendix A:

Figure1 142

Figure2 144

Figure3 146

Figure4 148

Figure5 150

Figure 6 152

Supplementary Figure1 153

Supplementary Figure2..... 155

Chapter 1

Introduction: epigenetic regulation in neural crest development

Na Hu and Marianne Bronner

To be submitted

Introduction

Neural crest cells are a population of multipotent stem cells that are induced during gastrulation at the neural plate border, between the neural and non-neural ectoderm. By neurulation, definitive neural crest cells are specified and initiate neural crest marker expression as premigratory cells within the dorsal neural tube. They then emerge from the neural tube by undergoing an epithelial to mesenchymal transition (EMT) whereby they delaminate from the neuroepithelium, assume a mesenchymal morphology and migrate extensively to different parts of the body (Figure1). After migration, they differentiate into numerous derivatives including neurons and glia of the peripheral nervous system, melanocytes, portions of the cardiac outflow tract, craniofacial bone and cartilage, and smooth muscle of major blood vessels (Sauka-Spengler and Bronner-Fraser 2008; Sauka-Spengler and Bronner 2010; Bronner and LaBonne 2012). Understanding neural crest development is important because these cells are involved in a variety of birth defects, diseases and cancers such as cleft lip and palate, heart defects, Hirschprung's disease, melanoma and neurofibromatosis.

There is good evidence that transcriptional events are critical for many aspects of neural crest (NC) development. A neural crest gene regulatory network (GRN) (Meulemans and Bronner-Fraser 2004) comprised of transcriptional and signaling events has been proposed to function in a feed-forward series of regulatory circuits (Sauka-Spengler and Bronner-Fraser 2006; Betancur et al. 2010). This neural crest GRN appears to

be highly conserved throughout vertebrates, including basal agnathans (Sauka-Spengler et al. 2007), suggesting that these regulatory mechanisms were in place more than 550 million years ago. However, the current formulation of the NC GRN is far from complete and it is becoming increasingly clear that additional inputs play critical roles in neural crest formation and migration.

As one example, there is growing evidence to support roles for epigenetic inputs as critical for many aspects of neural crest development, most notably in controlling the timing of gene expression at different developmental stages. Below, I summarize the process of neural crest formation (Figure 2) and discuss the role of epigenetic regulation during neural crest development, neural crest related birth defects and diseases.

Neural crest induction

The process of neural crest induction is mediated by signaling ligands including BMPs, Wnts and FGFs that are secreted from neighboring tissues such as the neural and non-neural ectoderm as well as the underlying mesoderm (Figure 1). During gastrulation, these signals establish the neural plate border region between the neural and non-neural ectoderm and initiate neural crest induction (Heeg-Truesdell and LaBonne 2004; Steventon et al. 2005; Basch and Bronner-Fraser 2006; Stuhlmiller and Garcia-Castro 2012). The neural plate border region has the competence to form not only neural crest cells but also other cell types within the central nervous system (CNS). Signaling inputs in this region up-regulate a group of transcription factors called ‘neural plate border specifier genes’

including *Msx1/2*, *Pax3/7*, *Dlx5*, *Gbx2* and *Zic*. The collective and overlapping expression of these genes confers upon the neural plate border region the unique ability to form neural crest cells.

Neural crest specification

During neurulation, neural plate border circuitry activates a set of transcription factors called the ‘neural crest specifier genes’ in the dorsal neural tube. These include genes like *AP2 α* , *n-Myc*, *Id*, *Snail2*, *FoxD3*, *Ets-1*, *Sox8/9/10*, with some differences in the timing of their initial expression. These factors function to control cell cycle, proliferation, and survival, while maintaining multipotency, initiating delamination, and promoting their epithelial-to-mesenchymal transition (EMT). A bona fide neural crest cell is first recognizable in the dorsal neural tube by its expression of transcription factors such as *FoxD3*, *Sox9*, *Snail2*, and *Sox10*. These genes regulate downstream effector genes to promote EMT and migration, at which point the neural crest cells become an identifiable population of multipotent migratory stem cells (Gammill and Bronner-Fraser 2003; Barembaum and Bronner-Fraser 2005; Sauka-Spengler and Bronner-Fraser 2008).

Neural crest EMT and migration

During the epithelial to mesenchymal transition process, neural crest cells alter cell junctions, adhesive properties and morphology to acquire cell motility, which enables them

to migrate long distances to their final destinations. For example, they switch from expression of Type I cadherins (characteristic of epithelial cells) to Type II cadherins (of mesenchymal character) and lose tight junctions while establishing gap junctions. Neural crest specifier genes like Snail2 and FoxD3 regulate downstream genes to facilitate this process. As a result, N-cad and Cad6B are down-regulated and Cad7 is up-regulated along with gap junction proteins and integrins (Kerosuo and Bronner-Fraser 2012; Strobl-Mazzulla and Bronner 2012a). At this point, neural crest cells become a distinct group of mesenchymal cells that delaminate from the neuroepithelium and migrate out of the dorsal neural tube.

During their migration, neural crest cells interact with each other and with their environment via signaling receptors such as Neuropilins, Robo and Ephrin receptors, which respond to ligands that guide them to specific destinations and facilitate their differentiation (Sauka-Spengler and Bronner-Fraser 2008; Betancur et al. 2010).

At the end of migration, the expression of most neural crest specifier genes is down-regulated. However, expression of some factors like Sox10 and FoxD3 remain on in a subset of cells and contribute to terminal differentiation (Kelsh 2006). Depending on the axial location and time of emigration, neural crest cells give rise to a wide variety of derivatives such as peripheral neurons and glia, craniofacial skeleton, cartilage derivatives, and melanocytes. (Le Douarin 1982; Betancur et al. 2010).

Signaling pathways utilized during neural crest EMT are common to many other developmental EMTs (Lim and Thiery 2012). Signaling molecules like TGF- β family, Wnt and FGF and transcription factors like Snail genes are common to EMTs during both gastrulation and neural crest cell emigration (Acloque et al. 2009). Not surprisingly, abnormal activation of EMT programs in carcinoma cells also utilizes similar mechanisms to delaminate from an epithelial tumor as those used by neural crest cells, and this process results in the formation of invasive migratory tumor cells (Strobl-Mazzulla and Bronner 2012a). Key neural crest transcription factors such as Snail, Sip1, Twist are common regulators in both neural crest development and tumor progression. The recurrence of EMT in adult disease may reflect a reactivation of developmental programs functioning at the cellular level. Thus, an in-depth understanding of neural crest EMT may contribute to our understanding of cancer metastasis and help guide the design of anti-invasive drugs.

Developmental defects, diseases and syndromes

Many of the most common human birth defects are related to abnormal neural crest development. Neural crest malformation can lead to craniofacial defects like cleft lip and palate, heart septation defects, and agangliogenesis of the colon (Tennyson et al. 1986; Youn et al. 2003; Jiang et al. 2006). In addition, neural crest cells are involved in a variety of diseases and syndromes such as Hirschsprung's disease (HSCR), Wardenburg syndrome (WS), CHARGE syndrome and Williams Syndrome (Inoue et al. 2002; Ahola et al. 2009; Yoshimura et al. 2009; Bajpai et al. 2010; Kim et al. 2011). Understanding the

normal mechanisms of neural crest development will contribute to the discovery of therapeutic treatments on birth defects, cancers, and other diseases associated with aberrant neural crest cells.

Epigenetic regulation

In addition to transcription factors and signaling proteins, epigenetic regulators play an essential role in controlling proper neural crest development. Epigenetic modifications are defined as mechanisms that regulate gene expression without altering the underlying sequence of DNA (Bernstein et al. 2007; Bird 2007). Epigenetic modifiers can alter chromatin structure and genome function through different processes such as DNA modifications or histone modifications, or can work as a complex to regulate higher-level chromatin conformation in an ATP-dependent manner. Depending on the specific type of regulator, the outcome can either lead to gene activation, in which the chromatin is relaxed and DNA is accessible to transcription factors, or to gene repression, where chromatin is tightly packed and inaccessible to transcriptional regulators.

Epigenetic modifiers are key regulators of developmental events and aberrant epigenetic marks are associated with many types of cancers, and disease states (Portela and Esteller 2010). Different types of DNA and histone modifications and family members of chromatin remodeling complexes have been reviewed recently in (Liu and Xiao 2011). Here, we focus on various epigenetic regulators that have been shown to play a role in

neural crest development and neural crest related diseases. The epigenetic machinery falls into the following groups: DNA methylation, histone methylation, histone acetylation, ATP-dependent chromatin remodeling complex, and other regulators that work with the epigenetic machinery to regulate neural crest development.

DNA methylation

During development, epigenetic repression is used to shut down alternative pathways during cell type specification and lineage commitment (Cedar and Bergman 2008). One common type of gene repression in mammalian cells occurs via DNA methylation. DNA methylation is one of the most important epigenetic mechanisms regulating many different events including gene expression, genome imprinting, inactivation of the silent X chromosome, and genome stability (Ooi et al. 2009). After fertilization, repressive parental DNA methylation is erased or gradually lost, reprogramming the cells of the early embryo to enable reacquisition of pluripotency (Mayer et al. 2000). As development proceeds, new DNA methylation marks are established to gradually restrict the cell's potential (Mayer et al. 2000; Reik 2007; Borgel et al. 2010). In mammalian cells, 60-90% of the cytosines are methylated in the context of CpG dinucleotides or CpG islands (Gardiner-Garden and Frommer 1987) (Namiyama et al. 2004). This process is mediated by the family of DNA methyltransferases: DNMT1, DNMT2, DNMT3L, DNMT3A and 3B. These enzymes catalyze the transfer of a methyl group on Cytosine using AdoMet (S-adenosyl-L-methionine) as a donor (Turek-Plewa and Jagodzinski 2005), thereby inhibiting

interaction of some proteins with DNA, while facilitating the binding of others (Prokhortchouk and Defossez 2008).

The DNMTs can be categorized into two main groups with DNMT1 representing the maintenance methyltransferase and DNMT3A and 3B acting as de novo methyltransferases. DNMT1 preferably attacks the newly synthesized strand of DNA during chromatin replication, repairing and maintaining the pattern of methylation according to the parent strand (Chen and Li 2006). DNMT2 is a tRNA methyltransferase (Goll et al. 2006); its role in development has yet to be studied. The de novo methyltransferases (DNMT3s) are the major players in tissue specific regulation during development. They establish the initial CpG methylation pattern. They consist of two enzymatically active methyltransferases DNMT3A and DNMT3B and one regulatory factor DNMT3L that augments the function of DNMT3A (Jurkowska et al. 2011b; Siddique et al. 2012) and promotes the activity of both DNMT3A and 3B (Wienholz et al. 2010).

De novo DNMTs recognize CpG islands and newly methylate DNA by catalyzing the transfer of a methyl group to cytosine residues (Cheng and Blumenthal 2008). Such methylation of CpG sites in the promoter region of a gene is thought to inhibit gene expression, as shown in cancer and stem cells (Momparler and Bovenzi 2000; Miranda and Jones 2007; Suzuki and Bird 2008; Altun et al. 2010). DNMT3A (Jurkowska et al. 2011a) and its paralog DNMT3B have been shown to be vital for normal mammalian development and play important roles in disease (Jaenisch and Bird 2003; Linhart et al. 2007; Ehrlich et

al. 2008; Yan et al. 2011). For example, DNMT3A double knockout mice die several weeks after birth, and DNMT3B double knockout embryos have rostral neural tube defects and growth impairment (Okano et al. 1999), suggesting a neural crest related phenotype.

In the chick embryo, DNMT3A is predominantly expressed in the neural crest territory and its loss of function results in down regulation/loss of neural crest specifier genes Sox10, Snail2, FoxD3, etc. and the expansion of neural genes Sox2 and Sox3 into the neural crest territory [this thesis and (Hu et al. 2012)]. Intriguingly, DNMT3A plays an early function in repressing the neural genes Sox2 and Sox3 in the presumptive neural crest region, and this down-regulation of neural genes in the dorsal neural fold is a prerequisite to activate neural crest specifier genes (Hu et al. 2012).

Although classically thought to act as repressors, DNMTs can also function as activators in some cases. Whereas traditional DNMT3A promoter methylation represses transcription, DNMT3A non-promoter DNA methylation has been shown to facilitate transcription by antagonizing Polycomb repression (Wu et al. 2010). In addition, DNMT3A can act as a co-repressor. In episomal cell lines, DNMT3A binds histone deacetylases and is recruited by a sequence-specific repressor RP58 to silence transcription, independent of its de novo methylation function (Fuks et al. 2001).

Mutations in human DNMT3B are found in ICF (immunodeficiency-centromeric instability-facial anomalies) syndrome, comprised of facial abnormalities such as widened

nasal bridge and hypotelorism, neurological dysfunction and other related defects (Ehrlich et al. 2008; Jin et al. 2008). These defects are consistent with an important role for DNMT3B in neural crest development. In zebrafish, DNMT3B and histone methyltransferase G9a cooperate to regulate neurogenesis through Lef1 and play a critical role in forming the precursors of craniofacial structures, brain and retina (Rai et al. 2010). In human embryonic stem cells, knockdown of DNMT3B accelerates neural and neural crest differentiation and increases the expression of neural crest specifier genes (Pax3, Pax7, FoxD3, Sox10 and Snail2). In addition, H3K27me3 and polycomb complex protein are reduced at the promoter regions of neural crest specifier genes upon knock-down of DNMT3B in hESCs (Martins-Taylor et al. 2012).

DNMT3B expression is significantly up-regulated during neural crest induction in chicken embryos (Adams et al. 2008). In my recent unpublished work, I show that DNMT3B influences the ability of neural tube cells to produce emigrating neural crest cells (Hu et al., in preparation). Knock-down of DNMT3B in chick causes an excess of neural crest emigration and up-regulation of neural crest genes Sox10, Snail2 and FoxD3, consistent with the data from human embryonic stem cells. In older embryos, this results in precocious neuronal differentiation of the trigeminal ganglia (Hu et al., unpublished). In contrast to the human syndrome and stem cell studies, however, conditional knock-down of DNMT3B in the mouse neural crest using Wnt1- or Sox10-cre does not produce an apparent craniofacial phenotype (Jacques-Fricke et al. 2012). Wnt-1-Cre driven knock-out of DNMT3B exhibits only mild migration defects of dispersed Sox10 positive cells, that

recover during cranial gangliogenesis (Jacques-Fricke et al. 2012). This could reflect differences between species, or may indicate that the primary function of DNMT3B is in non-neural crest tissue.

In addition to embryonic development, DNA methyltransferases are also thought to be involved in metastasis. Many tumor suppressor genes are silenced in a variety of human cancer cells by promoter methylation whereas some pro-oncogenic genes are activated by hypomethylation. In human prostate cancer cells, increased binding of DNMT3B to E-cadherin (a tumor suppressor gene) promoter was detected. This leads to promoter hypermethylation, resulting in less cell aggregation and increased metastasis (Kwon et al. 2010). In addition, DNMT1, 3A and 3B proteins have been detected in retinoblastomas whereas there are no DNMT proteins in normal retinas. Increased levels of DNMTs correlate with retinoblastoma tumorigenesis (Qu et al. 2010). Given that neural crest and cancer EMT and migration share many similar players and neural crest derived cells are prone to metastasis leading to neuroblastoma, melanoma, and neurofibroma, understanding how DNMTs regulate neural crest EMT and migration may also shed light on the mechanisms leading to cancer progression and metastasis.

Histone modifications

Histone proteins associate with compacting DNA strands and organize them into structural components called nucleosomes. Each nucleosome contains eight histones: two

of each of the core histones H2A, H2B, H3 and H4 form octameric structures called nucleosome cores around which DNA is wrapped with unstructured tails (Gibney and Nolan 2010). The core histone proteins are highly conserved throughout evolution and their tails are subject to post-translational modifications such as: methylation, acetylation, deacetylation, phosphorylation, ubiquitination, sumoylation, etc. (Berger 2007; Kouzarides 2007). New histone marks and new types of histone modification continue to be discovered throughout time (Tan et al. 2011). Among these modifications, histone methylation and acetylation are, to date, the best studied in neural crest cells and they play an essential role in neural crest development.

Histone methylation is associated with both active and repressive transcription (Kouzarides 2007). Histone methyltransferases add methylation while histone demethylases remove methylation marks. H3K4me3 (Histone 3 Lysine 4 trimethylation) established by Trithorax group proteins is indicative of transcriptionally permissive chromatin states, and is mostly found in the promoter regions of genes (Barski et al. 2007; Pan et al. 2007; Akkers et al. 2009; Cheung et al. 2010). H3K36me3 is associated with euchromatic regions that are associated with active transcription and is mostly found in gene bodies. In contrast, H3K27me3 catalyzed by Polycomb repressive complex (Schwartz et al. 2006; Tolhuis et al. 2006; Swigut and Wysocka 2007; Simon and Kingston 2009) and H3K9me3 (Nielsen et al. 2001; Shi et al. 2003; Allan et al. 2012) are associated with transcriptional repression.

Histone demethylases such as members of the Jumonji family revert histone methylation (Tan et al. 2008). In neural crest development, a histone demethylase of the Jumonji family JmjD2A (also known as KDM4A) is the first epigenetic gene discovered to regulate neural crest specification via modulating H3K9me3 of neural crest genes (Strobl-Mazzulla et al. 2010). JmjD2A is expressed in the neural crest forming territory during neural crest specification and knocking down JmjD2A causes dramatic loss of neural crest specifier genes such as Sox10, Snail2, FoxD3, etc. In vivo ChIP assays reveal the direct interaction of JmjD2A with Sox10 and Snail2 promoter regions that are occupied with H3K9me3 (Strobl-Mazzulla et al. 2010). JmjD2A is required to demethylate Sox10 and Snail2 at the proper time and place to allow neural crest specification to occur.

Along similar lines, patients with mutations in the histone demethylase PHF8, a JmjC domain containing protein, have craniofacial deformities. PHF8 is capable of demethylating H4K20me1 and H3K9me1 around the transcription start site to activate transcription. In zebrafish, PHF8 directly regulates homeodomain transcription factor MsxB during cranial facial development especially in the lower jaw (Phillips et al. 2006; Qi et al. 2010). MsxB was previously implicated in regulation of neural crest development (Phillips et al. 2006).

The Polycomb Repression Complex modifies chromatin to allow epigenetic silencing of genes through H3K27me3. Aebp2, a component of the Polycomb Repression Complex 2 (Kim et al. 2009), is expressed in the neural crest territory in mouse and

heterozygous mutants carry phenotypes similar to human patients with Hirschsprung's disease (HSCR) and Waardensburg syndrome (WS), both diseases are caused by migratory and developmental defects in neural crest cells (Inoue et al. 2002; Ahola et al. 2009; Kim et al. 2011). Expression levels of key neural crest genes such as Sox10, Pax3 and Snail2 are elevated in these heterozygous mutants, further suggesting that *Aebp2* misregulation is responsible for HSCR and WS through improper regulation of the neural crest genes (Kim et al. 2011).

Histone acetylation is associated with active transcription and histone de-acetylation silences transcription (Jenuwein and Allis 2001). HATs and HDACs are two classes of enzymes that antagonize each other (Shahbazian and Grunstein 2007). HATs (histone acetyltransferases) transfer acetyl groups to lysines, and their binding is correlated with active transcription (Carrozza et al. 2003; Shahbazian and Grunstein 2007). Acetylation neutralizes the charge of lysine residues and weakens their interactions with negatively charged DNA, thus allowing the chromatin structure to open up and increasing the accessibility of transcription factors (Ekwall 2005; Wang et al. 2009). HATs have also been identified as co-transcriptional activators (Roth et al. 2001; Yang 2004). In contrast, HDACs (histone deacetylases) de-acetylate lysine residues and one of their major functions is to remove acetyl groups added by HATs (Wang et al. 2002). As a result, chromatin is reset to its tightly packed state (Hsieh et al. 2004). As a consequence, HDACs have been identified as transcriptional co-repressors (Kadosh and Struhl 1997; Rundlett et al. 1998).

Epigenetic annotation such as histone acetylation is closely associated with enhancer activity and is a new, powerful tool to identify neural crest cis-regulatory regions together with conserved regulatory regions. For example, H3K27ac is associated with active enhancers (Heintzman et al. 2009; Creyghton et al. 2010; Rada-Iglesias et al. 2011; Bonn et al. 2012; Cotney et al. 2012). In human neural crest cells derived from hESC, ChIP-seq against various histone marks reveals that active enhancer regions are enriched with H3K27ac and H3K4me1 while lacking H3K4me3 (Rada-Iglesias et al. 2012). Neural crest enhancer elements that are conserved between human and chicken are both enriched for H3K27ac. Many have now been identified as a result of these studies and it will be interesting to monitor their functional characterization.

In neural crest development, the HDAC inhibitor Trichostatin A (TSA) promotes trunk neural crest cell specification (Murko et al. 2013). In chick, in ovo treatment with the inhibitor TSA induces neural crest markers *Bmp4*, *Pax3*, *Sox9* and *Sox10*, and dysregulates the proper timing of cadherins expressions such as *Cad6B* and *N-cad*. As a result, there is premature loss of epithelial characteristics.

The HDAC repression complex plays an essential role in regulating neural crest migration. Premigratory neural crest cells from the dorsal neural tube undergo an epithelial to mesenchymal transition to gain migratory properties and travel to distant parts of the body. The transcriptional repressor *Snail2* has been reported to directly repress the

adhesion molecule Cadherin6B in premigratory neural crest cells (Hatta et al. 1987; Nakagawa and Takeichi 1995; Taneyhill et al. 2007). Epigenetic regulation has been shown to play a critical underlying molecular role in this repression (Strobl-Mazzulla and Bronner, 2012). Interaction between an adaptor protein, PHD12, and Snail2 makes it possible to recruit the repressive complex Sin3A/HDAC to the Cad6B promoter region. As a result, Cad6B transcription is repressed via histone deacetylation. The dual specificity of epigenetic regulators such as PHD12 and transcription factors such as Snail2 are required to cooperatively regulate the process of neural crest EMT (Strobl-Mazzulla and Bronner 2012b).

HDACs play important roles in regulating downstream neural crest differentiation as well. HDAC1 mutant zebrafish embryos exhibit a severe reduction in the number of melanoblast expressing MITFa (a critical transcription factor for melanoblast development) and retain prolonged FoxD3 expression in neural crest cells. FoxD3 physically interacts with the MITFa promoter and reducing FoxD3 expression in HDAC1 mutants partially rescues the melanoblast defects. Thus, during normal melanogenesis, HDAC1 is required to repress FoxD3 expression which in turn de-represses MITFa to allow melanophore specification, migration and differentiation (Ignatius et al. 2008).

In another example, HDAC3 is crucial for the regulation of smooth muscle differentiation and cardiac outflow tract formation during cardiac neural crest development in mouse (Singh et al. 2011). Similarly, during cranial neural crest differentiation into the

skull, conditional deletion of HDAC8 driven by Wnt1-Cre in mice results in loss of specific cranial skeletal elements. HDAC8 epigenetically controls skull morphogenesis in neural crest-derived cells by repressing homeobox transcription factors Otx2 and Lhx1 (Haberland et al. 2009).

In zebrafish craniofacial morphogenesis, embryos treated with HDAC4 morpholino exhibit loss of cranial neural crest derived palatal skeletal precursor cells and this later results in defects in the developing palate including cleft plate and a shortened face (DeLaurier et al. 2012). In human development, HDAC4 is also highly associated with neural crest related diseases and syndromes. Haploinsufficiency of HDAC4 is associated with brachydactyly mental retardation syndrome with features such as craniofacial and skeletal abnormalities (Williams et al. 2010). In addition, high throughput SNP analysis has linked HDAC4 with nonsyndromic oral clefts, a common birth defect closely related to neural crest development (Park et al. 2006). Moreover, infants exposed to the drug valproic acid (VPA) (an HDAC inhibitor) during pregnancy have an increased risk of neural crest and neural tube related malformations including cleft lip and palate, and cardiovascular defects (Alsdorf and Wyszynski 2005; Wyszynski et al. 2005).

In summary, HDACs execute important functions in the control of both enhancer activity and promoter regions of transcription factors to regulate gene expression. Their activity affects numerous aspects of neural crest development ranging from specification to migration and differentiation.

ATP-dependent chromatin remodelers

The ATP-dependent chromatin remodeling complexes such as SWI/SNF, ISWI, and CHD regulate gene expression by changing the position or structures of higher order chromatin in an ATP-dependent manner. They create nucleosome-free regions to facilitate access of DNA to transcription factors and regulatory proteins (Kwon and Wagner 2007; Wu et al. 2009). CHD7, an ATP-dependent chromatin domain helicase DNA-binding domain member, cooperates with PBAF (SWI/SNF chromatin remodeling complex (Muchardt and Yaniv 2001)) to promote neural crest specification in hESC induced neural crest cells. CHD7 activates core neural crest transcriptional circuitry including Sox9 and Twist through directly regulating the enhancer regions of these genes (Bajpai et al. 2010). Sixty-seven percent of CHARGE syndrome (a rare genetic disorder) patients have CHD7 mutations (Zentner et al. 2010). CHD7 impairment in *Xenopus* embryos recapitulates major CHARGE syndrome features such as craniofacial malformations, peripheral nervous system abnormalities and heart defects (Bajpai et al. 2010). Consistent with this, CHD7 deficient mice exhibit craniofacial abnormalities (Bosman et al. 2005; Hurd et al. 2007; Layman et al. 2009). Taken together, these data suggest that CHARGE syndrome is a result of CHD7 malfunction in early neural crest development. In addition, in zebrafish, Brg1, a member of the SWI/SNF chromatin-remodeling complex, plays an important role in neural crest induction, possibly via regulating the promoter region of Snail2 (Eroglu et al. 2006).

WSFT, Williams syndrome transcription factor, is a major subunit for two distinct ATP-dependent chromatin remodeling complexes: WINAC and WICH. It is one of the genes associated with Williams syndrome, a developmental disorder in which patients have problems in neural crest derived tissues. These include facial abnormalities, heart defects, and neural problems, among other defects. In *Xenopus* embryos, WSFT is expressed in the migratory neural crest and branchial arches. Knock-down of WSFT perturbs Snail and Snail2 expression in the branchial arches. There are severe defects in neural crest migration and maintenance, whereas neural crest induction is unaffected (Barnett et al. 2012). In mice, WSFT heterozygous mutants have cardiovascular abnormalities that phenocopy Williams syndrome patients (Yoshimura et al. 2009). Taken together, these data suggest that malfunction of WSFT during neural crest development is a major contributor to Williams syndrome.

Other epigenetic regulators

The reduced folate carrier (RFC) is a membrane-bound receptor involved in folate uptake by cells. Mice lacking RFC1 develop multiple defects including neural tube, craniofacial and heart abnormalities (Gelineau-van Waes et al. 2008). In *Xenopus*, XRFC is expressed exclusively in the neural crest domain and its morpholino-mediated knockdown down-regulates neural crest markers such as *Zic1*, *Snail2*, and *FoxD3* (Li et al. 2011). As a result, *Twist1* positive neural crest cells fail to migrate ventrally and embryos exhibit similar phenotypes to those observed in mice. In animal cap assays, knock-down of RFC reduces the levels of H3K4me1 and H3K4me3. Over expressing lysine transferase hMLL1

in XRFC MO treated embryos fully rescues *Zic1* and *FoxD3* expression and partially rescues *Snail2* and *Twist1* expression (Li et al. 2011). Taken together, these data suggest that an RFC mediated folate metabolic pathway controls neural crest development through epigenetic mechanisms.

Leo1 is a component of the Polymerase-Associated Factor (PAF1) complex associated with chromatin remodeling and gene regulation (Krogan et al. 2003; Simic et al. 2003; He et al. 2004). In zebrafish mutants with truncated *Leo1* protein, there is reduced expression of *Crestin*, *Gch2*, and *Miffta* in neural crest derived cells (Nguyen et al. 2010). As a consequence, mutants have phenotypes such as reduced numbers of melanocyte, craniofacial cartilage, and glial cells. It is interesting to speculate that *Leo 1* may be essential for neural crest differentiation, possibly through epigenetic regulations.

Perspective and overview

It is now clear that, in addition to transcriptional regulators, epigenetic modifiers serve as important inputs that are crucial for proper neural crest development. At a given time point, epigenetic modifiers control aspects of neural crest development in a spatially and temporally specific manner. They are capable of communicating at both the promoter and enhancer regions to render DNA in an accessible state for transcription, poise an enhancer region for future activation, or remove active marks to turn off transcription. Furthermore, these regulators cross-talk and work together to achieve their goals. For

example, DNA methyltransferases often work with histone methyltransferases to shut down alternative pathways and histone demethylases read and remove repressive marks and work along with acetylases to activate transcription at the appropriate time. Each cell lineage is marked with different combinations of epigenetic modifications at a given developmental time point. Uncovering these marks in neural crest cells will be critical for understanding both neural crest development and related diseases.

In the remaining chapters, I elaborate on my research discoveries in avian embryos to demonstrate the necessity of de novo DNA methylation in neural crest specification and the neural crest epithelial to mesenchymal transition (EMT). Neural crest precursors initially reside within the dorsal neural tube and they subsequently segregate and emigrate out of the neural tube to become a distinct stem cell population. The molecular mechanisms underlying the neural tube to neural crest transition are a long-standing mystery. In Chapter 2, I show that the DNA methyltransferase, DNMT3A, promotes neural crest cell specification by directly mediating repression of the neural genes. DNMT3A plays a critical function in the neural versus neural crest cell fate decision. Shortly after their overt specification, neural crest cells undergo a process of EMT that allows them to emigrate out of the dorsal neural tube and migrate extensively to different parts of the body. In chick, neural crest EMT occurs over a defined period of approximately one day. Little is known about the mechanisms that end EMT and limit the ability of the CNS to produce neural crest. In Chapter 3, I show that DNMT3B influences the ability of neural tube cells to produce emigrating neural crest cells. The results show that it is required for the proper

timing of cessation of neural crest emigration from the dorsal neural tube at cranial levels.

Taken together, the data show that DNA methylation plays a dual role in neural crest development with each DNMT paralogue primarily functioning during distinct temporal window.

Chick as a research model system

Most scientists who study the functions of DNMTs use stem cells that can be maintained in culture under artificial conditions and obtained in large quantities for biochemical analysis. In contrast, we are studying events that occur in living embryos in order to understand the mechanism of DNMTs in their endogenous environment. To do so, we have adapted chick embryos as a research model to study the in vivo functions of DNMTs.

Chick embryos have many advantages for characterizing developmental events. Birds like humans are amniotes, but develop outside the mother in a morphologically similar manner to human embryos at comparable stages. Thus, they are easily accessible to experimental manipulations at early developmental stages, allowing temporally and spatially controlled genetic perturbations. For example, we can perform electroporations in half embryos or half neural tubes throughout early stages, leaving the other half as an internal control. Thus, we can compare the effects of protein knockdown using

morpholinos on the experimental versus control side of the same embryo, eliminating differences due to stage variation and allowing us to characterize phenotypes accurately.

In addition, we have adapted cell biological protocols to the chick system so that reasonably small amounts of cells can be used to perform biochemistry and high throughput analysis. For example, we can dissect small amounts of tissue for micro-Chromatin Immunoprecipitation analysis to verify direct interactions between proteins and DNA *in vivo*, and NanoString technology to evaluate the loss of function effects on hundreds of genes simultaneously from samples of a single embryo.

Moreover, several neural crest enhancers are functional in chick, which allows us to perform ectopic expression of constructs specifically in the neural crest cells for overexpression or rescue experiments. By electroporating enhancer regions mediating GFP expression, it is possible to use FACS to isolate pure neural crest cells for biochemistry analysis.

In the remaining chapters of my thesis, I use chick as a model system to characterize the roles of DNMT3A and 3B in neural crest specification and EMT.

Figure1. An overview of neural crest development

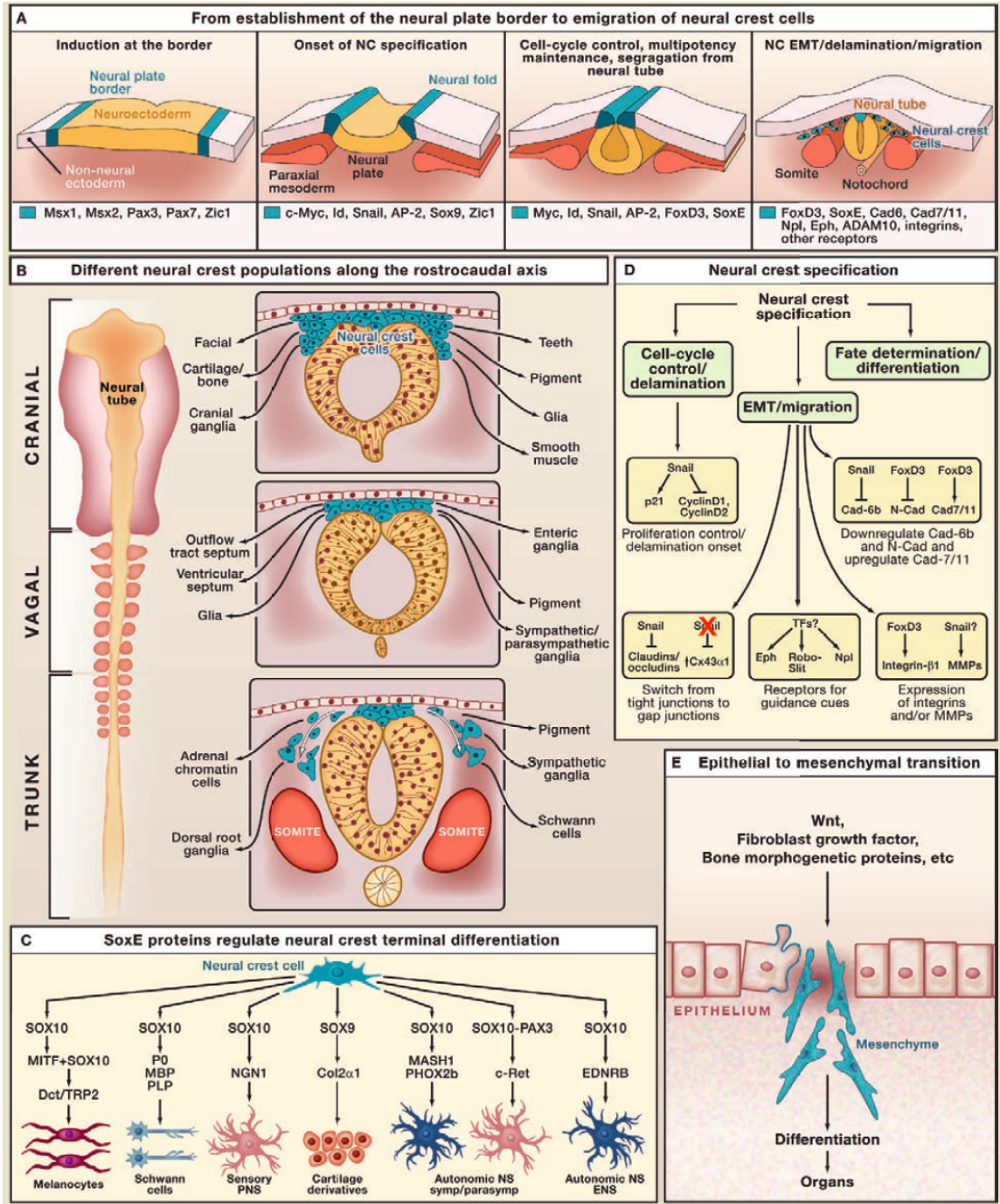


Figure1. An overview of neural crest development from (Sauka-Spengler and Bronner 2010). This diagram summarizes key regulatory events involved in neural crest formation, migration, and differentiation during vertebrate development.

Figure 2. Regulatory steps in neural crest formation

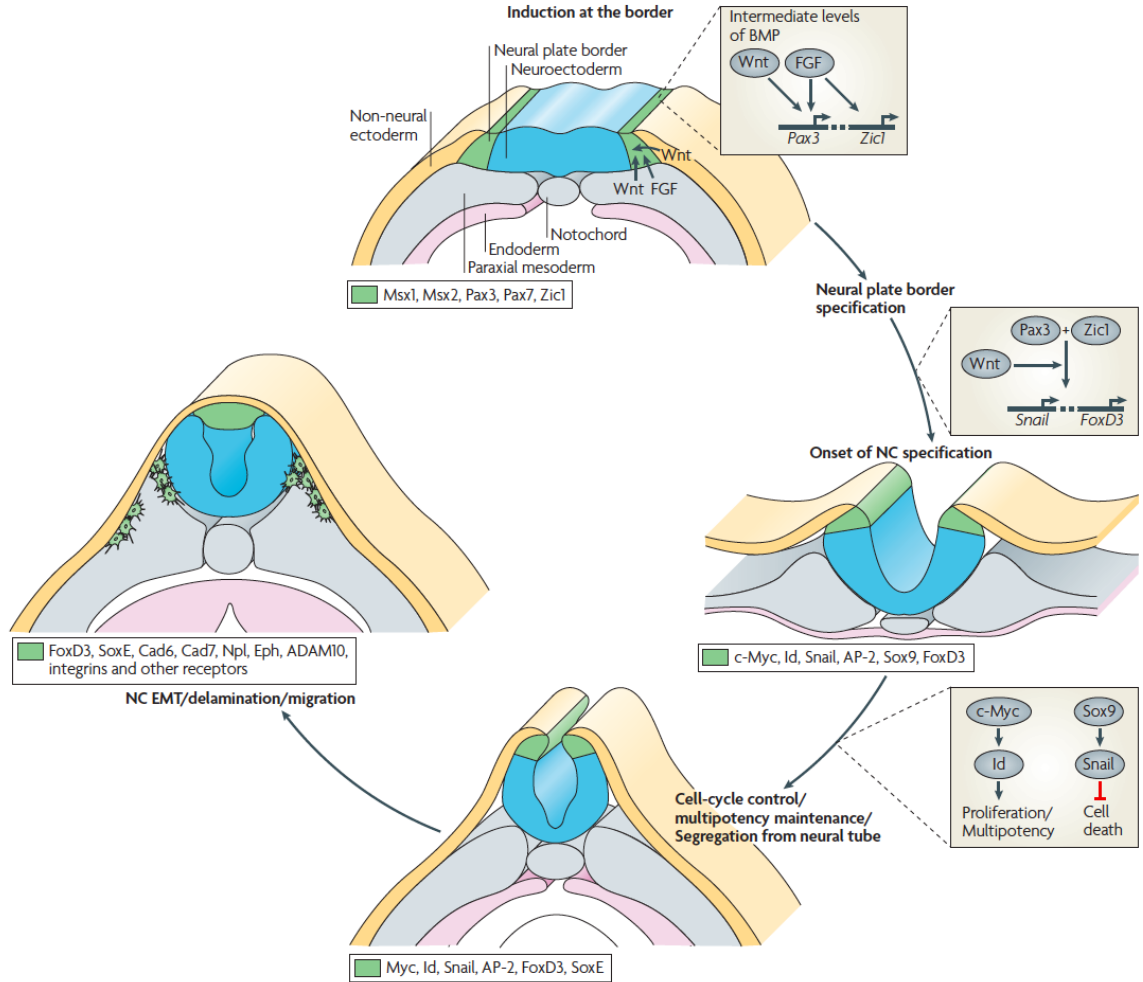


Figure 2. Regulatory steps in neural formation from (Sauka-Spengler and Bronner-Fraser 2008). Signals such as FGF, Wnt, and BMP induce neural crest at the neural plate border and turn on neural plate border specifiers such as Pax3 and Zic1. Pax3 and Zic1 in turn act synergistically to up-regulate neural crest specifiers such as Snail and FoxD3. During this stage, neural crest cells go through cell cycle control, multipotency maintenance, and

delaminate from the dorsal neural tube. Neural crest specifiers such as Sox10 and FoxD3 persist in delaminating neural crest cells and control expression of downstream effector genes such as Cadherin-7, matrix metalloprotease-10, integrins, neuropilins, and other transmembrane receptors (Sauka-Spengler and Bronner 2008).

Table 1. Summary of epigenetic regulation in neural crest development

St. of NC Development	Gene Name	Epigenetic Mark	On/Off	Targets	Notes
Neural Crest Specification	DNMT3A	DNA methylation targeting CpG islands	OFF	Sox2/3, SoxE, Snail2, FoxD3	neural to neural crest transition
	Jmjd2A	histone deacetylase targeting H3K9me3	ON	Sox10, Snail2	neural crest specification
	CHD7	ATP-dependent chromatin remodeler	ON	Sox9, Twist	neural crest specification, CHARGE syndrome
	Brg1	chromatin remodeler	ON	Snail2	neural crest induction
	TSA	HDAC inhibitor	ON	Bmp4, Pax3, Sox9, Sox10	trunk crest specification
Neural Crest EMT and migration	PHD12	histone deacetylase complex member	OFF	Cad6B	neural crest EMT
	HDAC8		OFF		facial skeleton
	DNMT3B	DNA methylation targeting CpG islands	OFF	Sox10, Snail2, FoxD3	timing of neural crest emigration
	RFC	co-factor of hMLL1 lysine transferase targeting H3K4me	ON	Zic1, Snail2, FoxD3	dorsal to ventral migration
Neural Crest Differentiation	PHF8	histone demethylase targeting H4K20me1 and H3K9me1	ON	MSXB	cranial facial jaw development
	HDAC1	removes acetylation	OFF	FoxD3, MITFa	melanoblast development
	HDAC3	removes acetylation	OFF		smooth muscle and cardiac outflow tract
	HDAC8	removes acetylation	OFF	Otx2, Lhx1	cranial differentiation into skull

	DNMT3B	DNA methylation	OFF	Lef1	craniofacial structures, brain and retina development
	HDAC4	removes acetylation	OFF		palatal skeleton formation
	G9a	histone methylation	OFF	Lef1	craniofacial structures, brain and retina development
	VPA	HDAC inhibitor	ON		neural tube defects, cleft lip and palate, and cardiovascular defects
Syndromes and diseases	WSTF	ATP-dependent chromatin remodeler	ON	Snail, Snail2	Williams syndrome
	Aebp2	Polycomb repression associated with H3K27me3	OFF	Sox10, Pax3, Snail2	Hirschsprung's disease and Warrensburg syndrome
	HDAC4	removes acetylation	OFF		brachydactyly mental retardation syndrome, oral clefts

Table 1. Summary of epigenetic regulators in neural crest specification, EMT, migration, differentiation, and neural crest related diseases and syndromes. ON/OFF column indicates whether the epigenetic regulator acts to turn the transcription of its target gene(s) on or off. Targets column represents direct and/or indirect downstream targets. Notes column characterizes the specific timing during neural crest development, specific neural crest derived structures, and diseases/defects that the regulator is known to play a role in. Stage (St.) Neural Crest (NC)

*Chapter 2***DNA methyltransferase3A as a molecular switch mediating the
neural tube to neural crest fate transition****Na Hu, Pablo Strobl-Mazzulla, Tatjana Sauka-Spengler and Marianne Bronner***Genes and Development*

Nov 01 2012

Abstract

The neural crest is an important embryonic stem cell type that forms much of the peripheral nervous system, facial skeleton and pigmentation of the vertebrate body. Originating within the dorsal neural tube, the events that cause neural crest cells to segregate from a central nervous system fate are unknown. Here, we show that DNA methyltransferase 3A (DNMT3A) promotes neural crest cell specification by directly mediating repression of the neural genes, Sox2 and Sox3. DNMT3A is expressed in the newly induced neural plate border region from which neural crest cells originate. Its loss of function at the border leads to ectopic upregulation of Sox2 and Sox3 in the dorsal neural tube at the expense of neural crest markers, in a cell autonomous manner. In vivo Chromatin immunoprecipitation of neural folds further demonstrates that DNMT3A specifically associates with CpG islands in the Sox2 and Sox3 promoter regions, resulting in methylation leading to their repression. The results suggest that DNMT3A functions in the embryo as a molecular switch between central nervous system versus peripheral cell lineages, repressing neural to favor neural crest cell fate.

Introduction

During development, neural crest stem cells contribute to many uniquely vertebrate derivatives, including peripheral ganglia and the craniofacial skeleton (Le Douarin 1982).

Although neural crest precursors initially reside within the neural tube, they subsequently segregate from other neuroepithelial cells by a heretofore unknown mechanism. Whereas the remainder of the neural tube will form the central nervous system (CNS), neural crest cells undergo an epithelial to mesenchymal transition, emigrate from the CNS and migrate into the periphery. Single cell lineage analysis has shown that individual cells within the dorsal neural tube can contribute to both the CNS and neural crest (Bronner-Fraser and Fraser 1988) suggesting that premigratory dorsal neural tube cells are not yet committed to a neural crest fate. Subsequently, a subpopulation of dorsal neural tube cells produces bona fide neural crest cells that migrate extensively to populate diverse derivatives, ranging from peripheral neurons to craniofacial cartilage and melanocytes. The molecular mechanisms underlying the neural tube to neural crest transition are a long-standing mystery. In this study, we have explored the possibility that silencing via promoter DNA methylation may play a role in this cell fate choice during embryonic development.

De novo DNA methyltransferases recognize CpG islands and newly methylate DNA by catalyzing transfer of a methyl group to cytosine residues (Cheng and Blumenthal 2008). In cancer and stem cells, when such CpG island methylation occurs in the promoter region, gene expression is inhibited ((Momparler and Bovenzi 2000; Miranda and Jones 2007; Altun et al. 2010). De novo DNA methyltransferases, DNMT3A (Jurkowska et al. 2011a) and DNMT3B, are vital for normal mammalian development and have been implicated in disease (Linhart et al. 2007; Ehrlich et al. 2008; Yan et al. 2011). For example, DNMT3A $-/-$ mice die several weeks after birth and DNMT3B $-/-$ embryos have

rostral neural tube defects and growth impairment (Okano et al. 1999). Moreover, mutations in human DNMT3B result in immunodeficiency-centromeric instability-facial anomalies syndrome, in which patients exhibit craniofacial abnormalities (Jin et al. 2008), suggesting a defect in neural crest development. By contrast, the function of DNMT3A in early development is not understood. Here, we show that DNMT3A plays a critical function in de novo methylation during early nervous system and neural crest development.

Results and Discussion

Expression pattern of DNMT3A in the early chick embryo

As a first step in analyzing its possible function, we examined the expression pattern of DNMT3A transcripts by in situ hybridization. Intriguingly, DNMT3A is highly expressed at the neural plate border at gastrula stages, contrasting with low levels in the neural plate (Fig. 1A, st.5-7). Subsequently, transcripts are confined to the neural folds containing premigratory neural crest precursors (Fig. 1A, st.9), and later in migrating neural crest cells, labeled with HNK-1 antibody (Fig. S1A). Thus, at early developmental stages, DNMT3A is selectively expressed in tissues associated with neural crest and early neural tube development.

Knock-down of DNMT3A blocks neural crest specification, as assayed by FoxD3 expression, in a cell autonomous manner

To test the functional consequences of loss of DNMT3A during neural crest specification, we designed two different fluorescein tagged translation blocking antisense morpholino oligonucleotides (MO) targeted against DNMT3A. These were electroporated into one half of the early chick embryo at gastrulation stages 4/5, with the uninjected side serving as an internal control. To verify that the knock-down was effective, we performed Western blots comparing protein levels in the electroporated side versus control half of the same embryo and found that a band corresponding to DNMT3A protein was significantly decreased in the presence of DNMT3A MO (Fig. 1B). We examined the effects of loss of DNMT3A on expression of FoxD3, as it is one of the earliest neural crest markers to appear in the dorsal neural tube. FoxD3 was dramatically down-regulated after loss of DNMT3A on the morpholino-electroporated side of the embryo (Fig. 1C, D), in an apparently dose-dependent fashion as the severity of the phenotype increased with the amount of morpholino introduced (Fig. S1B).

To control for the specificity of action of DNMT3A morpholino and demonstrate that the observed phenotype was not due to off-target binding, we co-electroporated DNMT3A MO with a construct encoding exogenous DNMT3A under the control of a cranial FoxD3 enhancer, NC1, which turns on at early St.8. This enhancer drives exogenous DNMT3A only in premigratory cranial neural crest cells. Despite the fact that the morpholino was introduced much earlier, this resulted in marked rescue of the loss-of-function phenotype, restoring FoxD3 expression (Fig. 2A, B). To examine whether the

catalytic activity of DNMT3A was important for its function, we co-electroporated DNMT3A morpholino and a rescue construct in which the catalytic domains of DNMT3A were removed. Under identical co-electroporation conditions as above, this mutated form of DNMT3A failed to rescue the loss-of-function phenotype (Fig. S2A, B). This demonstrates that catalytic activity is critical for DNMT3A function during neural crest development.

Although we hypothesize that DNMT3A acts in a cell autonomous fashion in the presumptive neural crest cells, it is possible that aberrant interactions between neural crest precursors and more ventral neural tube cells results in a neural crest phenotype. DNMT3A is expressed at high levels at the neural plate border, neural folds and premigratory neural crest, but is also expressed in the neural tube, albeit at much lower levels. To test if the function of DNMT3A is cell autonomous, we compared its effect on the neural crest versus the rest of the neural tube. Because we cannot selectively target the neural crest region in a predictable fashion, we electroporated the morpholino into the entire neural tube on one side of each embryo, and the neural tube with the exception of the dorsal neural fold region on the opposite side. In 100% of cases, we noted that down-regulation of FoxD3 only occurred when DNMT3A protein was down-regulated in the presumptive neural crest itself (Fig. 2C). The finding that FoxD3 is absent from cells containing DNMT3A MO but present in cells lacking DNMT3A MO in the dorsal neural fold region, definitively demonstrates that DNMT3A acts cell autonomously (Fig. S2D).

Multiplex analysis reveals that loss of DNMT3A up-regulates neural genes, while down-regulating neural crest specifier genes

In order to understand global and multiplexed changes in gene expression caused by DNMT3A knock-down, we performed NanoString analysis to monitor and quantify 73 transcripts including genes expressed in the neural crest, neural tube, neural plate, neural plate border, placodes, nonneural ectoderm, and those involved in cell proliferation and cell death. Each DNMT3A knockdown embryo was analyzed at late St.8, by comparing the morpholino electroporated side to the uninjected side of the same embryo. Because DNMTs are thought to inhibit transcription by methylating the promoter region of target genes, we were particularly interested in genes that were up-regulated as a consequence of down-regulating DNMT3A, as these represent potential direct targets. Interestingly, the results show that transcriptional regulators characteristic of neural fate specification, Sox2 and Sox3, as well as the neural plate border gene, Zic1, some EMT and placode related genes were upregulated after DNMT3A knock-down (Fig. 3A, Fig. S3A, B, C).

Sox2 (Pevny and Lovell-Badge 1997; Graham et al. 2003) was of particular interest since its misexpression in the neural folds blocks expression of the neural crest gene, Snail2 (Wakamatsu et al. 2004). Furthermore, Sox2 is a well-known pluripotency gene and is one of the four genes necessary to reprogram somatic cells into pluripotent stem cells (Pawlak and Jaenisch 2011). Therefore, we used in situ hybridization to verify

the upregulation of Sox2 noted by NanoString analysis. The results show that loss of DNMT3A causes expansion of Sox2 into the neural crest territory whereas, on the control side of the same embryo, Sox2 is absent from the neural crest domain (Fig. 3B). Interestingly, this is accompanied by changes in morphology of the dorsal neural tube, which appears less broad and more neuroepithelial than the control side. In contrast to Sox2, the pluripotency genes, Nanog and Oct4/PouV, exhibited little or no expression in the cranial neural tube (Canon et al. 2006); and unpublished observation). Moreover, their expression was unchanged after DNMT3A knock-down (data not shown).

Sox2 and Sox3 are paralogues with overlapping function. Therefore, we examined the effects of DNMT3A knock-down on Sox3 expression and found that, like Sox2, it is upregulated in the dorsal neural tube after morpholino knock-down (Figure 3B). Thus, both genes are affected similarly, though Sox2 comes on earlier than Sox3 and appears to be the dominant neural specifier. Like Sox2 and Sox3, Zic1 also was upregulated in the dorsal neural tube after loss of DNMT3A (Fig. 3B).

Concomitant with up-regulation of Sox2, neural crest specification markers were down-regulated in DNMT3A knockdown embryos as shown in our NanoString data (Fig. 3A). This was verified by in situ hybridization for other neural crest specifiers and dorsal neural tube genes, including Sox9, Sox10, Snail2, Ets1, Wnt1, and N-Myc. Like FoxD3, all of these appeared to be down-regulated upon loss of DNMT3A (Fig. 4). Given that Wnt signaling has been implicated in neural crest specification and Wnt1 was down-regulated

after DNMT3A knock-down, we tested whether activated b-catenin could rescue the DNMT3A morpholino phenotype. However, the results show no change in FoxD3 expression (Fig. S4A, B).

Co-immunostaining of Sox2 and FoxD3 in a single embryo treated with DNMT3A MO further demonstrates that loss of DNMT3A up-regulates neural genes such as Sox2, while down-regulating neural crest specifier genes such as FoxD3 (Fig. 3C, Fig. S3E). We noted no significant change in cell death as shown by Casp-3 staining (Fig. S4C). In addition, there was no change in expression of neural plate border genes like Msx1 and BMP4 in the dorsal neural tube (Fig. S4D).

To demonstrate a direct link between Sox2 upregulation and the reduction of neural crest gene expression, we electroporated a construct containing avian Sox2 (Wakamatsu et al. 2004) into stage 4-5 neural plate, resulting in over-expression throughout the neural tube including ectopic expression in the dorsal region. Consistent with our findings after DNMT3A knock-down, this caused down-regulation of the neural crest specifier genes FoxD3, Sox10, and Snail2 (Fig. S5). For the reciprocal experiment, we examined whether morpholino knock-down of Sox2 and/or Sox3 was sufficient to induce neural crest cell fate in the neural tube. Loss of Sox2, Sox3 or both in combination failed to convert neural tube to neural crest cells. However, these factors are critical for normal neural induction and their loss, as expected, led to severe neural defects.

Neural specifier genes Sox2 and Sox3 are direct targets of DNMT3A

The Nanostring and in situ data raise the intriguing possibility that de novo methylation of the Sox2 promoter region by DNMT3A may be essential for repression of the Sox2 in the dorsal neural folds, and necessary for the switch in its identity from neural to neural crest. To test this in the in vivo context, we used Chromatin Immunoprecipitation (ChIP) followed by qPCR to assess whether Sox2 is a direct target of DNMT3A. To this end, dorsal neural folds were dissected from stage 8 embryos and processed for microChIP as previously described (Betancur et al. 2010; Strobl-Mazzulla et al. 2010). The data show that DNMT3A associates with the Sox2 promoter region, but not with the N2 enhancer region of Sox2 (Uchikawa et al. 2003)(Fig. 5). Similar to Sox2, ChIP analysis shows that DNMT3A also occupies the promoter region of Sox3, the paralogue of Sox2 (Fig. 5). In contrast, Zic1, which was also upregulated after DNMT3A knock-down, does not appear to be a direct target of DNMT3A, since ChIP analysis failed to show binding at its promoter region (data not shown).

We further examined the methylation pattern of Sox2 and Sox3 in the dorsal neural tube of stage 8. As expected, the results show that both Sox2 and Sox3 are methylated in the vicinity of their promoters (Fig. S2C). Taken together, these findings definitively show that DNMT3A directly binds to the promoter regions of Sox genes and represses their transcription via methylation, thus allowing the acquisition of neural crest gene expression.

Our data show that DNA methylation acts as a molecular switch to turn off neural tube transcription factors, thus facilitating neural crest gene expression and fate acquisition. Previous studies on the molecular mechanisms of DNMT3A function have been focused on hematopoietic, neural stem cells and glioma cells in tissue culture. These studies using in vitro data show that DNMT3A can promote cell differentiation by repressing pluripotency genes (Trowbridge and Orkin 2012). Consistent with this, our results in the developing embryo demonstrate that DNMT3A promotes neural crest cell type specification in an in vivo context by repressing neural genes like Sox2 and Sox3. Although the mechanism by which DNMT3A is recruited to the promoter region of target genes is unknown, it has been shown to interact with numerous factors on transcription factor arrays (Hervouet et al. 2009). Although these have yet to be validated, particularly in vivo, this list includes some neural plate border and neural crest specifier genes like Msx1, tfAP2a, Id2 and Myc. Thus, it is intriguing to speculate that DNMT3A may be recruited to the Sox2 promoter by some of these factors that are selectively expressed in the neural crest forming domain.

In some cases, de novo methyltransferases can also mediate methylation-independent gene repression, by co-localizing with heterochromatin and associating with HP1 and MeCBP (methyl-CpG-binding protein). For example, in zebrafish neurogenesis, DNMT3B cooperates with histone methyltransferase G9a to inhibit expression of Lef1 (Rai et al. 2010). Thus, it is particularly interesting that, in the neural folds, DNMT3A acts via regulation of the promoter region rather than the enhancer region as demonstrated by our ChIP data. This shows that, in addition to cis-regulatory events, epigenetic influences are a

critical mechanism for regulating transcription. Our discovery that DNA methylation promotes neural crest specification at the expense of neural tube identity provides important insights into the mechanisms that determine whether a cell becomes part of the central nervous system or peripheral nervous system.

Materials and methods

Embryos

Fertilized chicken eggs were incubated at 37°C to desired stages.

In situ hybridization

Embryos were fixed with 4%paraformaldehyde, washed with PBS/0.1%Tween, dehydrated in MeOH, and stored at -20°C. Whole mount in situ hybridization was performed as described (Wilkinson 1992; Aclouque et al. 2008). Dioxigenin-labeled RNA probes were made from DNA plasmids or ESTs of DNMT3A, Sox2, Sox9, Sox10, Snail2, FoxD3, Wnt1, Ets1, Nmyc, Msx1, and Bmp4. Embryos were sectioned at 16-18µm.

Electroporation

Embryos were electroporated at St.4-5 as described (Sauka-Spengler and Barembaum 2008) using DNMT3AMO1 (over ATG codon): TGGGTGTGTCCTGC TTTCCACCAT and/or DNMT3AMO2 (95 nucleotides upstream ATG): CAGTGTCCCCACGGCGCTTCCTGCT. The rescue construct included the coding

region of DNMT3A (NM001024832.1) under control of NC1 or empty NC1 as control. For each embryo, 0.6mM MO+0.5ug/ul DNA was used for knockdown experiments and 0.4mM MO+1.5ug/ul DNA for rescue experiments. MO was targeted to presumptive neural crest region with 5pulses of 5.2 V in 50 ms at 100ms intervals. Electroporated embryos were maintained in culture dishes with 1ml albumen, then fixed.

NanoString nCounter

Half dorsal neural folds of DNMT3AMO treated embryos were dissected in lysis buffer (Ambion RNAqueous-Micro Isolation kit). RNA lysates were hybridized to the probe set and incubated overnight at 65°C, washed and eluted according to nCounter Prep Station Manual and counted by nCounter Digital Analyzer.

Chromatin Immunoprecipitation

Dorsal neural tubes from 25 St.8 embryos were dissected and extracted (3 experiments/condition). Cells were crosslinked and sonicated to yield 300-800bp fragments. Samples were evenly split for DNMT3A antibody (Abcam), control rabbit anti-IgG (Abcam) and Input. Antibodies were preincubated with ProteinA magnetic beads (Invitrogen) before incubation with sonicated protein-DNA complex. Samples were washed, eluted and reverse crosslinked. Final DNA pulldown was purified and served as a template for qPCR of the Sox2 promoter region. Three replicates were loaded for each sample and results were quantified using DDCT method. Analysis was done using Applied Biosystems manual instructions.

Acknowledgments: We thank Drs. M. Simoes-Costa and M. Barembaum for helpful discussions. We are grateful to Dr. Yoshio Wakamatsu for kindly providing the Sox2 over-expression construct. This work was supported by F31DE021643 and 5 T32 GM07616 to N.H. and HD037105 and DE16459 to M.E.B.

Figure 1

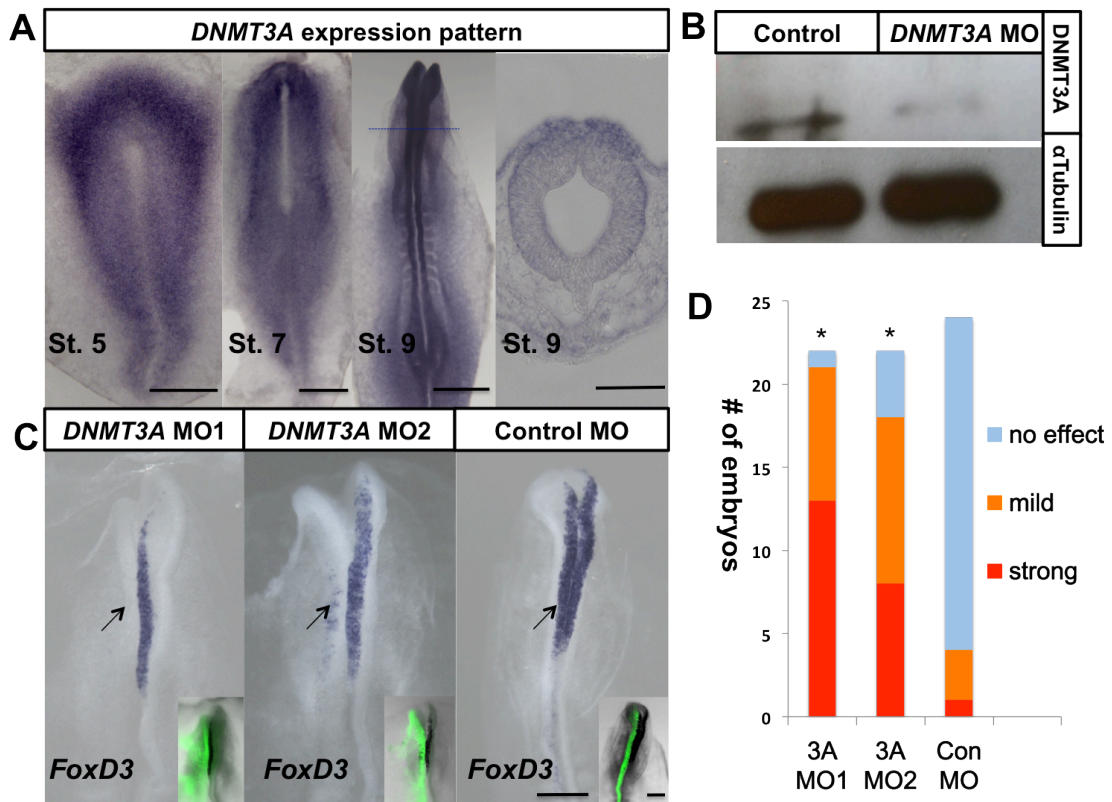


Figure 1. DNMT3A is expressed at sites of neural crest formation and its loss of function blocks expression of neural crest specifier gene, *FoxD3*. (A) Expression pattern of DNMT3A in St.5-9 chick embryo by in situ hybridization. DNMT3A is strongly expressed in the neural plate border (St.5-7) and dorsal neural tube (St.9). Scale bar =500um in whole mount, 100um in section (B) Western blot of dorsal neural tubes (5 pooled embryos) shows that DNMT3A protein level was reduced on the electroporated compared with control side; α -tubulin levels were unchanged. (C) Two morpholinos against DNMT3A (MO1&MO2, FITC-inset) caused reduction of *FoxD3* expression at St.8 after electroporation (left; arrowhead) compared with the contralateral internal control side

or control morpholino electroporated embryos. Scale bar = 200um **(D)** Quantitation of numbers of DNMT3A MO and Control MO treated embryos with either strong or mild loss of FoxD3 expression of MO versus control side of same embryo. Asterisk indicates significant differences ($P < 0.01$) by contingency table followed by chi-square test. See also Figure S1.

Figure 2

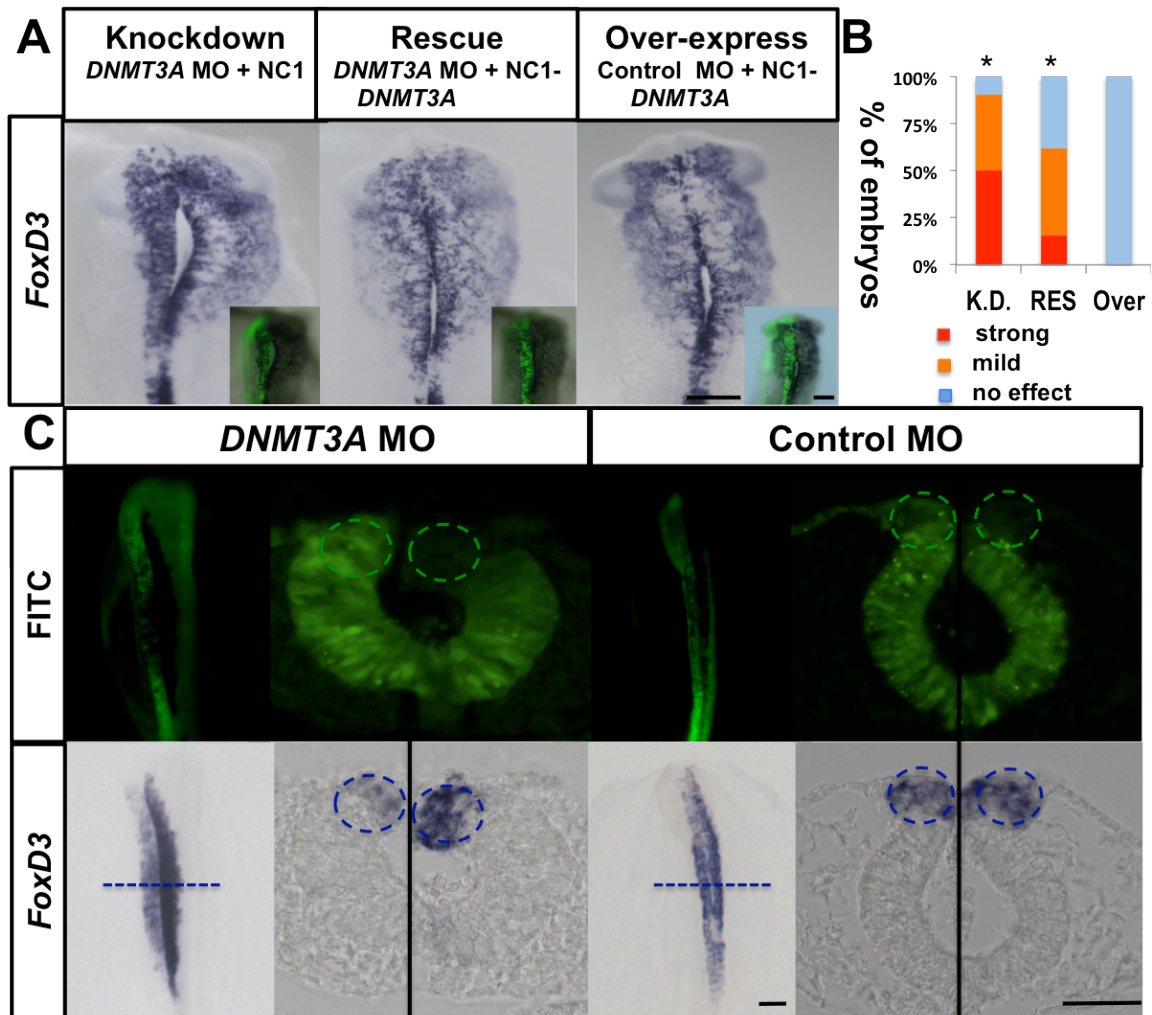


Figure 2. Loss of FoxD3 is rescued by exogenous DNMT3A in a neural crest cell autonomous manner. (A) Expression of DNMT3A protein in premigratory neural crest rescues the loss of FoxD3 phenotype: Each embryo was electroporated on the left side with either DNMT3A MO or control MO (green in inset) in combination with either a DNMT3A rescue construct (NC1-DNMT3A) or empty vector (NC1 alone). The rescue construct contains the coding region of DNMT3A under control of a cranial neural crest

specific enhancer for FoxD3 plus HSV-tk basal promoter. At St.10, the loss of neural crest marker FoxD3 was largely rescued by NC1-DNMT3A plus DNMT3A MO. Overexpression of DNMT3A rescue construct alone did not alter FoxD3 expression. Scale bar = 500um **(B)** Quantitation of the percentage of DNMT3A knockdown (K.D.), Rescue (RES), and Overexpression (Over) embryos in (a) with either strong or mild loss of FoxD3 expression. $P < 0.01$ by contingency table followed by chi-square test. K.D. n=10, RES n=13, Over n=5. **(C) Effect of DNMT3A loss of function is cell autonomous to the neural crest forming region:** DNMT3A MO or Control MO was electroporated throughout the neural tube on the left side, and into the neural tube with the exception of the dorsal neural folds (circled) on the right side. Loss of FoxD3 only occurred when the dorsal neural fold was electroporated with DNMT3A MO, as evident in transverse section. DNMT3A MO n=8/8, Control MO n=12/12, $p < 0.01$ by contingency table followed by chi-square test. Scale bar = 100um See also Figure S2.

uninjected sides. **(B)** Transverse sections of St.8 embryos electroporated with DNMT3A MO (FITZ-inset) confirms that Sox2, Sox3 and Zic1 expression was expanded into the neural crest territory (blue circle) when compared to internal control side, n=12/12. Scale bar = 200um in whole mount, 100um in section. **(C)** Transverse section of St.8 embryos electroporated with DNMT3A MO (green) confirms that Sox2 (red) protein expression was expanded into the neural crest territory (red circle) when compared to the internal control side while FoxD3 (blue) protein expression was missing in the neural crest territory (blue circle). n=7/8. Control morpholino treated embryos show equivalent Sox2 and FoxD3 expression on both sides (Figure S3). Scale bar = 100um

Figure4

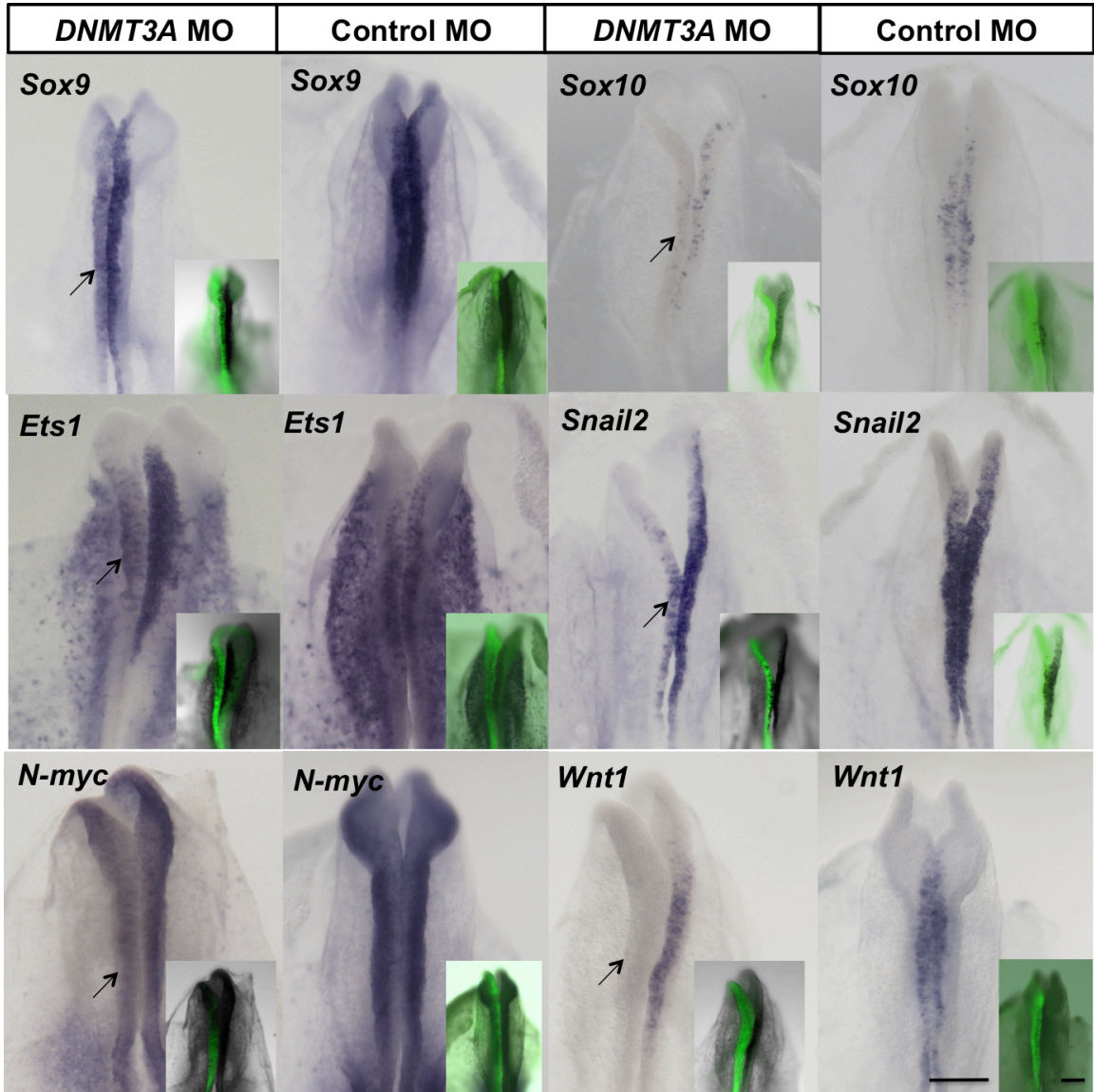


Figure 4. Neural crest specifier and dorsal neural tube genes are down-regulated after knock-down of DNMT3A. DNMT3A MO or Control MO was electroporated into the left side of embryo (FITC-inset, green) and the subsequent effects on expression patterns of

neural crest and dorsal neural tube genes were examined by whole mount in situ hybridization. Sox9, Sox10, Ets1, Snail2, N-myc and Wnt1 are down-regulated (arrowhead) upon introduction of DNMT3A MO when compared to the internal control side or control morpholino electroporated embryos. Scale bar = 200um

Figure 5

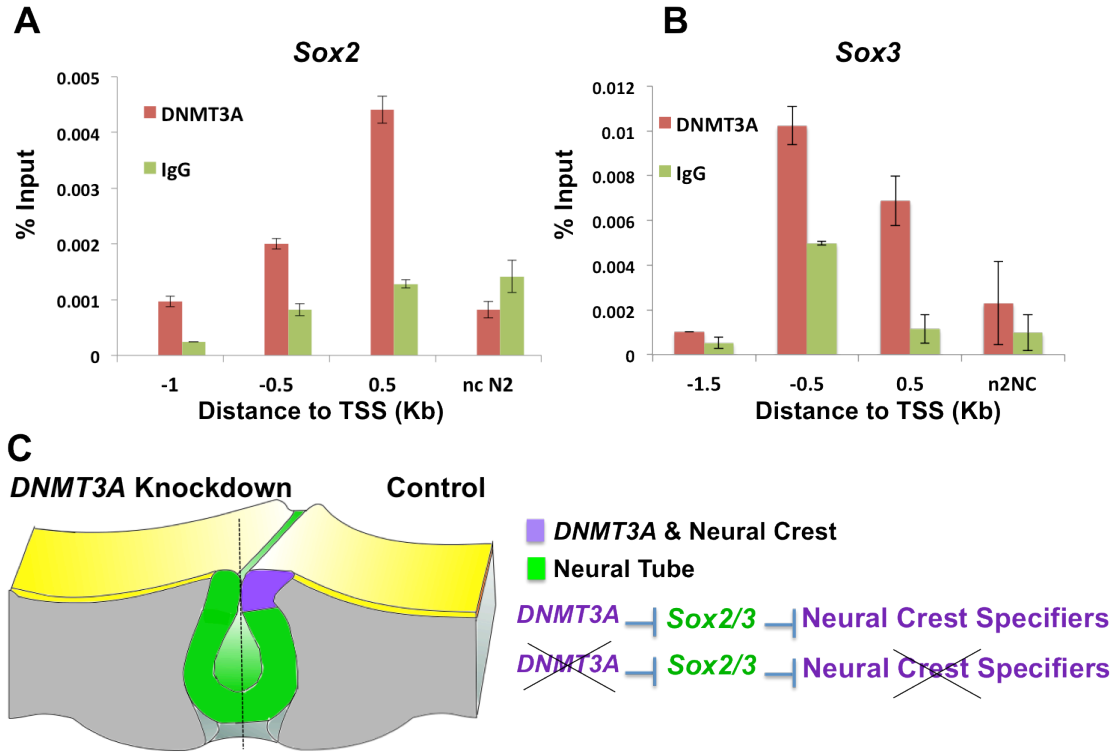


Figure 5. Sox2 and Sox3 are direct targets of DNMT3A. Chromatin immunoprecipitation (ChIP) was used to detect binding of DNMT3A in the vicinity of transcriptional start site (TSS) of Sox2 and Sox3. The y axis represents input percentage (ChIP enriched/input) and x axis the distance from the TSS in kilobases (kb). **(A)** The results show high occupancy of DNMT3A at 0.5kb from the TSS of Sox2 at St.8. DNMT3A significantly binds to Sox2 at 0.5kb (0.0044% input) compared to negative control region ncN2 (0.0008% input) or IgG binding at 0.5kb (0.0013%input). Graph shows mean value \pm standard deviation (SD) of a representative experiment. **(B)** The

results show high occupancy of DNMT3A at -0.5kb and 0.5kb from the TSS of Sox3 at St.8. DNMT3A significantly binds to Sox3 at -0.5kb (0.0102% input) and 0.5kb (0.0069% input) compared to a negative control region ncN2 (0.0023% input) or IgG binding at -0.5kb (0.0049%input) and 0.5kb (0.0011%input). Graph shows mean value \pm standard deviation (SD) of a representative experiment. **(C) Schematic diagram summarizing effects of DNMT3A knockdown.** In wildtype (control side), DNMT3A (purple) directly represses Sox2/3 in the dorsal neural tube, thus facilitating expression of neural crest specifier genes like Snail2, FoxD3 and Sox10. After DNMT3A knockdown, Sox2/3 expression expands into the dorsal neural tube region, in turn resulting in down-regulation of FoxD3, Snail2, Sox10 and other neural crest specifiers, and thus conferring a neural tube rather than neural crest fate.

Figure S1

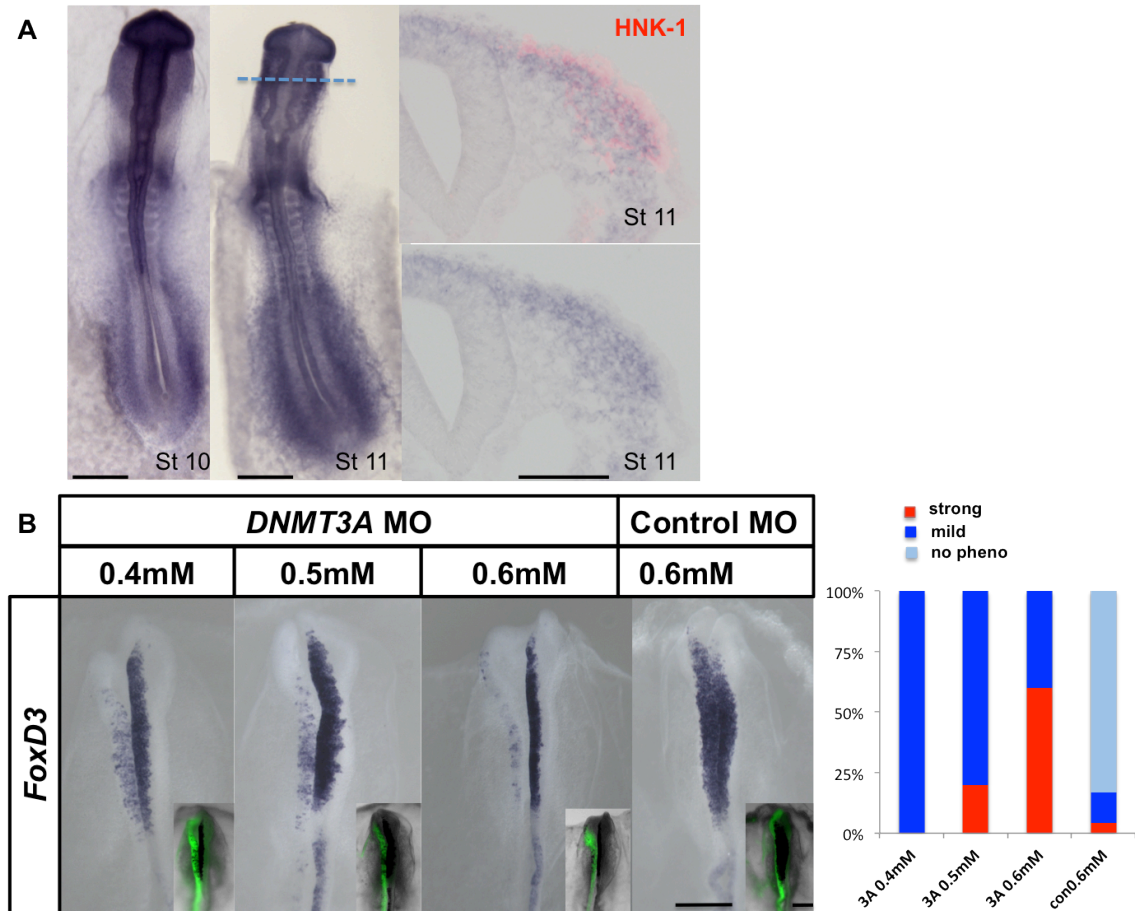


Figure S1, related to Figure 1. (A) DNMT3A is expressed in the domain where neural crest cells are formed. Expression pattern of DNMT3A in the early chick embryo by in situ hybridization at stages 10-11. DNMT3A is expressed in the dorsal neural tube and migratory neural crest cells, which are identified by HNK-1 antibody staining. Scale bar = 500 in whole mount, 100 in section **(B) The decrease in FoxD3 expression corresponds with increases in the amount of DNMT3A morpholino introduced, suggesting dose-**

dependence. $P < 0.01$ by contingency table followed by chi-square test. Graph shows quantification of percentage of embryos with strong or mild loss of neural crest specifier FoxD3 expression when comparing MO side versus control side of same embryo. 3A = DNMT3A. Con=control. Pheno=phenotype. DNMT3A MO 0.4mM n=15, 0.5mM n=10, 0.6mM n=17; Con0.6mM n=22. Scale bar = 200um

Figure S2

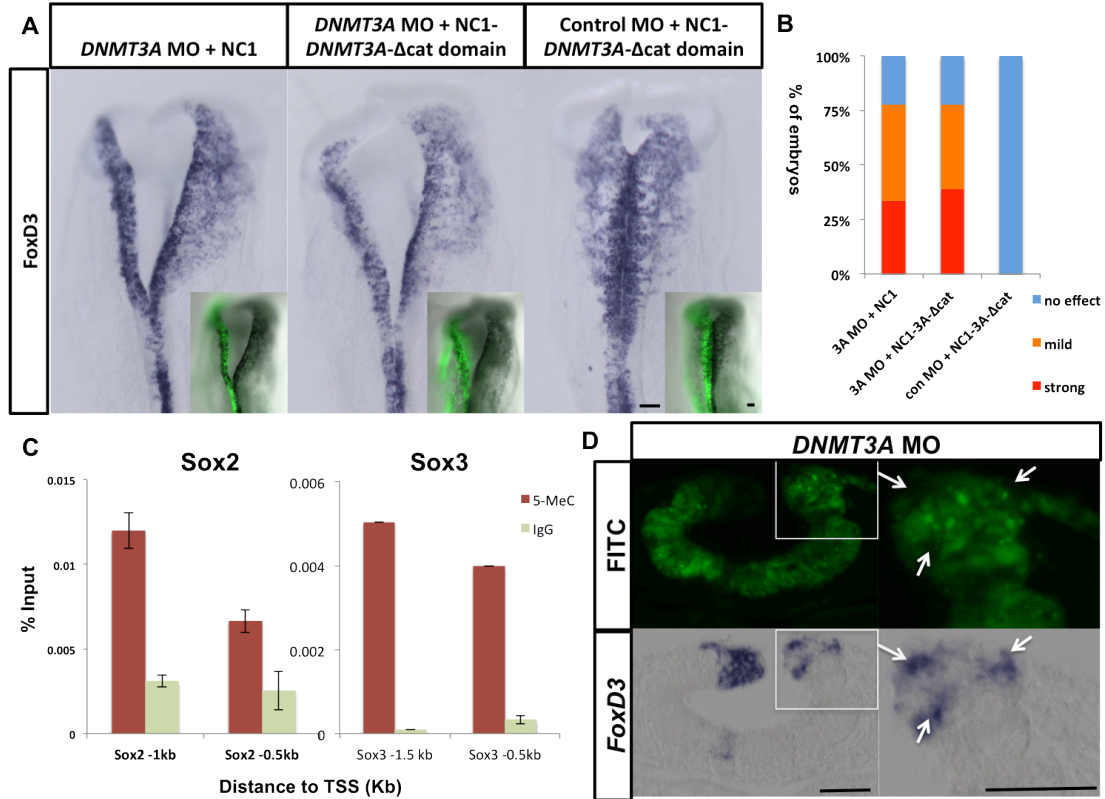


Figure S2, related to Figure 2. A mutated version of DNMT3A fails to rescue the loss-of-function phenotype. (A) Each embryo was electroporated on the left side with either DNMT3A MO or control MO (green in inset) in combination with a construct containing either a mutated form of DNMT3A in which the catalytic domains of DNMT3A were removed (NC1-DNMT3A Δ cat domain) or an empty vector (NC1). The construct is under control of a cranial neural crest specific enhancer for FoxD3 plus HSV-tk basal promoter. At St.10, this mutated form of DNMT3A failed to rescue the loss-of-function phenotype. Over-expression of this construct alone did not alter FoxD3 expression. Scale bar = 200 μ m

(B) Quantitation of the percentage of embryos in (a) with either strong or mild loss of FoxD3 expression. 3A MO + NC1 n=18, 3A MO + NC1-3A- Δ cat n=18, con MO + NC1-3A- Δ cat n=6. **(C) Both Sox2 and Sox3 are methylated in the vicinity of their promoters.** Chromatin immunoprecipitation (ChIP) was used to detect binding of 5-methyl cytosine (5-MeC) in the vicinity of transcriptional start site (TSS) of Sox2 and Sox3. The y axis represents input percentage (ChIP enriched/input) and x axis the distance from the TSS in kilobases (kb). The results show high occupancy of 5-MeC at the TSS of Sox2 and Sox3 at St.8. 5-MeC significantly binds to Sox2 at -1kb (0.0120% input) and -0.5kb (0.0067% input) compared to IgG binding at -1kb (0.0031%input) and -0.5kb (0.0026%input). 5-MeC significantly binds to Sox3 at -1.5kb (0.0050% input) and -0.5kb (0.0040% input) compared to IgG binding at -1.5kb (0.0001%input) and -0.5kb (0.0003%input). Graph shows mean value \pm standard deviation (SD) of a representative experiment. **(D) The loss of neural crest specifier gene expression is cell autonomous.** FoxD3 is absent from cells containing DNMT3A MO but present in cells lacking DNMT3A MO (pointed by arrow) in the dorsal neural fold region. Scale bar = 50um

Figure S3

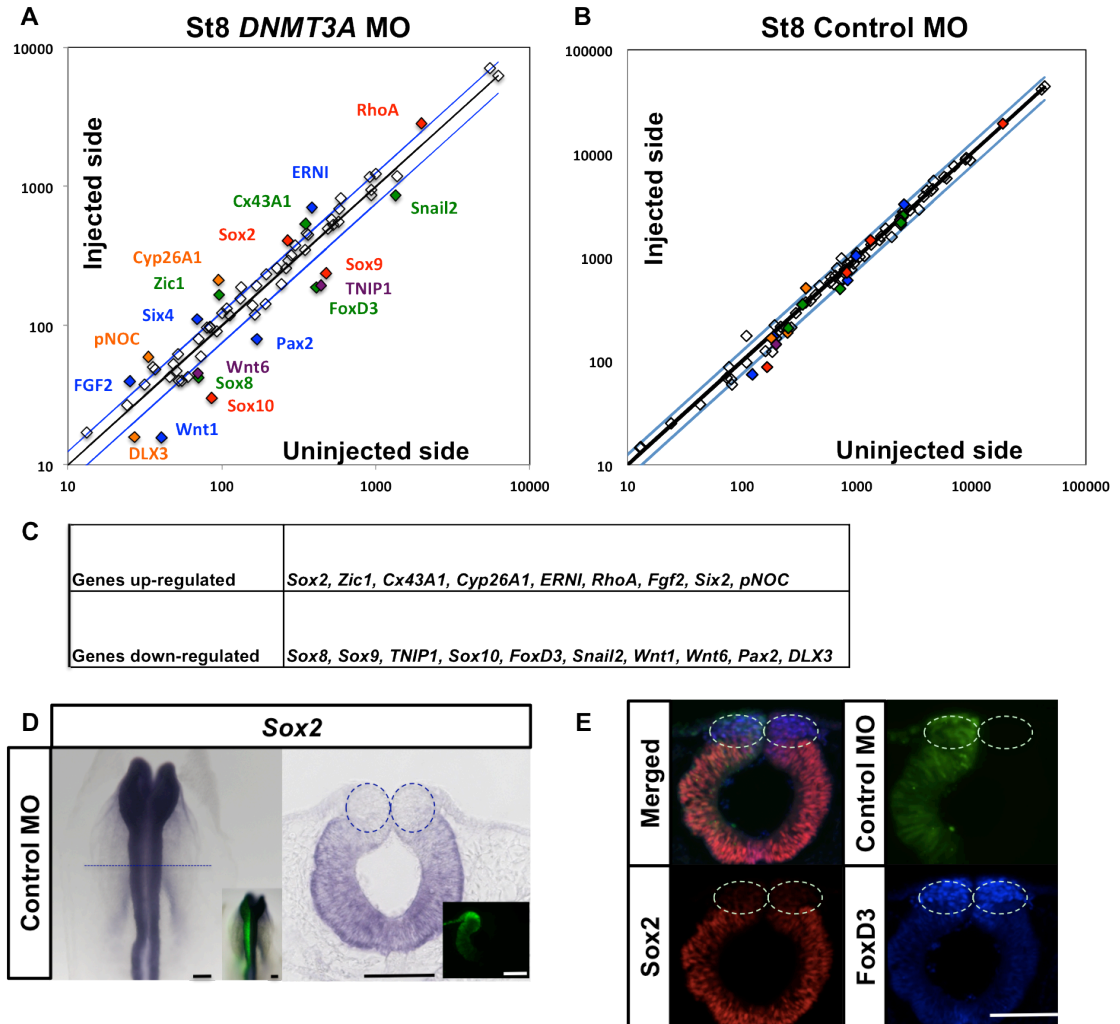


Figure S3, related to Figure3. (A-B) Identifying putative downstream targets of DNMT3A using Nanostring. The injected side of DNMT3A MO treated embryos shows >25% up-regulation of neural tube genes *Sox2, Zic1*, EMT related genes *RhoA, Cx43A1*, placode related genes *Cyp26A1, Six4*, as well as *ERNI* and *FGF2* ($n=3$); in addition, there was >25% reduction of neural crest specifier genes *Snail2, Sox9, TNIP1, FoxD3, Sox8*,

Sox10, dorsal neural tube genes Wnt1, Wnt6 and placode genes DLX3 and Pax2; in contrast, no significant differences were noted in gene expression between control morpholino and uninjected side of the same embryo (n=3). **(C)** Genes up and down regulated for >25% upon introduction of DNMT3A MO. **(D)** Control morpholino treated embryos have equivalent Sox2 expression on both sides of the embryo. n=9/9. Scale bar = 100um **(E)** Control morpholino treated embryos have equivalent Sox2 and FoxD3 protein expression on both sides of the embryo. n=10/10. Scale bar = 100um

Figure S4

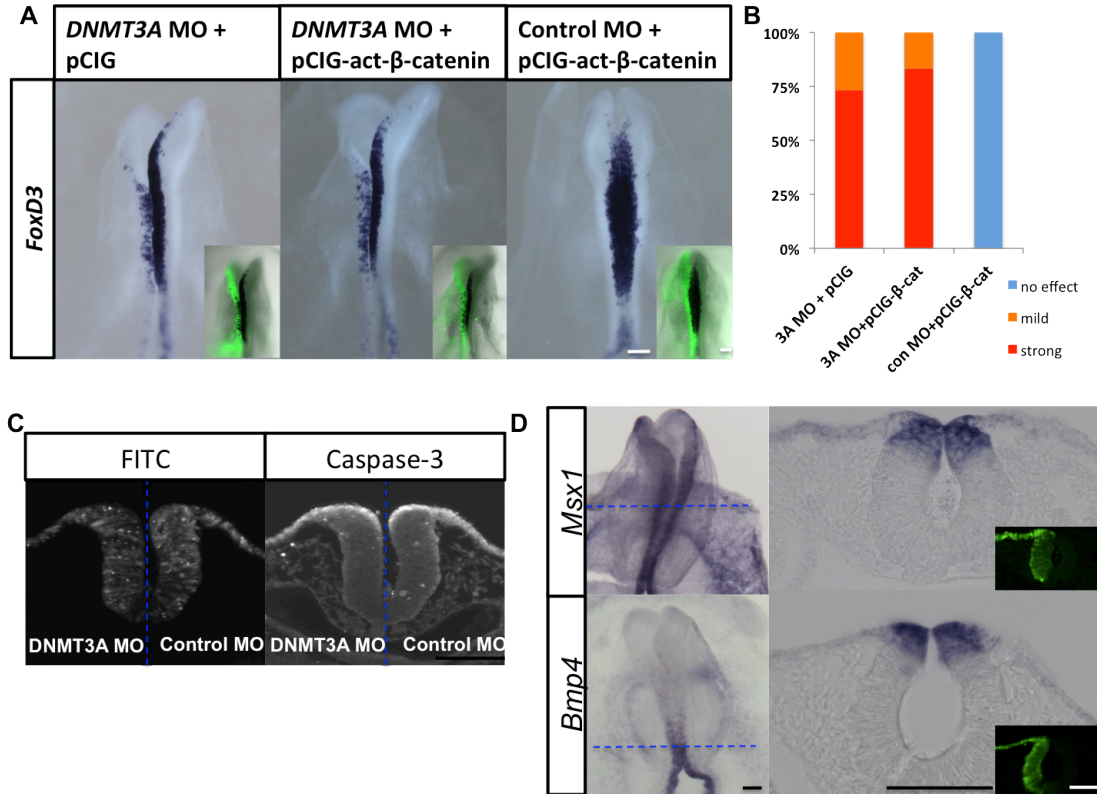


Figure S4, related to Figure 4. Activated β -catenin fails to rescue the loss of FoxD3 phenotype. (A) Each embryo was electroporated on the left side with either *DNMT3A* MO or control MO (green in inset) in combination with either an activated β -catenin driven by pCIG (pCIG-act- β -catenin) or an empty vector (pCIG). We tested whether activated β -catenin could rescue the *DNMT3A* morpholino phenotype. However, the results show no change in *FoxD3* expression. (B) Quantitation of the percentage of embryos in (a) with either strong or mild loss of *FoxD3* expression. 3A MO + pCIG n=15, 3A MO + pCIG- β -catenin n=12, con MO + pCIG- β -catenin n=8. Scale bar = 100um (C) **Knock-down of**

DNMT3A does not increase cell death. DNMT3A MO was electroporated into the left side and Control MO into the right side of the same embryo. Embryos were fixed and sectioned at stage 9 and stained for Casp-3 immunoreactivity. Casp-3 positive cells were counted and compared between the left and right side. No difference was found between the two sides in n=3/3 embryos. Figure shows one representative section. Scale bar = 100um **(D) DNMT3A loss of function does not effect neural plate border genes Msx1 and BMP4,** shown in whole mount and transverse section. DNMT3A MO was electroporated to left side of each embryo (FITC-inset). n=6/6. Scale bar = 100um

Figure S5

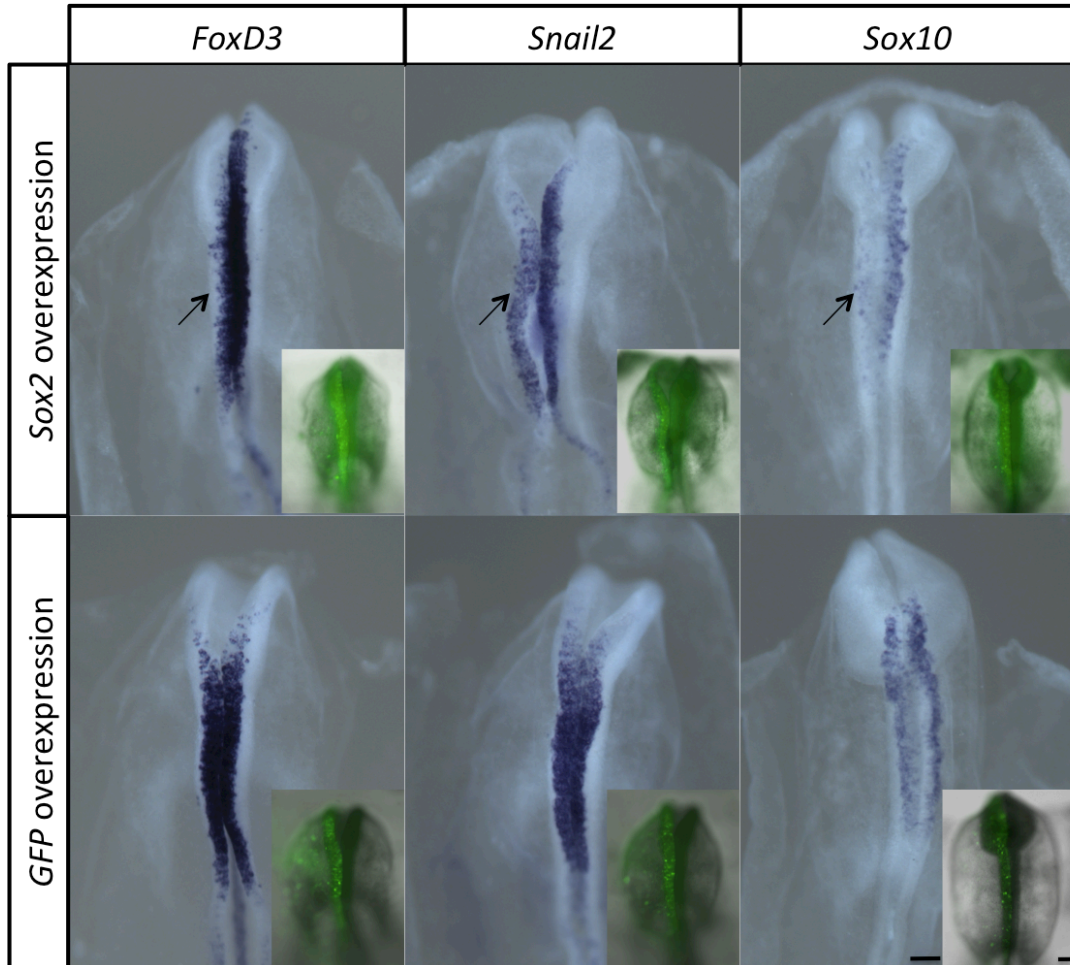


Figure S5. Over-expression of Sox2 causes down-regulation of the neural crest specifiers genes FoxD3, Sox10 and Snail2. Overexpression construct containing avian Sox2 (green in inset) or GFP (Wakamatsu et al., 2004) was electroporated into the left side of stage 4-5 embryos. Consistent with our findings after DNMT3A knock-down, over-expression of Sox2 caused down-regulation of the neural crest specifier genes FoxD3, Sox10, and Snail2(arrowhead). Scale bar = 100um

Table1**qPCR Primers:**

sox2 -1kb Forward	GATGTCGGGAGAAGCCATAG
sox2 -1kb Reverse	GGTTGGAAGGAAGGAGAGA
sox2-0.5kb Forward	ACTCCCCAAAACCACACTTG
sox2-0.5kb Reverse	GTGTTTGCAAAGGGGGTAA
sox20.5kb Forward	TTGCTGATCTCCGAGTTGTG
sox20.5kb Reverse	GATGGAAACCGAGCTGAAAC
Sox2 ncN2 Forward	GGGAAAGCTCTGTTTAGCC
Sox2 ncN2 Reverse	TTTTCGTCTTCGGCATTITT
Sox3-1.5kb Forward	AGGAGAAAGAGCGCAGACAG
Sox3-1.5kb Reverse	GTTCCCTCCGTGTGAAAGAA
Sox3-0.5kb Forward	CTCTCCAAACCGACCCATTA
Sox3-0.5kb Reverse	AGGAGGGGGAAGGAGTTTTTC
Sox3+0.5kb Forward	CACAACCTCGGAGATCAGCAA
Sox3+0.5kb Reverse	CAGCAAGGTCTTGGTCTTCC

Chapter 3

**Loss of DNA methyltransferase3B prolongs neural crest EMT and causes
premature neuronal differentiation**

Na Hu, Pablo Strobl-Mazzulla and Marianne Bronner

To be submitted

Abstract

The neural crest is a multipotent stem cell-like population that undergoes an epithelial to mesenchymal transition (EMT) to leave the central nervous system (CNS), migrate extensively and form numerous derivatives including peripheral ganglia and the craniofacial skeleton. In chick, neural crest EMT occurs over a defined period of approximately one day. Little is known about the mechanisms that limit the ability of the CNS to produce neural crest. Here, we show that DNA methyltransferase (DNMT) 3B influences the ability of neural tube cells to produce emigrating neural crest cells. DNA methyltransferase 3B is expressed in the dorsal portion of the developing neural tube from early stages. Interestingly, morpholino-mediated knock-down in chick causes an excess of neural crest emigration, by extending the time that the neural tube is competent to generate migratory neural crest cells. Concomitant with up-regulation of neural crest genes, like *Snail2*, *Sox10* and *FoxD3*, there is a loss of neural tube markers such as *Wnt3A*. In older embryos, this resulted in precocious neuronal differentiation. These results support an important role for DNA methylation in regulating the duration of neural crest production by the neural tube and the timing of their differentiation.

Introduction

The neural crest is a multipotent population, unique to vertebrates, that contributes to a wide variety of derivatives including sensory and autonomic ganglia of the peripheral nervous system, cartilage and bone of the face, and pigmentation of the skin. Neural crest progenitors arise at the neural plate border, between neural and non-neural ectoderm, and after neurulation, reside within the dorsal aspect of the central nervous system. They then undergo an epithelial to mesenchymal transition (EMT) and delaminate from the neural tube as migratory, mesenchymal cells that navigate to diverse and sometimes distant locations. The timing of both onset and cessation of neural crest emigration from the neural tube is stereotypic. For example, in birds, neural crest cells initiate emigration shortly after neural tube closure and cease emigration about one day later. The proper timing and degree of neural crest production and appropriate migration is critical for normal development of the peripheral nervous system and craniofacial skeleton. Indeed, dysregulation of these events can result in neural crest related birth defects and peripheral neuropathies.

The initiation of neural crest emigration from the neural tube has been the subject of many studies. At trunk levels, for example, it has been reported that neural crest delamination depends upon appropriate levels of BMP signaling which in turn regulate the G1/S cell cycle transition of emigrating neural crest cells in a Wnt-dependent manner (Burstyn-Cohen et al. 2004). In addition, transcription factors like Snail2 play an important

role in EMTs of cancer cells as well as neural crest cells (Cano et al. 2000; del Barrio and Nieto 2002; Strobl-Mazzulla and Bronner 2012b). In contrast, the mechanisms that limit the ability of the neural tube to produce neural crest cells over time are poorly understood. Single cell lineage analyses of the newly closed neural tube have shown that individual precursor cells can give rise to both neural crest and neural tube derivatives (Bronner-Fraser and Fraser 1988; McKinney et al. 2013). This raises the intriguing possibility that unknown factors, such as epigenetic modifiers, may progressively limit the ability of presumptive central nervous system cells to produce neural crest cells, by influencing the balance between neural tube versus neural crest cell fate. Consistent with this possibility, we recently found that a DNA methyltransferase (DNMT3A) plays an early function in repressing the neural genes Sox2 and Sox3 in the presumptive neural crest region, and this is a prerequisite for neural crest specification (Hu et al. 2012).

DNA methyltransferases function in de novo methylation, catalyzing transfer of a methyl group to the cytosine residues on DNA (Cheng and Blumenthal 2008). Generally, most mammalian genomes are highly methylated at CpG islands within promoter regions, where DNA methylation has a repressive effect. A similar situation has been observed for cancer and stem cells (Mompalmer and Bovenzi 2000; Miranda and Jones 2007; Altun et al. 2010). Both DNMT3B and its paralog, DNMT3A, are essential for de novo methylation and have been shown to play important roles in disease as well as mammalian development (Linhart et al. 2007; Ehrlich et al. 2008). Whereas mouse knock-outs of DNMT3A were nonviable, DNMT3b *-/-* embryos have rostral neural tube defects and growth impairment

(Okano et al. 1999). Moreover, mutations in human DNMT3B are found in ICF (immunodeficiency-centromeric instability-facial anomalies) syndrome, comprised of facial abnormalities, neurological dysfunction and other related defects (Jin et al. 2008). Similarly, in zebrafish, loss of DNMT3 causes defects in craniofacial structures and abnormal neurogenesis (Rai et al. 2010). In human embryonic stem cells, knockdown of DNMT3B accelerates neural and neural crest differentiation and increases the expression of neural crest specifier genes (Pax3, Pax7, FoxD3, Sox10 and Snail2). DNMT3B expression is significantly upregulated during neural crest induction in chicken embryos (Adams et al. 2008). All of these data are consistent with an important role for DNMT3B in neural crest development. In contrast to the human syndrome and stem cells data, however, conditional knock-down of DNMT3B in the mouse neural crest using Wnt1- or Sox10-cre does not produce an apparent craniofacial phenotype (Jacques-Fricke et al. 2012). Both DNMT3B null and Wnt-1 cre driven DNMT3B knockout mice exhibit only mild migration defects, reflected by dispersed Sox10 positive cells that recover during cranial gangliogenesis. This could reflect differences between species, or may indicate that the primary function of DNMT3b is in non-neural crest tissue.

To resolve the possible species specific roles of DNMT3B in the neural crest, we turned to the chick embryo, which affords several advantages. Bird embryos are easily accessible to experimental perturbation at early stages of development, while developing in a manner that is morphologically nearly identical to that of human embryos at comparable stages. This allows for temporally and spatially controlled manipulation of gene

expression. Moreover, it is possible to perform perturbations that affect only one side of the embryo, with the opposite side serving as an internal control. Using this paradigm, our results show that knock-down of DNMT3B in the cranial neural crest during stages of neural crest EMT prolongs the production of neural crest cells by the neural tube, and up-regulates expression of key neural crest transcription factors like Sox10, Snail2 and FoxD3. Our findings suggest an important role for DNMT3B in regulating the length of time during which the neural tube is able to produce migratory neural crest cells, thus affecting the numbers of migrating neural crest cells and the timing of their differentiation.

Results

In a screen for genes up regulated during neural crest development, we identified several epigenetic factors, including the DNA methyltransferase 3B (DNMT3B) (Gammill and Bronner-Fraser 2002; Adams et al. 2008).

DNMT3B is expressed in regions of neural crest formation and migration

As a first step in establishing its functional significance, we examined the expression patterns of DNMT3B transcripts during early stages of chick embryonic development ranging from gastrulation to the formation of neural crest derivatives, focusing on the cranial neural crest. The results show that DNMT3B is expressed in the dorsal neural tube and migratory crest cells (Fig.1). It is initially expressed throughout the

neural tube at stage 8 but becomes restricted to the dorsal neural tube by stage 10. Using HNK-1 staining as a marker for migrating neural crest cells, we found co-localization of DNMT3B with HNK-1positive migrating neural crest cells as well as neural crest derivatives. In addition, DNMT3B also was expressed in the gastrula-stage embryo, with broad expression throughout the neural plate and at the neural plate border where neural crest cells are induced (Fig.1). Since the expression of DNMT3B becomes exclusively expressed in the neural crest territory during the migratory stages, we hypothesize that it plays a crucial role in neural crest migration.

Loss of function of DNMT3B causes prolonged production of neural crest cells from the neural tube, but does not affect neural crest induction

To examine whether DNMT3B played a role in neural crest specification similar to its paralog DNMT3A (Hu et al. 2012), we tested the effects of its loss-of-function on neural crest gene expression. We used fluorescein-tagged antisense morpholino oligonucleotides (MO) to the region overlapping ATG codon to block translation of DNMT3B protein at early stages. MOs plus carrier DNA were injected into one half of embryos at stage 4, with the uninjected side serving as an internal control. Despite the fact that DNMT3B is expressed as early as stage 4, no changes in expression of neural crest markers Sox10 or FoxD3 were noted at stages of neural crest induction (data not shown).

To test whether DNMT3B played a later role in neural crest development, the above experiments were repeated in ovo as the neural folds were elevating during stage 8 (Fig. 2B). Subsequent effects on neural crest production were examined at stage 12, by which time cranial neural crest emigration has ended in control embryos. The effects of DNMT3B knock-down were evaluated by analyzing neural crest and neural tube genes expression. Interestingly, the results suggested that morpholino-mediated knock-down of DNMT3B caused excess and/or prolonged emigration of the neural crest cells. The neural crest specifier genes Sox10 and Snail2 come on shortly before initiation of migration and later are maintained on migrating neural crest cells. In situ hybridization for Sox 10 and Snail2 reveals differences in the patterns of neural crest emigration and/or gene expression between the control and experimental side. Whereas Sox10 or Snail2 positive neural crest cells were observed some distance away from the neural tube on the control side, they appeared to be continuing to emigrate from the morpholino-treated side (Fig. 2A, C, D). Furthermore, we noted no alterations in the time of onset of neural crest emigration (Sup Fig.1).

To demonstrate morpholino specificity, control morpholino was injected in a similar fashion as function-blocking morpholino. These control embryos displayed equivalent migratory patterns on both sides, consistent with the fact that emigration of cranial neural crest cells had ceased by stage 12 (Fig. 2A, C, D). To further demonstrate specificity, co-electroporation of a second DNMT3B morpholino different in sequence than the first morpholino produced an identical phenotype (Fig. 2A).

To definitively test the effects of DNMT3B knock-down on the time course of neural crest emigration, we labeled neural tubes with the lipophilic dye, DiI, at time points after neural crest cell emigration had concluded in the head (stage 12). Normally, cranial neural crest cells emigrate from the neural tube for 8 to 16 hours, depending upon the exact axial level, with the last cells emigrating at midbrain levels by the 14-15 somite stage (stage 11). Accordingly, when embryos treated with control morpholinos were labeled with DiI at stage 12, DiI label remained within the cranial neural tube (Fig.2E n = 7/7), with no DiI labeled neural crest cells observed migrating at the level of the midbrain or rostral hindbrain. In contrast, in DNMT3B-MO treated embryos, DiI-labeled migrating neural crest cells continued to emigrate from the neural tube at the midbrain and rostral hindbrain levels on the morpholino-injected side (Figure 2E; n = 4/9 embryos). A few DiI-labeled cells also were noted on the contralateral side. These likely represent ones generated from the morpholino-treated side that crossed the midline, given that approximately 20% of neural crest cells “cross” to the opposite side (McKinney et al. 2013). These results definitively show that DNMT3B morpholino-treated neural tubes continue to produce cranial neural crest cells on the injected side well beyond the time neural crest emigration normally had ceased in control embryos.

Multiplex analysis reveals that loss of DNMT3B up-regulates neural crest specifier genes, while down-regulating dorsal neural tube genes

In order to understand global changes in gene expression caused by DNMT3B knock-down, we performed Nanostring analysis to monitor and quantify 73 transcripts including genes expressed in the neural crest, neural tube, neural plate, neural plate border placodes, nonneural ectoderm, and those involved in cell proliferation and cell death. Each DNMT3B knockdown embryo was analyzed at stage 12, by comparing the morpholino electroporated side to the uninjected side of the same embryo. Because DNMTs are thought to inhibit transcription by methylating the promoter region of target genes, we were particularly interested in genes that were up-regulated as a consequence of down-regulating DNMT3B, as these represent potential direct targets. Interestingly, the results show that neural crest specifier genes Sox9, Sox10, Snail2, and FoxD3 were all up-regulated as a result of DNMT3B knock-down (Fig. 3A). In contrast, the dorsal neural tube gene Wnt3A and Type I cadherin Ncad were both down-regulated. Cell proliferation was unchanged as indicated by the PCNA marker. This further supports the possibility that the prolonged emigration of neural crest cells after DNMT3B knock-down occurs at the expense of dorsal neural tube cells. To verify changes in Wnt3A expression, we performed in situ hybridization and indeed observed loss of Wnt3A mRNA expression on the DNMT3B morpholino-treated side of the neural tube (Fig. 3B). In contrast, expression of neural tube genes Sox2 and Sox3 were not affected at stage 12.

Loss of DNMT3B results in extra migratory neural crest cells

To examine if the prolonged emigration of neural crest cells upon loss of DNMT3B results in more migratory neural crest cells, we collected embryos at later stages and examined the expression of HNK1 epitope, a marker for migratory neural crest cells. When compared to the control side of each embryo, the DNMT3B knockdown side had many more neural crest cells as shown in both whole mount embryos and in transverse sections (Fig. 4A, 4B). There was no apparent increase in cell death between the control and experimental side of the embryos, as assayed by Caspase 3 staining as a marker (data not shown). Similar to stage 12, excess neural crest cells were noted on the DNMT3B knockdown side at stage 13 (Fig.4C).

Loss of DNMT3B results in premature differentiation of the trigeminal ganglia

To examine later effects of DNMT3B knock-down, embryos were stained with Tuj1 as a marker of neuronal differentiation in the trigeminal ganglia. Surprisingly, we observed premature differentiation of trigeminal neurons and early condensation of the ganglion on the DNMT3B morpholino-treated side of the embryo (Fig. 5). Whereas neuronal differentiation was just beginning on the uninjected side or in control morpholino treated stage 13 embryos, we observed a well-differentiated and condensed trigeminal ganglia with obvious ophthalmic and maxillo-mandibular lobes on the DNMT3B morpholino treated side.

Discussion

De novo DNA methylation may be one of the main epigenetic marks used for cell fate restriction of progenitor cells during cell fate differentiation. The paralogues DNMT3A and DNMT3B both have been implicated in de novo DNA methylation and have some overlapping functions. However, they also seem to play distinctive roles during development. This is evidenced by the observation that DNMT3A-null mice die several weeks after birth, whereas DNMT3B-null mice are nonviable and embryos exhibit severe defects including rostral neural tube defects and growth impairment (Okano et al. 1999). Moreover, our recent work in chick embryos shows that DNMT3A plays an important role during neural crest specification by acting as a molecular switch mediating the neural tube-to-neural crest fate transition (Hu et al. 2012), whereas DNMT3B lacks a function at this stage of development. DNMT3A promotes neural crest specification by repressing, via promoter DNA methylation, neural genes like Sox2 and Sox3 in the neural crest territory. These data provide insights into the mechanisms that determine whether a cell becomes part of the central nervous system or peripheral nervous system. On the other hand, mutations in human DNMT3B result in ICF (immunodeficiency-centromeric instability-facial anomalies) syndrome, in which patients exhibit facial abnormalities (Jin et al. 2008), suggesting a defect related to abnormal neural crest development.

The present results demonstrate the necessity of de novo DNA methylation, exerted by DNMT3B, for proper timing of the cessation of neural crest emigration from the dorsal

neural tube at cranial levels. A recent report in mice using neural crest-specific conditional deletion of DNMT3B failed to detect obvious defects in neural crest migration or differentiation and morphogenesis into craniofacial and cardiac structures (Jacques-Fricke et al. 2012). One possibility for the difference between these findings in different species is that the neural crest defect obtained in DNMT3B mutant mice may be due to a requirement for this protein in neighboring cell types. Alternatively, this may reflect a species difference. Chick lacks DNMT3L, which is present in mouse. Since DNMT3A and 3B are paralogues, it may not be surprising that each paralogue assumed slightly different roles in different species. In chick, we find that DNMT3A and 3B are not redundant to one another during neural crest development, but they may be different and somewhat overlapping in the mouse. Although DNMT3B null mice have mostly normal neural crest development, Jacques-Fricke and colleagues do describe ectopic migrating neural crest cells dispersed dorsal to the normal neural crest streams (Jacques-Fricke et al. 2012). This is similar to the prolonged emigration of neural crest cells we observed in our DNMT3B MO treated chick embryos, which results in abnormally migrating neural crest cells. However, this may be a less obvious phenotype in the null mice, since it is not possible to compare control and experimental sides in the same embryo in mice as it is in chick. Finally, DNMT3B may be required in mouse neural crest development prior to the onset of Wnt1-driven cre expression, resulting in a less obvious phenotype.

In addition to de novo DNA methyltransferases, other epigenetic regulators such as histone demethylases and histone deacetylases have also been shown to play a crucial role

regulating the timing of neural crest specification or migration. Histone demethylases such as members of the Jumonji family revert histone methylation (Tan et al. 2008). In neural crest development, histone demethylase of the Jumonji family JmjD2A (also known as KDM4A) is discovered to regulate neural crest specification (Strobl-Mazzulla et al. 2010). JmjD2A is expressed in the neural crest territory during neural crest specification and knocking down JmjD2A causes dramatic loss of neural crest specifier genes such as Sox10, Snail2, FoxD3, etc. In vivo ChIP assays reveal direct interaction of JmjD2A with Sox10 and Snail2 promoter regions (Strobl-Mazzulla et al. 2010). JmjD2A is required to demethylate Sox10 and Snail2 at the proper time and place to allow neural crest specification to take place.

Moreover, histone deacetylase (HDAC) repression complex plays an essential role in regulating neural crest migration. Premigratory neural crest cells from the dorsal neural tube undergo an epithelial to mesenchymal transition to gain migratory property and travel to distant parts of the body. The transcriptional repressor Snail2 has been reported to directly repress the adhesion molecule Cadherin6B in premigratory neural crest cells (Hatta et al. 1987; Nakagawa and Takeichi 1995; Taneyhill et al. 2007). Epigenetic regulation has been shown to play a critical underlying molecular role in this repression (Strobl-Mazzulla and Bronner 2012b). In particular, an interaction between PHD12, a member of the histone deacetylase complex, and Snail2 makes it possible to recruit the repressive complex Sin3A/HDAC to Cad6B promoter region and as a result turn off Cad6B transcription via histone deacetylation to allow neural crest cells to gain migratory property (Strobl-

Mazzulla and Bronner 2012b). Overall, epigenetic regulators influence neural crest formation throughout different temporal time points.

One of the main questions in vertebrate development is to understand what regulates the spatial and temporal progression of the genetic program underlying neural crest development in such an exquisite manner. Our results in avian embryos suggest that *de novo* DNA methylation, exerted by both DNMT3A and DNMT3B, plays a dual role in neural crest development. First, DNMT3A appears to limit the spatial boundary between neural crest versus neural tube progenitors, repressing the expression of neural marker in the neural crest forming territory. Second, DNMT3B appears to restrict the temporal window during which the neural crest cells emigrate from the dorsal neural tube. Thus, interfering with DNMT3A or 3B results in craniofacial problems, but each appears to primarily function during a different temporal window of neural crest development.

Materials and methods

Embryos

Fertilized chicken eggs were incubated at 37°C to desired stages.

In situ hybridization

Dioxigenin-labeled RNA probes were made from cDNA plasmids or ESTs of DNMT3B,

Sox10, Snail2, Wnt3A, Sox2, and Sox3. Embryos were fixed with 4% paraformaldehyde, washed with PBS/0.1% Tween, dehydrated in MeOH, and stored at -20C. Whole mount chick in situ hybridization was performed according to the methods in (Acloque et al. 2008); Wilkinson 1992). Embryos were imaged and subsequently sectioned at 14-16 μm .

Immunohistochemistry

Anti-TuJ1 (Covance) was used and diluted 1:250 and anti-HNK1 was diluted 1:10. Secondary antibodies against the primary antibody subtype were conjugated to Alexa Fluor 488, 568, or 350 dyes (Molecular Probes). Images were taken on a Zeiss Axioskop2 plus fluorescence microscope.

In ovo electroporation

Embryos were electroporated at stage 8 as described in (Sauka-Spengler and Barembaum 2008) using DNMT3B MO1 (over ATG codon): CGAGGCTCGTTACCATGCTCATCGC and DNMT3B MO2 (upstream of ATG): GAACGGAGTGATGACAATGATACCT. DNMT3B MOs or Control MOs were introduced into the open neural tube at stage 8. A charge was applied to transfect the morpholino into the right side of the neural tube. The embryos were then sealed and incubated at 37°C until they reach the indicated stage of analysis.

NanoString nCounter

Half dorsal neural folds of DNMT3B MO treated embryos were dissected in lysis buffer

(Ambion RNAqueous-Micro Isolation kit) at St.12. RNA lysates were hybridized to the probe set and incubated overnight at 65°C, washed and eluted according to nCounter Prep Station Manual and counted by nCounter Digital Analyzer.

Acknowledgments: We thank Drs. T. Sauka-Spengler, M. Simoes-Costa and M. Barembaum for helpful discussions. This work was supported by F31DE021643 and 5 T32 GM07616 to N.H. and HD037105 and DE16459 to M.E.B.

Figures and Figure Legends

Figure1

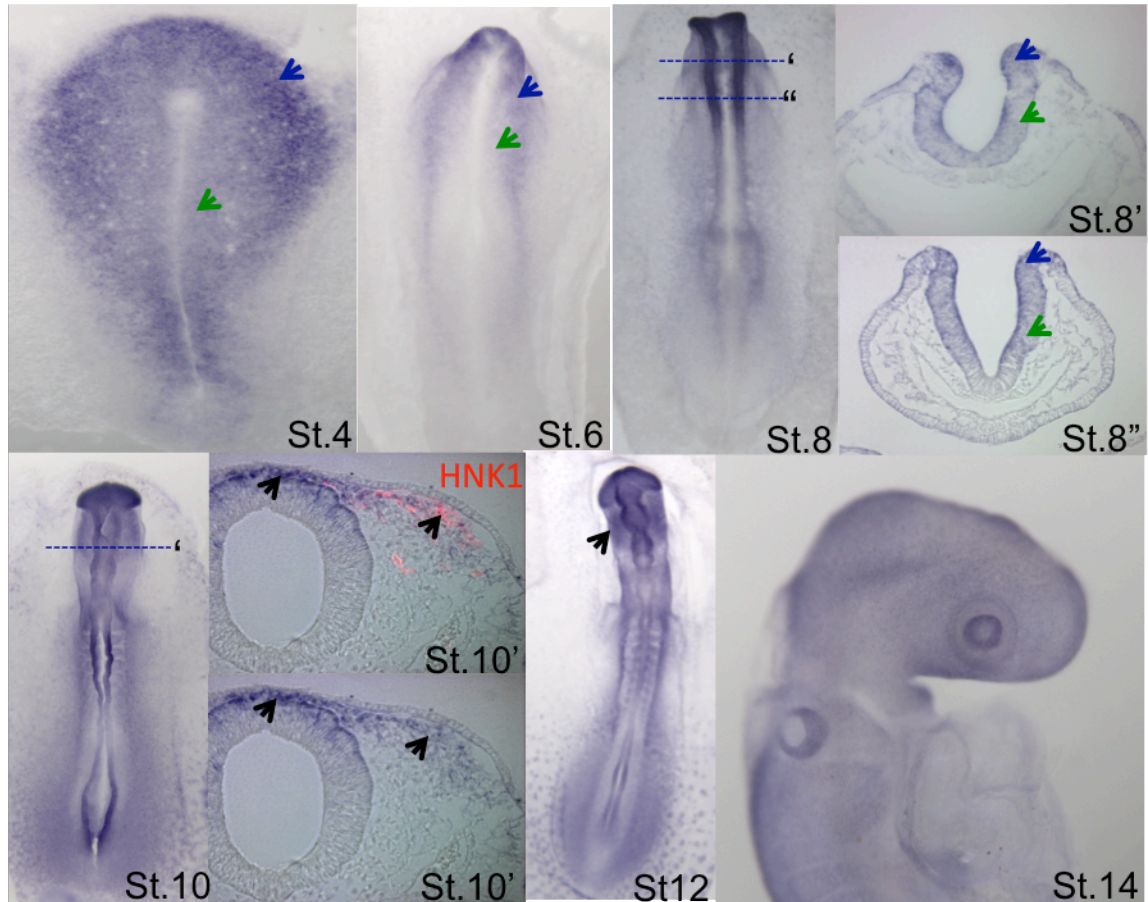


Fig. 1 DNMT3B is expressed in the neural crest territory at the proper time and stage.

Expression pattern of DNMT3B in St.4-14 chick embryo by in situ hybridization. During St.4-8, DNMT3B is expressed throughout the neural plate (green arrowhead) and neural plate border (blue arrowhead). During the migratory stages (St. 10-11), expression of DNMT3B is restricted to the dorsal neural tube and migratory neural crest cells (black arrowhead). Using HNK-1 staining (red) as a marker for migrating neural crest cells, we

found co-localization of DNMT3B with HNK-1positive migrating neural crest cells as well as neural crest derivatives. DNMT3B is not expressed at St.14. Dashed line shows the level of cranial region being cross-sectioned.

Figure 2

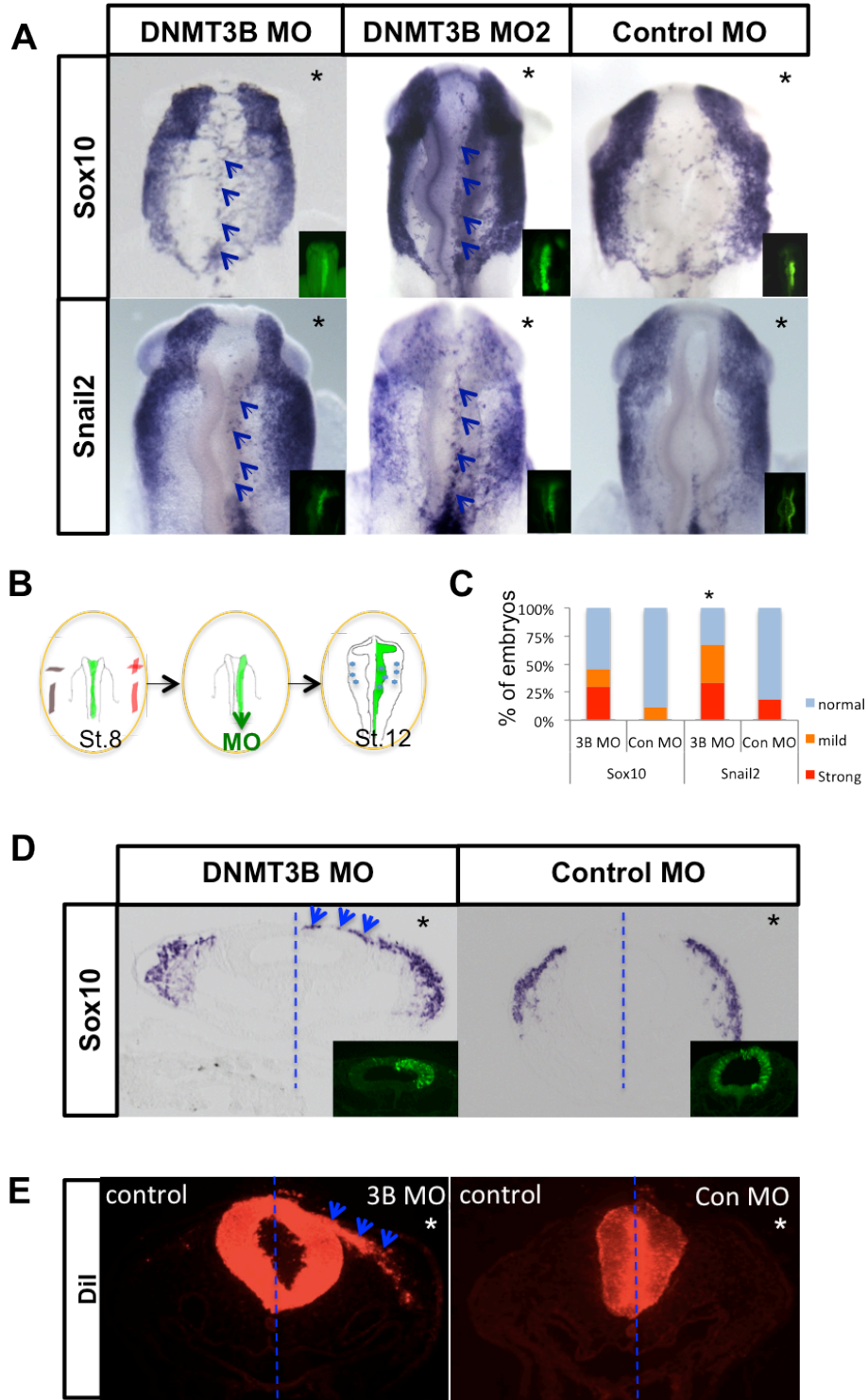


Fig. 2 Loss of function of DNMT3B causes prolonged migration of neural crest cells using Sox10, Snail2 and Dil as markers. (A) Two morpholinos against DNMT3B (MO1&MO2, FITC-inset) caused prolonged emigration of neural crest cells. The right side of each neural tube was electroporated with DNMT3B MO or control morpholino. Cranial neural crest cells marked by Sox 10 or Snail2 appear to keep emigrating from the neural tube for longer time periods (arrow) on the side electroporated with DNMT3B MO when compared to their internal control side. Embryos electroporated with control morpholino appear normal. Asterisk marks the side of morpholino injection. **(B)** Schematic graph summarizing in ovo electroporation. Morpholino was introduced at St.8 and electroporated onto the right side of the neural tube in each embryo. Embryos were incubated until St.12, at which time neural crest cells at this axial level have normally ceased emigration. **(C)** Quantitation of percentage of DNMT3B MO or Control MO treated embryos with either strong or mild prolonged emigration phenotype using Sox10 or Snail2 as markers. Expression was compared between MO treated side and control side of the same embryo. Sox10, n=21 with DNMT3B MO, n=9 with Control MO; Snail2, n=18 with 3B MO, n=11 with Control MO. Asterisk on graph means $P < 0.05$ using Chi-square contingency test. **(D)** Transverse sections of embryos treated with DNMT3B MO versus Control MO. Sox10 positive neural crest cells continue to emigrate out of the neural tube (arrows) on DNMT3B MO treated side compared with the internal control side. In Control MO treated embryos, emigration has ceased on both sides. FITC-inset shows morpholino incorporation. Asterisks mark side of MO injection. **(E)** Embryos were electroporated with MO at St.8

into the right side of the neural tube (asterisk) and DiI was used to label the entire neural tube during early St.12, by which time emigration has ceased in normal embryos. Embryos were collected and sectioned at St.13. Prolonged emigration was observed (arrows) on the side treated with DNMT3B MO while no emigration was observed on the uninjected side or Control MO treated side. 4/9 embryos treated with DNMT3B MO and 0/7 embryos treated with Control MO have prolonged emigration phenotype.

Figure3

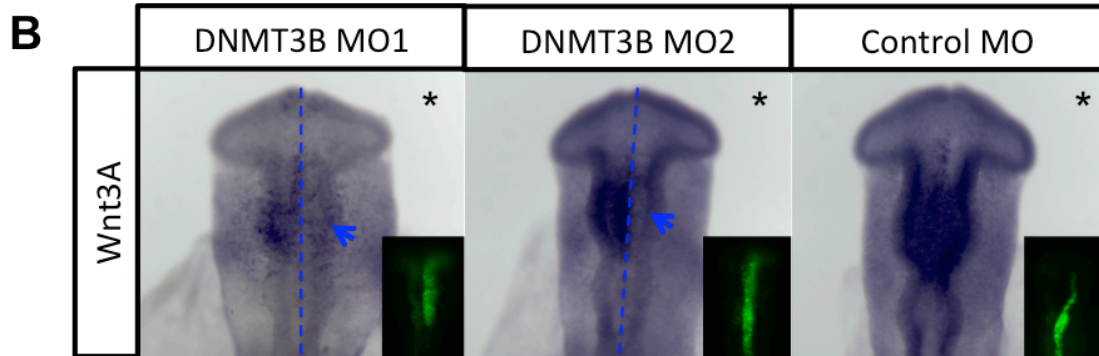
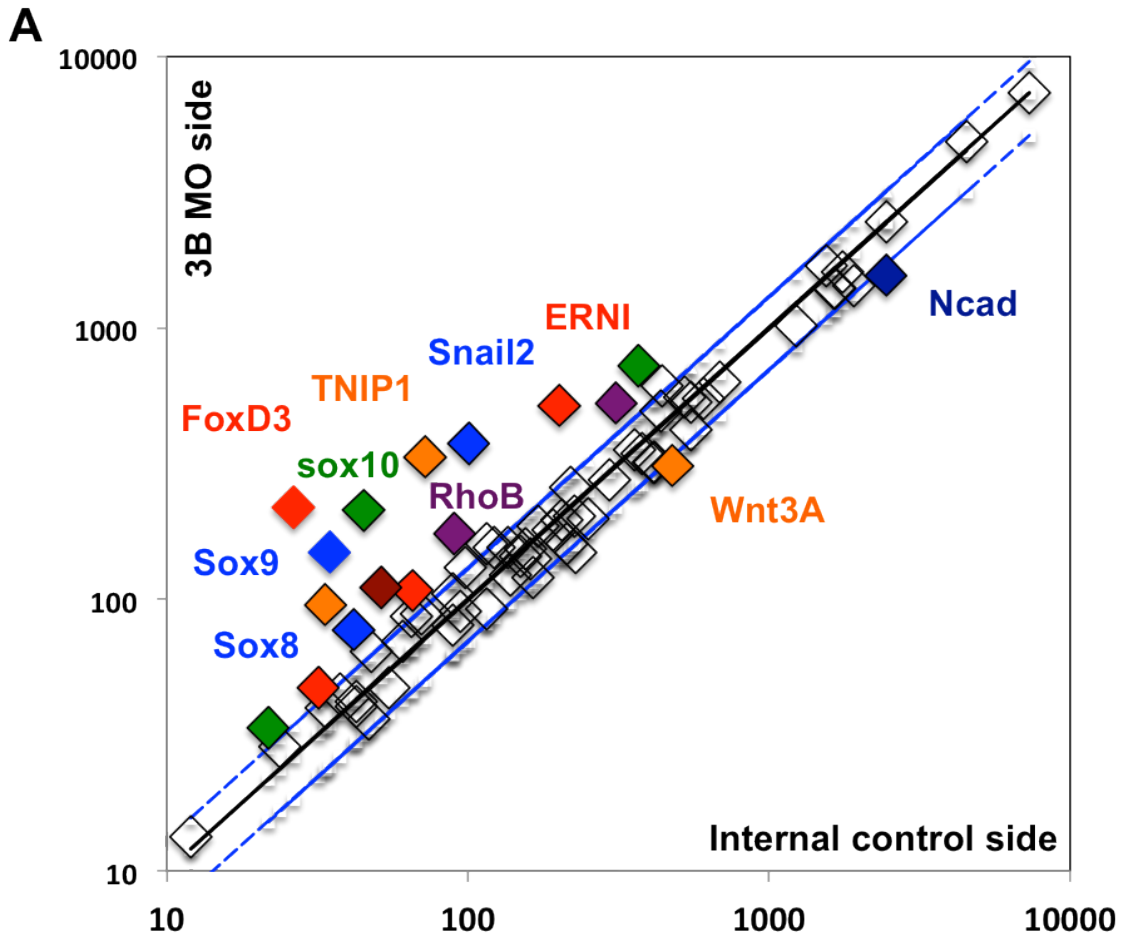


Fig. 3 Neural crest specifier genes such as Snail2, Sox10 and FoxD3 are up-regulated upon loss of DNMT3B as identified using multiplex Nanostring analysis and concomitantly, dorsal neural tube gene Wnt3A is down-regulated. (A) Nanostring analysis reveals genes up-regulated (above diagonal lines) and down-regulated (below diagonal lines) by DNMT3B knock-down. Injected side of DNMT3B MO treated embryos shows >25% up-regulation of neural crest specifier genes Sox10, Sox9, Snail2 and FoxD3; there was >25% down-regulation of dorsal neural tube gene Wnt3A and Type I cadherin Ncad. (n=5) **(B)** In situ data further verifies that loss of DNMT3B causes reduction of dorsal neural tube gene Wnt3A when compared to the internal control side and to control embryos, at the time window in which prolonged emigration of the neural crest cells were observed in DNMT3B MO treated embryos. 10/12 embryos treated with DNMT3B MO and 1/6 embryos treated with Control MO show reduction of Wnt3A.

Figure4

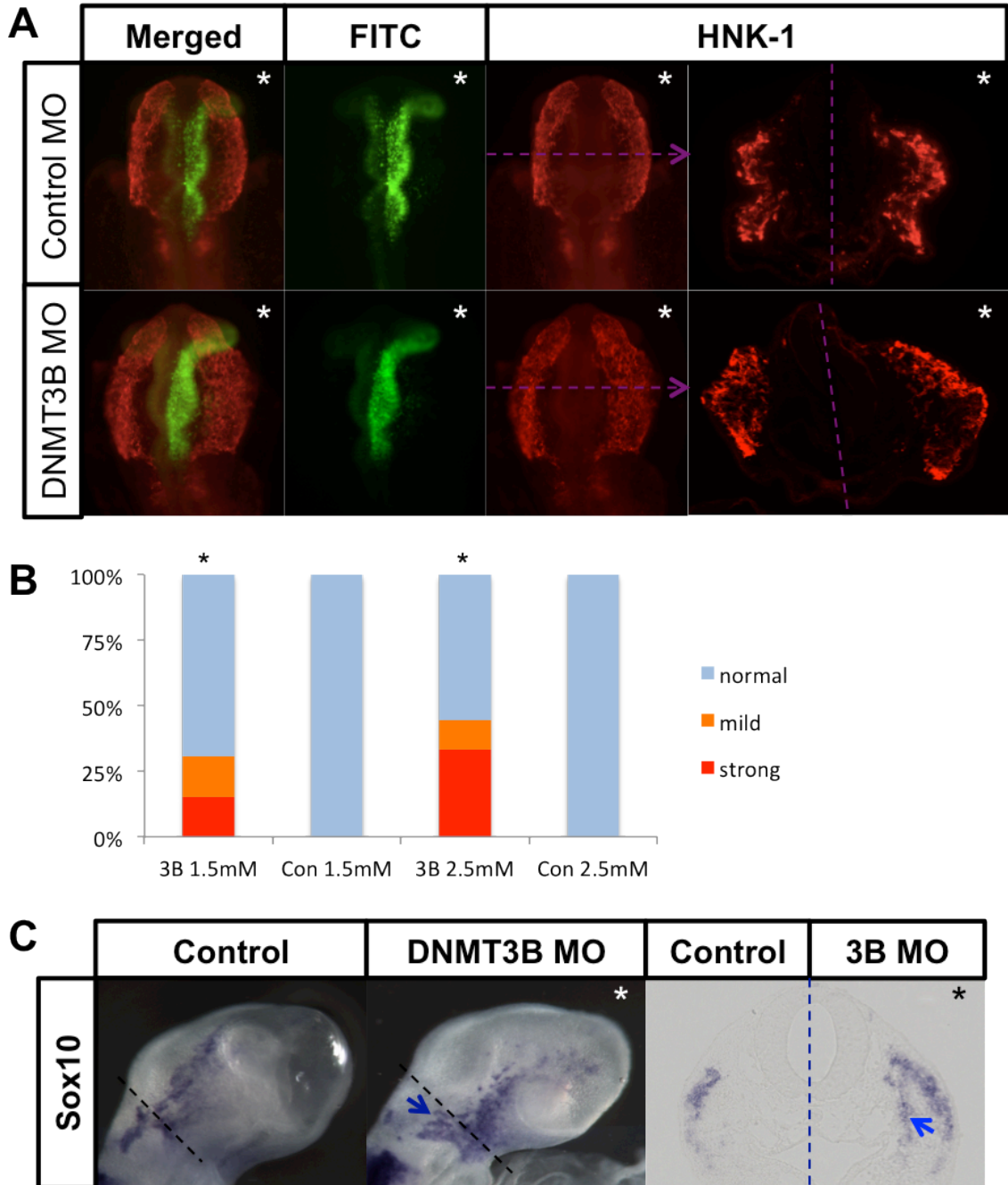


Fig. 4 DNMT3B knock-down results in extra migratory neural crest cells. (A) Embryos electroporated with DNMT3B MO or Control MO were immunostained with anti-HNK1 antibody and sectioned. DNMT3B MO injected side of the embryo (asterisk) show increased number of HNK1 positive neural crest cells in both whole mount and transverse section view. **(B)** Quantitation of percentage of DNMT3B MO (3B) or Control MO (Con) (in mM concentration) treated embryos with either strong or mild phenotype of generating extra migrating neural crest cells on the electroporated side versus internal control side. n=13 for 3B 1.5mM, n=8 for Con 1.5mM, n=9 for 3B 2.5mM, n=8 for Con 2.5mM. Asterisk on graph means $P < 0.05$ using Chi-square contingency test. **(C)** Embryos collected at St.13 continue to exhibit extra neural crest cells (arrow, n=5/7) using Sox10 as a marker on the DNMT3B MO treated side (asterisk) versus the control side in both whole mount and section view.

Figure5

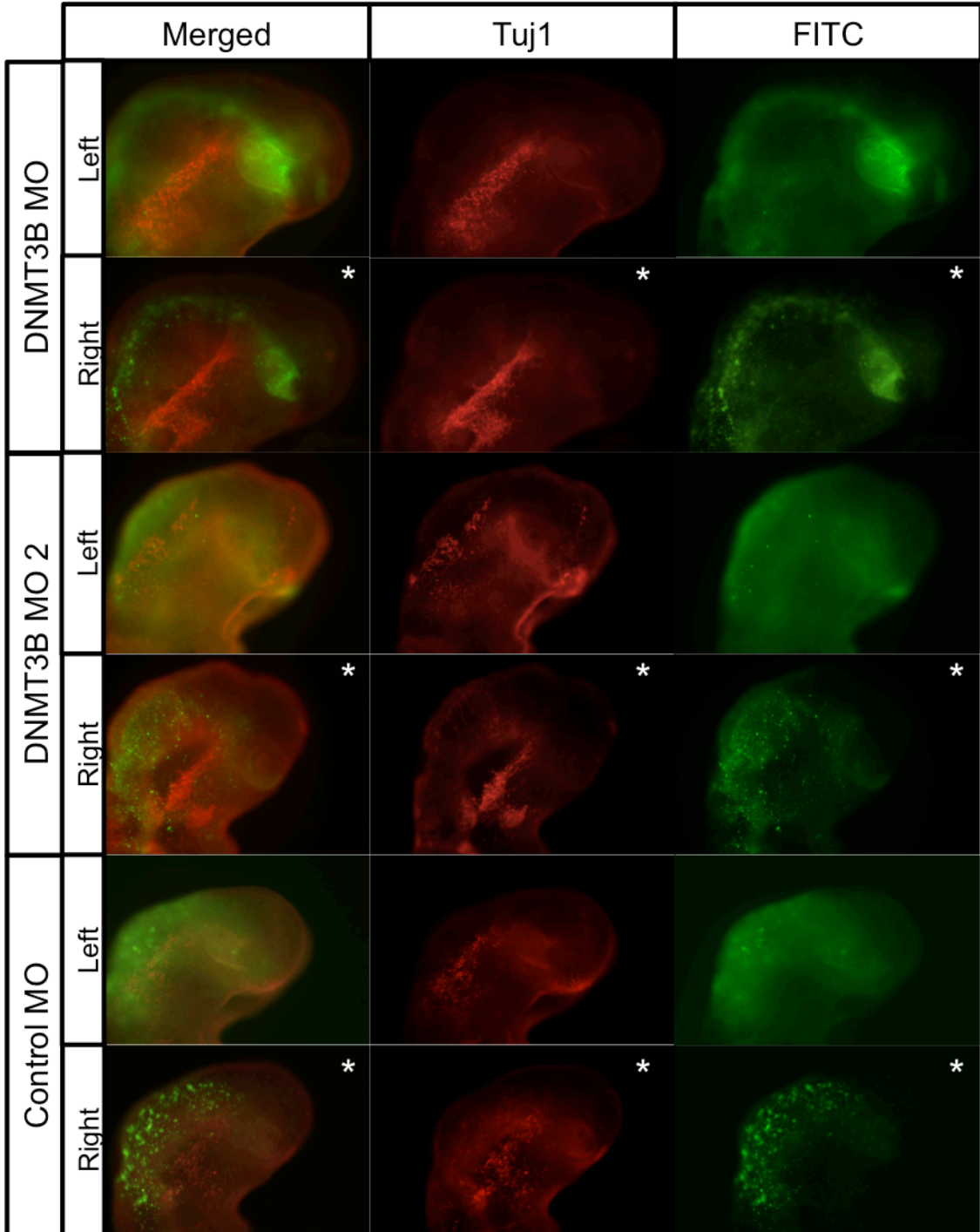


Fig. 5 DNMT3B knock-down results in premature differentiation of the trigeminal ganglia.

The right half (asterisk) of each embryo was electroporated with DNMT3B MO, DNMT3B MO2 or Control MO (FITC) and Tuj1 was used as a marker for neuronal differentiation in the forming trigeminal ganglia. Premature differentiation of the trigeminal ganglia (well-condensed ganglia with both ophthalmic, maxillo-mandibular lobes) was observed in DNMT3B MO treated side of the embryo when compared to control side that shows normal ganglion aggregation. 4/6 embryos treated with DNMT3B MO and 0/6 embryos treated with Control MO show premature differentiation of the trigeminal ganglia.

Figure S1

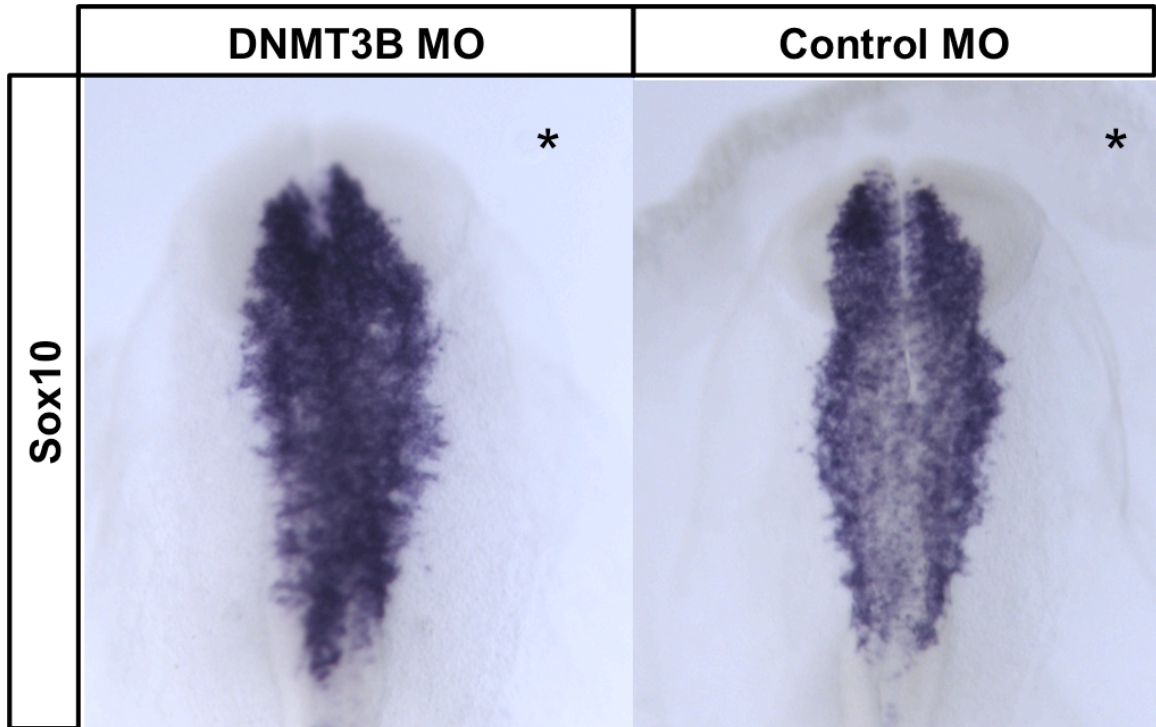


Fig. S1 Knockdown of DNMT3B does not affect early migrating neural crest cells.

Right side (asterisk) of each neural tube was electroporated with DNMT3B MO or control morpholino during St.8 and embryos were scored at early St.10, the onset of neural crest migration. Cranial neural crest cells marked by Sox10 seem to be normal between control and injected side of each embryo.

Chapter 4

Conclusions and future perspectives

Summary and Significance

In this thesis, I have dissected the roles of DNMT3A and DNMT3B in neural crest development in developing embryos. During neural crest specification, DNMT3A is expressed in the region where neural crest cells originate. Its loss of function leads to ectopic upregulation/expansion of neural genes Sox2 and Sox3 in the dorsal neural tube (neural crest forming region) at the expense of neural crest makers such as Snail2, Sox10 and FoxD3, in a cell autonomous manner. Using Nanostring multiplex analysis, we show concomitant upregulation of neural genes and down-regulation of neural crest genes in the same embryo after treatment with DNMT3A morpholino. We then confirmed that ectopic expression of neural genes such as Sox2 in the neural crest region is sufficient to inhibit neural crest markers Sox10, Snail2 and FoxD3. In vivo ChIP further demonstrates that DNMT3A specifically associates with CpG islands in the Sox2 and Sox3 promoter region, resulting in methylation leading to their repression. Therefore, during neural crest specification, DNMT3A first directly represses neural genes Sox2 and Sox3 in the dorsal neural tube, facilitating expression of neural crest markers Snail2, Sox10 and FoxD3. These data show that DNMT3A functions as a molecular switch mediating neural tube to neural crest fate transition.

During neural crest EMT, DNMT3B expression is restricted to the dorsal neural tube and migratory neural crest region. Its loss of function extends the time window of neural crest emigration, which results in an excess of migratory neural crest cells using

Sox10, Snail2, and FoxD3 as markers. In the meantime, there is a loss of the dorsal neural tube gene, Wnt3A, indicating that the excess neural crest cells formed at the expense of neural tube cells. In later stages, this is manifested in the premature neural differentiation of the trigeminal ganglia. The effect is particularly severe in the maxillo-mandibular lobe of the trigeminal ganglia, the lobe that is heavily contributed by cells of neural crest origin. The data suggest that DNMT3B plays an important role in regulating the duration of neural crest emigration and the timing of their differentiation into craniofacial ganglia.

This thesis project identified key molecular players necessary for neural crest cell fate specification and neural crest EMT. My results show that epigenetic regulation at the level of DNA modifications is a novel mechanism for regulation of neural crest development. Second, the data show that de novo DNMTs have a specific role at specific times in making key developmental decision for the embryo. Rather than acting ubiquitously, these enzymes appear to be exquisitely controlled in space and time. Third, I demonstrate that negative input is essential for promoting neural crest cell fate. In this case, Sox2/Sox3 must be turned off by DNMT3A in order to achieve a positive outcome of specifying neural crest cells. Fourth, my results provide the first molecular evidence that DNMT3B is involved in the termination of neural crest EMT. This promises to open future studies regarding factors that stop the generation of migrating neural crest cells from the dorsal neural tube. Finally, our work provides important insights into explaining the long-standing mystery of what makes a precursor cell part of the central nervous system versus peripheral nervous system.

In the future, these findings have implications for stem-cell therapy, by giving clues as to how to engineer stem or iPS cells to become neural crest cells. For example, ongoing research is attempting to define the conditions needed to induce iPS cells to neural crest derivatives. Our results showing that DNMT3A is important for converting CNS cells to neural crest cells will be useful in defining the steps needed to reprogram such iPS cells and then use them to repair human diseases.

Future Perspectives

From this study, I now propose some possible future directions that stem from this thesis to further dissect the molecular mechanisms of de novo DNA methylation in neural crest and neural crest related development.

Exploring epigenetic regulation in placode development

Given these results, we speculate that DNMTs may have important functions in the embryo at different places and times. One possible future direction is to examine the roles of these enzymes in placode development. Placodes are discrete, thickened regions of the head ectoderm that invaginate from the surface ectoderm and migrate into the adjacent mesenchyme. They form in pairs on both sides of the neural tube and contribute to the formation of the olfactory epithelium, trigeminal ganglia, lens of the eye, and structures in

the ear. Placode and neural crest precursors both originated from the neural plate border during gastrula stage. Later, neural crest cells occupy the dorsal neural tube region while placode cells reside outside of the neural plate as patches of thickened ectoderm. My preliminary data indicate that DNMT3A may be involved in olfactory placode formation. Knocking down DNMT3A at St.5 leads to loss of olfactory tissues at St.8 (Figure1). It will be interesting to characterize the involvement of DNMT3A in olfactory placode development and compare/contrast its mechanism of regulation with neural crest development. To do this, we would first characterize the expression of DNMT3A in the olfactory placode region to determine whether it co-localizes with olfactory placode markers. Loss of function experiments will then be performed and data will be collected at different stages of olfactory formation to examine the influence of DNMT3A on olfactory development. By in situ hybridization and immunostaining for olfactory placode markers we might be able to find potential direct targets. To further confirm a possible interaction we would perform ChIP followed by qPCR to identify a possible direct regulatory relationship between DNMT3A and genes involved in olfactory placode development.

Another possible direction is to investigate the roles of DNMT3A and/or 3B in trigeminal ganglia formation. The trigeminal ganglion is derived from a mixture of cells originating from both neural crest and placodes. My preliminary data shows that loss of DNMT3A and 3B in the neural crest cells eventually leads to premature ganglion formation. Depending on the stages examined, the maxillo-mandibular lobe appeared to be more severely affected by the loss of DNMT3A and 3B than the ophthalmic lobe (Figure

2). This is not surprising because the maxillo-mandibular lobe contains more of a neural crest contribution than the ophthalmic lobe. In the future, it will be interesting to examine the roles of DNMT3A and/or DNMT3B in the trigeminal placode. This could be done by specifically knocking down DNMT3A and/or 3B in the trigeminal placode cells and examining the formation of the trigeminal ganglion. This study would allow us to distinguish the differential contribution of DNMTs in neural crest cells versus placode cells, and how this ultimately affects the formation of the trigeminal ganglia.

Identification of co-factors of DNMTs in neural crest development

In chapter 2, we show that loss of DNMT3A maintains Sox2 and Sox3 expression in the dorsal neural folds, and this in turn leads to repression of neural crest specifier genes. However, it still remains unclear how DNMT3A's effect is restricted only to the dorsal neural fold region during neural crest specification. Identifying co-factors would inform about how spatial and temporal specificity is conferred by de novo DNA methylation. Although the mechanism by which DNMT3A is recruited to the promoter region of target genes is unknown, they have been shown to interact with numerous factors on transcription factor arrays (Hervouet et al. 2009). Although these have yet to be validated, particularly in vivo, this list includes some neural plate border and neural crest specifier genes like Msx1, tfAP2a, Id2 and Myc. Thus, it is intriguing to speculate that DNMT3A may be recruited to the promoter region of neural genes by some of these transcription factors that are selectively expressed in the neural crest forming domain. To test the possible interactions

of these transcription factors with DNMT3A, dorsal neural folds of embryos at stages of neural crest induction and specification can be collected for co-IP analysis to find evidence of *in vivo* binding. To visualize protein interactions within living cells, Bimolecular fluorescence complementation (BiFC) can be used to capture DNMT3A interacting with its co-factors. For this, full length DNMT3A coupled to the Venus N-terminus domains, and neural crest co-factors of interest coupled to the Venus C-terminus domains can be transfected into chick fibroblasts and an interaction would be visible by a green fluorescent Venus signal since it is only detectable when two proteins directly interact with each other.

Identification of novel downstream targets of DNMTs in neural crest development

The availability of high throughput technologies such as RNA-seq and ChIP-seq, it will be of great benefit for the identification of novel regulators in neural crest development. For example, ChIP-seq can be used to map the genome-wide binding of DNMTs during different stages of neural crest development to obtain genome scale information of the downstream targets regulated by DNMTs as well as which positions DNMTs bind *in vivo*. To pinpoint the methylated sites, this experiment can be further modified to incorporate bisulfite treatment that converts unmethylated cytosine to uracil while leaving methylated cytosine unchanged. By comparing sequence data from treated and untreated DNA, methylation sites can be identified. A good quality antibody is crucial to perform such types of experiments in order to get high signal and low background.

Alternatively, morpholino knockdown followed by RNA-seq is another possibility to find novel targets. For this, embryos would be treated with DNMT3A and/or 3B morpholino on one side, leaving the other side as internal control. Neural crest tissues from morpholino treated sides and control sides can be dissected, sequenced, compared for changes that occur in novel genes that are not included in our Nanostring probet set, which I described earlier. From our previous study we know that DNMT3A mediates neural versus neural crest cell fate choice and DNMT3B regulates neural crest EMT. Therefore, changes in genes involved with cell fate choice and EMT will be particularly interesting to us as they are very likely to be direct targets. Although this alternate experiment would not isolate direct binding targets, it is still informative in terms of identifying potential novel targets of DNMTs. These candidates will be further validated in vivo for expression at proper times and places and their specific functions in neural crest development will also be further studied in chick. From this study, we hope to uncover novel genes involved in neural crest development and bring new additions to our current neural crest gene regulatory network.

Cis-regulatory analysis to identify DNMT3A and DNMT3B enhancers

Since DNMTs play a crucial and specific role in neural crest development and their tissue specific expression changes considerably during chick developmental stages, it would be interesting to dissect the cis-regulatory regions of DNMTs and investigate how their transcription is being controlled. Putative regulatory regions can be cloned into

expression vectors and electroporated in chick to study their individual expression. Once an enhancer region(s) is narrowed down to its minimal size and still capable of driving expression, mutational studies can be carried out to identify specific functional binding sites in the region. This study will identify the direct regulatory inputs of DNMTs and give us a more global picture of neural crest formation.

Establish direct relationships between DNMT3B and regulatory regions of EMT genes and neural crest specifier genes

From Chapter 3, we concluded that DNMT3B controls the termination time of neural crest EMT and/or maintenance of neural crest specifier expression. One possible mechanism is that DNMT3B represses EMT genes and thus terminates emigration of neural crest cells from the neural tube. Alternatively, DNMT3B may initially affect the maintenance of neural crest specifiers and affects on EMT genes may be the consequence of that. It is also possible that DNMT3B initially effects both EMT genes and neural crest specifier genes. It will be interesting to distinguish these possibilities by performing ChIP followed by qPCR to look at the occupancy of DNMT3B on the promoter regions of EMT genes and neural crest specifier genes.

Taken together, we are just beginning to understand the contributions of epigenetic regulatory mechanisms in neural crest development. This is an important and open area for future investigations. Understanding the normal mechanisms of neural crest development

will contribute to the discovery of therapeutic treatments on birth defects, cancers, and other diseases associated with aberrant neural crest cells.

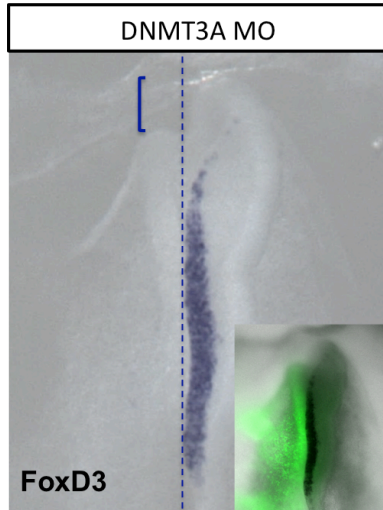
Figure. 1

Figure1. Preliminary data indicates that DNMT3A is involved in olfactory placode formation. Knocking down DNMT3A during St.5 leads to loss of olfactory tissues (bracket) at St.8. FITC inset shows DNMT3A MO was introduced to the left side of embryo, leaving the right side as internal control.

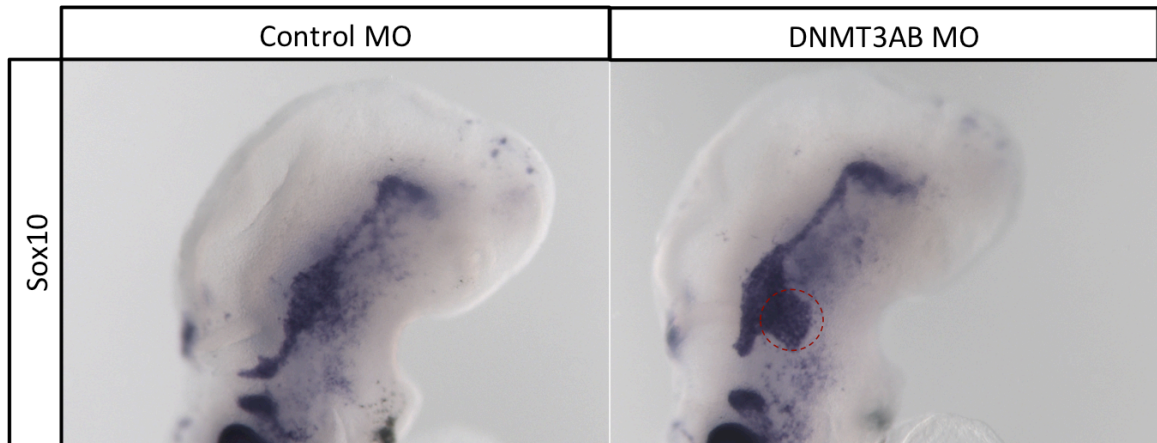
Figure. 2

Figure2. Preliminary data show loss of DNMT3A and 3B in neural crest cells results in premature formation of the trigeminal ganglion, especially the maxillo-mandibular lobe

(circled in red). Embryos were electroporated with DNMT3A and 3B morpholino into the neural tube at St.8 and examined at St.13/14.

BIBLIOGRAPHY

- Acloque H, Adams MS, Fishwick K, Bronner-Fraser M, Nieto MA. 2009. Epithelial-mesenchymal transitions: the importance of changing cell state in development and disease. *J Clin Invest* **119**: 1438-1449.
- Acloque H, Wilkinson DG, Nieto MA. 2008. In situ hybridization analysis of chick embryos in whole-mount and tissue sections. *Methods Cell Biol* **87**: 169-185.
- Adams MS, Gammill LS, Bronner-Fraser M. 2008. Discovery of transcription factors and other candidate regulators of neural crest development. *Dev Dyn* **237**: 1021-1033.
- Ahola JA, Koivusalo A, Sairanen H, Jokinen E, Rintala RJ, Pakarinen MP. 2009. Increased incidence of Hirschsprung's disease in patients with hypoplastic left heart syndrome--a common neural crest-derived etiology? *J Pediatr Surg* **44**: 1396-1400.
- Akkers RC, van Heeringen SJ, Jacobi UG, Janssen-Megens EM, Francoijs KJ, Stunnenberg HG, Veenstra GJ. 2009. A hierarchy of H3K4me3 and H3K27me3 acquisition in spatial gene regulation in *Xenopus* embryos. *Dev Cell* **17**: 425-434.
- Allan RS, Zueva E, Cammas F, Schreiber HA, Masson V, Belz GT, Roche D, Maison C, Quivy JP, Almouzni G et al. 2012. An epigenetic silencing pathway controlling T helper 2 cell lineage commitment. *Nature* **487**: 249-253.
- Alsdorf R, Wyszynski DF. 2005. Teratogenicity of sodium valproate. *Expert Opin Drug Saf* **4**: 345-353.
- Altun G, Loring JF, Laurent LC. 2010. DNA methylation in embryonic stem cells. *J Cell Biochem* **109**: 1-6.
- Bajpai R, Chen DA, Rada-Iglesias A, Zhang J, Xiong Y, Helms J, Chang CP, Zhao Y, Swigut T, Wysocka J. 2010. CHD7 cooperates with PBAF to control multipotent neural crest formation. *Nature* **463**: 958-962.
- Barembaum M, Bronner-Fraser M. 2005. Early steps in neural crest specification. *Semin Cell Dev Biol* **16**: 642-646.
- Barnett C, Yazgan O, Kuo HC, Malakar S, Thomas T, Fitzgerald A, Harbour W, Henry JJ, Krebs JE. 2012. Williams Syndrome Transcription Factor is critical for neural crest cell function in *Xenopus laevis*. *Mech Dev* **129**: 324-338.
- Barski A, Cuddapah S, Cui K, Roh TY, Schones DE, Wang Z, Wei G, Chepelev I, Zhao K. 2007. High-resolution profiling of histone methylations in the human genome. *Cell* **129**: 823-837.
- Basch ML, Bronner-Fraser M. 2006. Neural crest inducing signals. *Adv Exp Med Biol* **589**: 24-31.
- Berger SL. 2007. The complex language of chromatin regulation during transcription. *Nature* **447**: 407-412.
- Bernstein BE, Meissner A, Lander ES. 2007. The mammalian epigenome. *Cell* **128**: 669-681.
- Betancur P, Bronner-Fraser M, Sauka-Spengler T. 2010. Assembling neural crest regulatory circuits into a gene regulatory network. *Annu Rev Cell Dev Biol* **26**: 581-603.
- Bird A. 2007. Perceptions of epigenetics. *Nature* **447**: 396-398.

- Bonn S, Zinzen RP, Girardot C, Gustafson EH, Perez-Gonzalez A, Delhomme N, Ghavi-Helm Y, Wilczynski B, Riddell A, Furlong EE. 2012. Tissue-specific analysis of chromatin state identifies temporal signatures of enhancer activity during embryonic development. *Nat Genet* **44**: 148-156.
- Borgel J, Guibert S, Li Y, Chiba H, Schubeler D, Sasaki H, Forne T, Weber M. 2010. Targets and dynamics of promoter DNA methylation during early mouse development. *Nat Genet* **42**: 1093-1100.
- Bosman EA, Penn AC, Ambrose JC, Kettleborough R, Stemple DL, Steel KP. 2005. Multiple mutations in mouse Chd7 provide models for CHARGE syndrome. *Hum Mol Genet* **14**: 3463-3476.
- Bronner ME, LaBonne C. 2012. Preface: the neural crest--from stem cell formation to migration and differentiation. *Dev Biol* **366**: 1.
- Bronner-Fraser M, Fraser SE. 1988. Cell lineage analysis reveals multipotency of some avian neural crest cells. *Nature* **335**: 161-164.
- Burstyn-Cohen T, Stanleigh J, Sela-Donenfeld D, Kalcheim C. 2004. Canonical Wnt activity regulates trunk neural crest delamination linking BMP/noggin signaling with G1/S transition. *Development* **131**: 5327-5339.
- Cano A, Perez-Moreno MA, Rodrigo I, Locascio A, Blanco MJ, del Barrio MG, Portillo F, Nieto MA. 2000. The transcription factor snail controls epithelial-mesenchymal transitions by repressing E-cadherin expression. *Nat Cell Biol* **2**: 76-83.
- Canon S, Herranz C, Manzanares M. 2006. Germ cell restricted expression of chick Nanog. *Dev Dyn* **235**: 2889-2894.
- Carrozza MJ, Utley RT, Workman JL, Cote J. 2003. The diverse functions of histone acetyltransferase complexes. *Trends Genet* **19**: 321-329.
- Cedar H, Bergman Y. 2008. Epigenetic silencing during early lineage commitment. in *StemBook*, Cambridge (MA).
- Chen T, Li E. 2006. Establishment and maintenance of DNA methylation patterns in mammals. *Curr Top Microbiol Immunol* **301**: 179-201.
- Cheng X, Blumenthal RM. 2008. Mammalian DNA methyltransferases: a structural perspective. *Structure* **16**: 341-350.
- Cheung I, Shulha HP, Jiang Y, Matevossian A, Wang J, Weng Z, Akbarian S. 2010. Developmental regulation and individual differences of neuronal H3K4me3 epigenomes in the prefrontal cortex. *Proc Natl Acad Sci U S A* **107**: 8824-8829.
- Cotney J, Leng J, Oh S, DeMare LE, Reilly SK, Gerstein MB, Noonan JP. 2012. Chromatin state signatures associated with tissue-specific gene expression and enhancer activity in the embryonic limb. *Genome Res* **22**: 1069-1080.
- Creyghton MP, Cheng AW, Welstead GG, Kooistra T, Carey BW, Steine EJ, Hanna J, Lodato MA, Frampton GM, Sharp PA et al. 2010. Histone H3K27ac separates active from poised enhancers and predicts developmental state. *Proc Natl Acad Sci U S A* **107**: 21931-21936.
- del Barrio MG, Nieto MA. 2002. Overexpression of Snail family members highlights their ability to promote chick neural crest formation. *Development* **129**: 1583-1593.
- DeLaurier A, Nakamura Y, Braasch I, Khanna V, Kato H, Wakitani S, Postlethwait JH, Kimmel CB. 2012. Histone deacetylase-4 is required during early cranial neural

- crest development for generation of the zebrafish palatal skeleton. *BMC Dev Biol* **12**: 16.
- Ehrlich M, Sanchez C, Shao C, Nishiyama R, Kehrl J, Kuick R, Kubota T, Hanash SM. 2008. ICF, an immunodeficiency syndrome: DNA methyltransferase 3B involvement, chromosome anomalies, and gene dysregulation. *Autoimmunity* **41**: 253-271.
- Ekwall K. 2005. Genome-wide analysis of HDAC function. *Trends Genet* **21**: 608-615.
- Eroglu B, Wang G, Tu N, Sun X, Mivechi NF. 2006. Critical role of Brg1 member of the SWI/SNF chromatin remodeling complex during neurogenesis and neural crest induction in zebrafish. *Dev Dyn* **235**: 2722-2735.
- Fuks F, Burgers WA, Godin N, Kasai M, Kouzarides T. 2001. Dnmt3a binds deacetylases and is recruited by a sequence-specific repressor to silence transcription. *EMBO J* **20**: 2536-2544.
- Gammill LS, Bronner-Fraser M. 2002. Genomic analysis of neural crest induction. *Development* **129**: 5731-5741.
- . 2003. Neural crest specification: migrating into genomics. *Nat Rev Neurosci* **4**: 795-805.
- Gardiner-Garden M, Frommer M. 1987. CpG islands in vertebrate genomes. *J Mol Biol* **196**: 261-282.
- Gelineau-van Waes J, Heller S, Bauer LK, Wilberding J, Maddox JR, Aleman F, Rosenquist TH, Finnell RH. 2008. Embryonic development in the reduced folate carrier knockout mouse is modulated by maternal folate supplementation. *Birth Defects Res A Clin Mol Teratol* **82**: 494-507.
- Gibney ER, Nolan CM. 2010. Epigenetics and gene expression. *Heredity (Edinb)* **105**: 4-13.
- Goll MG, Kirpekar F, Maggert KA, Yoder JA, Hsieh CL, Zhang X, Golic KG, Jacobsen SE, Bestor TH. 2006. Methylation of tRNA^{Asp} by the DNA methyltransferase homolog Dnmt2. *Science* **311**: 395-398.
- Graham V, Khudyakov J, Ellis P, Pevny L. 2003. SOX2 functions to maintain neural progenitor identity. *Neuron* **39**: 749-765.
- Haberland M, Mokalled MH, Montgomery RL, Olson EN. 2009. Epigenetic control of skull morphogenesis by histone deacetylase 8. *Genes Dev* **23**: 1625-1630.
- Hatta K, Takagi S, Fujisawa H, Takeichi M. 1987. Spatial and temporal expression pattern of N-cadherin cell adhesion molecules correlated with morphogenetic processes of chicken embryos. *Dev Biol* **120**: 215-227.
- He Y, Doyle MR, Amasino RM. 2004. PAF1-complex-mediated histone methylation of FLOWERING LOCUS C chromatin is required for the vernalization-responsive, winter-annual habit in Arabidopsis. *Genes Dev* **18**: 2774-2784.
- Heeg-Truesdell E, LaBonne C. 2004. A slug, a fox, a pair of sox: transcriptional responses to neural crest inducing signals. *Birth Defects Res C Embryo Today* **72**: 124-139.
- Heintzman ND, Hon GC, Hawkins RD, Kheradpour P, Stark A, Harp LF, Ye Z, Lee LK, Stuart RK, Ching CW et al. 2009. Histone modifications at human enhancers reflect global cell-type-specific gene expression. *Nature* **459**: 108-112.
- Hervouet E, Vallette FM, Cartron PF. 2009. Dnmt3/transcription factor interactions as crucial players in targeted DNA methylation. *Epigenetics* **4**: 487-499.

- Hsieh J, Nakashima K, Kuwabara T, Mejia E, Gage FH. 2004. Histone deacetylase inhibition-mediated neuronal differentiation of multipotent adult neural progenitor cells. *Proc Natl Acad Sci U S A* **101**: 16659-16664.
- Hu N, Strobl-Mazzulla P, Sauka-Spengler T, Bronner ME. 2012. DNA methyltransferase3A as a molecular switch mediating the neural tube-to-neural crest fate transition. *Genes Dev* **26**: 2380-2385.
- Hurd EA, Capers PL, Blauwkamp MN, Adams ME, Raphael Y, Poucher HK, Martin DM. 2007. Loss of *Chd7* function in gene-trapped reporter mice is embryonic lethal and associated with severe defects in multiple developing tissues. *Mamm Genome* **18**: 94-104.
- Ignatius MS, Moose HE, El-Hodiri HM, Henion PD. 2008. *colgate/hdac1* Repression of *foxd3* expression is required to permit *mitfa*-dependent melanogenesis. *Dev Biol* **313**: 568-583.
- Inoue K, Shilo K, Boerkoel CF, Crowe C, Sawady J, Lupski JR, Agamanolis DP. 2002. Congenital hypomyelinating neuropathy, central dysmyelination, and Waardenburg-Hirschsprung disease: phenotypes linked by *SOX10* mutation. *Ann Neurol* **52**: 836-842.
- Jacques-Fricke BT, Roffers-Agarwal J, Gammill LS. 2012. DNA methyltransferase 3b is dispensable for mouse neural crest development. *PLoS One* **7**: e47794.
- Jaenisch R, Bird A. 2003. Epigenetic regulation of gene expression: how the genome integrates intrinsic and environmental signals. *Nat Genet* **33 Suppl**: 245-254.
- Jenuwein T, Allis CD. 2001. Translating the histone code. *Science* **293**: 1074-1080.
- Jiang R, Bush JO, Lidral AC. 2006. Development of the upper lip: morphogenetic and molecular mechanisms. *Dev Dyn* **235**: 1152-1166.
- Jin B, Tao Q, Peng J, Soo HM, Wu W, Ying J, Fields CR, Delmas AL, Liu X, Qiu J et al. 2008. DNA methyltransferase 3B (DNMT3B) mutations in ICF syndrome lead to altered epigenetic modifications and aberrant expression of genes regulating development, neurogenesis and immune function. *Hum Mol Genet* **17**: 690-709.
- Jurkowska RZ, Jurkowski TP, Jeltsch A. 2011a. Structure and function of mammalian DNA methyltransferases. *Chembiochem* **12**: 206-222.
- Jurkowska RZ, Rajavelu A, Anspach N, Urbanke C, Jankevicius G, Ragozin S, Nellen W, Jeltsch A. 2011b. Oligomerization and binding of the Dnmt3a DNA methyltransferase to parallel DNA molecules: heterochromatic localization and role of Dnmt3L. *J Biol Chem* **286**: 24200-24207.
- Kadosh D, Struhl K. 1997. Repression by *Ume6* involves recruitment of a complex containing *Sin3* corepressor and *Rpd3* histone deacetylase to target promoters. *Cell* **89**: 365-371.
- Kelsh RN. 2006. Sorting out *Sox10* functions in neural crest development. *Bioessays* **28**: 788-798.
- Kim H, Kang K, Ekram MB, Roh TY, Kim J. 2011. *Aebp2* as an epigenetic regulator for neural crest cells. *PLoS One* **6**: e25174.
- Kim H, Kang K, Kim J. 2009. *AEBP2* as a potential targeting protein for Polycomb Repression Complex PRC2. *Nucleic Acids Res* **37**: 2940-2950.
- Kouzarides T. 2007. Chromatin modifications and their function. *Cell* **128**: 693-705.

- Krogan NJ, Dover J, Wood A, Schneider J, Heidt J, Boateng MA, Dean K, Ryan OW, Golshani A, Johnston M et al. 2003. The Paf1 complex is required for histone H3 methylation by COMPASS and Dot1p: linking transcriptional elongation to histone methylation. *Mol Cell* **11**: 721-729.
- Kwon CS, Wagner D. 2007. Unwinding chromatin for development and growth: a few genes at a time. *Trends Genet* **23**: 403-412.
- Kwon O, Jeong SJ, Kim SO, He L, Lee HG, Jang KL, Osada H, Jung M, Kim BY, Ahn JS. 2010. Modulation of E-cadherin expression by K-Ras; involvement of DNA methyltransferase-3b. *Carcinogenesis* **31**: 1194-1201.
- Layman WS, McEwen DP, Beyer LA, Lalani SR, Fernbach SD, Oh E, Swaroop A, Hegg CC, Raphael Y, Martens JR et al. 2009. Defects in neural stem cell proliferation and olfaction in Chd7 deficient mice indicate a mechanism for hyposmia in human CHARGE syndrome. *Hum Mol Genet* **18**: 1909-1923.
- Le Douarin N. 1982. *The neural crest*. Cambridge University Press, New York.
- Li J, Shi Y, Sun J, Zhang Y, Mao B. 2011. Xenopus reduced folate carrier regulates neural crest development epigenetically. *PLoS One* **6**: e27198.
- Lim J, Thiery JP. 2012. Epithelial-mesenchymal transitions: insights from development. *Development* **139**: 3471-3486.
- Linhart HG, Lin H, Yamada Y, Moran E, Steine EJ, Gokhale S, Lo G, Cantu E, Ehrich M, He T et al. 2007. Dnmt3b promotes tumorigenesis in vivo by gene-specific de novo methylation and transcriptional silencing. *Genes Dev* **21**: 3110-3122.
- Liu Y, Xiao A. 2011. Epigenetic regulation in neural crest development. *Birth Defects Res A Clin Mol Teratol* **91**: 788-796.
- Martins-Taylor K, Schroeder DI, LaSalle JM, Lalande M, Xu RH. 2012. Role of DNMT3B in the regulation of early neural and neural crest specifiers. *Epigenetics* **7**: 71-82.
- Mayer W, Niveleau A, Walter J, Fundele R, Haaf T. 2000. Demethylation of the zygotic paternal genome. *Nature* **403**: 501-502.
- McKinney MC, Fukatsu K, Morrison J, McLennan R, Bronner ME, Kulesa PM. 2013. Evidence for dynamic rearrangements but lack of fate or position restrictions in premigratory avian trunk neural crest. *Development* **140**: 820-830.
- Meulemans D, Bronner-Fraser M. 2004. Gene-regulatory interactions in neural crest evolution and development. *Dev Cell* **7**: 291-299.
- Miranda TB, Jones PA. 2007. DNA methylation: the nuts and bolts of repression. *J Cell Physiol* **213**: 384-390.
- Momparler RL, Bovenzi V. 2000. DNA methylation and cancer. *J Cell Physiol* **183**: 145-154.
- Muchardt C, Yaniv M. 2001. When the SWI/SNF complex remodels...the cell cycle. *Oncogene* **20**: 3067-3075.
- Murko C, Lagger S, Steiner M, Seiser C, Schoefer C, Pusch O. 2013. Histone deacetylase inhibitor Trichostatin A induces neural tube defects and promotes neural crest specification in the chicken neural tube. *Differentiation* **85**: 55-66.
- Nakagawa S, Takeichi M. 1995. Neural crest cell-cell adhesion controlled by sequential and subpopulation-specific expression of novel cadherins. *Development* **121**: 1321-1332.

- Namihira M, Nakashima K, Taga T. 2004. Developmental stage dependent regulation of DNA methylation and chromatin modification in a immature astrocyte specific gene promoter. *FEBS Lett* **572**: 184-188.
- Nguyen CT, Langenbacher A, Hsieh M, Chen JN. 2010. The PAF1 complex component Leo1 is essential for cardiac and neural crest development in zebrafish. *Dev Biol* **341**: 167-175.
- Nielsen SJ, Schneider R, Bauer UM, Bannister AJ, Morrison A, O'Carroll D, Firestein R, Cleary M, Jenuwein T, Herrera RE et al. 2001. Rb targets histone H3 methylation and HP1 to promoters. *Nature* **412**: 561-565.
- Okano M, Bell DW, Haber DA, Li E. 1999. DNA methyltransferases Dnmt3a and Dnmt3b are essential for de novo methylation and mammalian development. *Cell* **99**: 247-257.
- Ooi SK, O'Donnell AH, Bestor TH. 2009. Mammalian cytosine methylation at a glance. *J Cell Sci* **122**: 2787-2791.
- Pan G, Tian S, Nie J, Yang C, Ruotti V, Wei H, Jonsdottir GA, Stewart R, Thomson JA. 2007. Whole-genome analysis of histone H3 lysine 4 and lysine 27 methylation in human embryonic stem cells. *Cell Stem Cell* **1**: 299-312.
- Park JW, Cai J, McIntosh I, Jabs EW, Fallin MD, Ingersoll R, Hetmanski JB, Vekemans M, Attie-Bitach T, Lovett M et al. 2006. High throughput SNP and expression analyses of candidate genes for non-syndromic oral clefts. *J Med Genet* **43**: 598-608.
- Pawlak M, Jaenisch R. 2011. De novo DNA methylation by Dnmt3a and Dnmt3b is dispensable for nuclear reprogramming of somatic cells to a pluripotent state. *Genes Dev* **25**: 1035-1040.
- Pevny LH, Lovell-Badge R. 1997. Sox genes find their feet. *Curr Opin Genet Dev* **7**: 338-344.
- Phillips BT, Kwon HJ, Melton C, Houghtaling P, Fritz A, Riley BB. 2006. Zebrafish msxB, msxC and msxE function together to refine the neural-nonneural border and regulate cranial placodes and neural crest development. *Dev Biol* **294**: 376-390.
- Portela A, Esteller M. 2010. Epigenetic modifications and human disease. *Nat Biotechnol* **28**: 1057-1068.
- Prokhortchouk E, Defossez PA. 2008. The cell biology of DNA methylation in mammals. *Biochim Biophys Acta* **1783**: 2167-2173.
- Qi HH, Sarkissian M, Hu GQ, Wang Z, Bhattacharjee A, Gordon DB, Gonzales M, Lan F, Ongusaha PP, Huarte M et al. 2010. Histone H4K20/H3K9 demethylase PHF8 regulates zebrafish brain and craniofacial development. *Nature* **466**: 503-507.
- Qu Y, Mu G, Wu Y, Dai X, Zhou F, Xu X, Wang Y, Wei F. 2010. Overexpression of DNA methyltransferases 1, 3a, and 3b significantly correlates with retinoblastoma tumorigenesis. *Am J Clin Pathol* **134**: 826-834.
- Rada-Iglesias A, Bajpai R, Prescott S, Brugmann SA, Swigut T, Wysocka J. 2012. Epigenomic annotation of enhancers predicts transcriptional regulators of human neural crest. *Cell Stem Cell* **11**: 633-648.

- Rada-Iglesias A, Bajpai R, Swigut T, Brugmann SA, Flynn RA, Wysocka J. 2011. A unique chromatin signature uncovers early developmental enhancers in humans. *Nature* **470**: 279-283.
- Rai K, Jafri IF, Chidester S, James SR, Karpf AR, Cairns BR, Jones DA. 2010. Dnmt3 and G9a cooperate for tissue-specific development in zebrafish. *J Biol Chem* **285**: 4110-4121.
- Reik W. 2007. Stability and flexibility of epigenetic gene regulation in mammalian development. *Nature* **447**: 425-432.
- Roth SY, Denu JM, Allis CD. 2001. Histone acetyltransferases. *Annu Rev Biochem* **70**: 81-120.
- Rundlett SE, Carmen AA, Suka N, Turner BM, Grunstein M. 1998. Transcriptional repression by UME6 involves deacetylation of lysine 5 of histone H4 by RPD3. *Nature* **392**: 831-835.
- Sauka-Spengler T, Barembaum M. 2008. Gain- and loss-of-function approaches in the chick embryo. *Methods Cell Biol* **87**: 237-256.
- Sauka-Spengler T, Bronner M. 2010. Snapshot: neural crest. *Cell* **143**: 486-486 e481.
- Sauka-Spengler T, Bronner-Fraser M. 2006. Development and evolution of the migratory neural crest: a gene regulatory perspective. *Curr Opin Genet Dev* **16**: 360-366.
- . 2008. A gene regulatory network orchestrates neural crest formation. *Nat Rev Mol Cell Biol* **9**: 557-568.
- Sauka-Spengler T, Meulemans D, Jones M, Bronner-Fraser M. 2007. Ancient evolutionary origin of the neural crest gene regulatory network. *Dev Cell* **13**: 405-420.
- Schwartz YB, Kahn TG, Nix DA, Li XY, Bourgon R, Biggin M, Pirrotta V. 2006. Genome-wide analysis of Polycomb targets in *Drosophila melanogaster*. *Nat Genet* **38**: 700-705.
- Shahbazian MD, Grunstein M. 2007. Functions of site-specific histone acetylation and deacetylation. *Annu Rev Biochem* **76**: 75-100.
- Shi Y, Sawada J, Sui G, Affar el B, Whetstine JR, Lan F, Ogawa H, Luke MP, Nakatani Y, Shi Y. 2003. Coordinated histone modifications mediated by a CtBP co-repressor complex. *Nature* **422**: 735-738.
- Siddique AN, Nunna S, Rajavelu A, Zhang Y, Jurkowska RZ, Reinhardt R, Rots MG, Ragozin S, Jurkowski TP, Jeltsch A. 2012. Targeted Methylation and Gene Silencing of VEGF-A in Human Cells by Using a Designed Dnmt3a-Dnmt3L Single-Chain Fusion Protein with Increased DNA Methylation Activity. *J Mol Biol.*
- Simic R, Lindstrom DL, Tran HG, Roinick KL, Costa PJ, Johnson AD, Hartzog GA, Arndt KM. 2003. Chromatin remodeling protein Chd1 interacts with transcription elongation factors and localizes to transcribed genes. *EMBO J* **22**: 1846-1856.
- Simon JA, Kingston RE. 2009. Mechanisms of polycomb gene silencing: knowns and unknowns. *Nat Rev Mol Cell Biol* **10**: 697-708.
- Singh N, Trivedi CM, Lu M, Mullican SE, Lazar MA, Epstein JA. 2011. Histone deacetylase 3 regulates smooth muscle differentiation in neural crest cells and development of the cardiac outflow tract. *Circ Res* **109**: 1240-1249.
- Steventon B, Carmona-Fontaine C, Mayor R. 2005. Genetic network during neural crest induction: from cell specification to cell survival. *Semin Cell Dev Biol* **16**: 647-654.

- Strobl-Mazzulla PH, Bronner ME. 2012a. Epithelial to mesenchymal transition: new and old insights from the classical neural crest model. *Semin Cancer Biol* **22**: 411-416.
- . 2012b. A PHD12-Snail2 repressive complex epigenetically mediates neural crest epithelial-to-mesenchymal transition. *J Cell Biol* **198**: 999-1010.
- Strobl-Mazzulla PH, Sauka-Spengler T, Bronner-Fraser M. 2010. Histone demethylase Jmjd2A regulates neural crest specification. *Dev Cell* **19**: 460-468.
- Stuhlmiller TJ, Garcia-Castro MI. 2012. Current perspectives of the signaling pathways directing neural crest induction. *Cell Mol Life Sci* **69**: 3715-3737.
- Suzuki MM, Bird A. 2008. DNA methylation landscapes: provocative insights from epigenomics. *Nat Rev Genet* **9**: 465-476.
- Swigut T, Wysocka J. 2007. H3K27 demethylases, at long last. *Cell* **131**: 29-32.
- Tan H, Wu S, Wang J, Zhao ZK. 2008. The JMJD2 members of histone demethylase revisited. *Mol Biol Rep* **35**: 551-556.
- Tan M, Luo H, Lee S, Jin F, Yang JS, Montellier E, Buchou T, Cheng Z, Rousseaux S, Rajagopal N et al. 2011. Identification of 67 histone marks and histone lysine crotonylation as a new type of histone modification. *Cell* **146**: 1016-1028.
- Taneyhill LA, Coles EG, Bronner-Fraser M. 2007. Snail2 directly represses cadherin6B during epithelial-to-mesenchymal transitions of the neural crest. *Development* **134**: 1481-1490.
- Tennyson VM, Pham TD, Rothman TP, Gershon MD. 1986. Abnormalities of smooth muscle, basal laminae, and nerves in the aganglionic segments of the bowel of lethal spotted mutant mice. *Anat Rec* **215**: 267-281.
- Tolhuis B, de Wit E, Muijters I, Teunissen H, Talhout W, van Steensel B, van Lohuizen M. 2006. Genome-wide profiling of PRC1 and PRC2 Polycomb chromatin binding in *Drosophila melanogaster*. *Nat Genet* **38**: 694-699.
- Trowbridge JJ, Orkin SH. 2012. Dnmt3a silences hematopoietic stem cell self-renewal. *Nat Genet* **44**: 13-14.
- Turek-Plewa J, Jagodzinski PP. 2005. The role of mammalian DNA methyltransferases in the regulation of gene expression. *Cell Mol Biol Lett* **10**: 631-647.
- Uchikawa M, Ishida Y, Takemoto T, Kamachi Y, Kondoh H. 2003. Functional analysis of chicken Sox2 enhancers highlights an array of diverse regulatory elements that are conserved in mammals. *Dev Cell* **4**: 509-519.
- Wakamatsu Y, Endo Y, Osumi N, Weston JA. 2004. Multiple roles of Sox2, an HMG-box transcription factor in avian neural crest development. *Dev Dyn* **229**: 74-86.
- Wang A, Kurdastani SK, Grunstein M. 2002. Requirement of Hos2 histone deacetylase for gene activity in yeast. *Science* **298**: 1412-1414.
- Wang Z, Zang C, Cui K, Schones DE, Barski A, Peng W, Zhao K. 2009. Genome-wide mapping of HATs and HDACs reveals distinct functions in active and inactive genes. *Cell* **138**: 1019-1031.
- Wienholz BL, Kareta MS, Moarefi AH, Gordon CA, Ginno PA, Chedin F. 2010. DNMT3L modulates significant and distinct flanking sequence preference for DNA methylation by DNMT3A and DNMT3B in vivo. *PLoS Genet* **6**.
- Wilkinson DG. 1992. *In Situ Hybridization: A Practical Approach*. IRL Press, Oxford.

- Williams SR, Aldred MA, Der Kaloustian VM, Halal F, Gowans G, McLeod DR, Zondag S, Toriello HV, Magenis RE, Elsea SH. 2010. Haploinsufficiency of HDAC4 causes brachydactyly mental retardation syndrome, with brachydactyly type E, developmental delays, and behavioral problems. *Am J Hum Genet* **87**: 219-228.
- Wu H, Coskun V, Tao J, Xie W, Ge W, Yoshikawa K, Li E, Zhang Y, Sun YE. 2010. Dnmt3a-dependent nonpromoter DNA methylation facilitates transcription of neurogenic genes. *Science* **329**: 444-448.
- Wu JI, Lessard J, Crabtree GR. 2009. Understanding the words of chromatin regulation. *Cell* **136**: 200-206.
- Wyszynski DF, Nambisan M, Surve T, Alsdorf RM, Smith CR, Holmes LB. 2005. Increased rate of major malformations in offspring exposed to valproate during pregnancy. *Neurology* **64**: 961-965.
- Yan XJ, Xu J, Gu ZH, Pan CM, Lu G, Shen Y, Shi JY, Zhu YM, Tang L, Zhang XW et al. 2011. Exome sequencing identifies somatic mutations of DNA methyltransferase gene DNMT3A in acute monocytic leukemia. *Nat Genet* **43**: 309-315.
- Yang XJ. 2004. Lysine acetylation and the bromodomain: a new partnership for signaling. *Bioessays* **26**: 1076-1087.
- Yoshimura K, Kitagawa H, Fujiki R, Tanabe M, Takezawa S, Takada I, Yamaoka I, Yonezawa M, Kondo T, Furutani Y et al. 2009. Distinct function of 2 chromatin remodeling complexes that share a common subunit, Williams syndrome transcription factor (WSTF). *Proc Natl Acad Sci U S A* **106**: 9280-9285.
- Youn YH, Feng J, Tessarollo L, Ito K, Sieber-Blum M. 2003. Neural crest stem cell and cardiac endothelium defects in the TrkC null mouse. *Mol Cell Neurosci* **24**: 160-170.
- Zentner GE, Layman WS, Martin DM, Scacheri PC. 2010. Molecular and phenotypic aspects of CHD7 mutation in CHARGE syndrome. *Am J Med Genet A* **152A**: 674-686.

Appendix A

**Altering Glypican-1 levels modulates canonical Wnt signaling
during trigeminal placode development**

Celia E. Shiau, Na Hu, Marianne Bronner-Fraser

Developmental Biology

Dec 01 2010

Abstract

Glypicans are conserved cell surface heparan sulfate proteoglycans expressed in a spatiotemporally regulated manner in many developing tissues including the nervous system. Here, we show that Glypican-1 (GPC1) is expressed by trigeminal placode cells as they ingress and contribute to trigeminal sensory neurons in the chick embryo. Either expression of full-length or truncated GPC1 *in vivo* causes defects in trigeminal gangliogenesis in a manner that requires heparan sulfate side chains. This leads to either abnormal placodal differentiation or organization, respectively, with near complete loss of the ophthalmic (OpV) trigeminal ganglion in the most severe cases after overexpression of full-length GPC1. Interestingly, modulating GPC1 alters levels of endogenous Wnt signaling activity in the forming trigeminal ganglion, as indicated by Wnt reporter expression. Accordingly, GPC1 overexpression phenocopies Wnt inhibition in causing loss of OpV placodal neurons. Furthermore, increased Wnt activity rescues the effects of GPC1 overexpression. Taken together, these results suggest that appropriate levels of GPC1 are essential for proper regulation of canonical Wnt signaling during differentiation and organization of trigeminal placodal cells into ganglia.

Introduction

Glypicans (GPCs) are a conserved family of cell surface heparan sulfate proteoglycans (HSPGs) that modulate major signaling pathways during embryonic

development of fruit flies to mammals (Fico et al., 2007 and Filmus et al., 2008).

Heparan sulfate side chains, attached to the core protein at conserved serine residues near the membrane anchored glycosyl-phosphatidylinositol (GPI) linkage, are thought to facilitate binding of growth factors and ligands, including Wingless/Wnt, Dpp/BMP, Fgf, and Hh, and are considered ligand carriers or coreceptors. Accordingly, functional perturbation of glypicans has been shown to cause significant defects in cell fate, cell movements, survival, and proliferation in mice, *Xenopus laevis*, *Drosophila*, and zebrafish (Filmus and Song, 2000, De Cat and David, 2001, Lin, 2004 and Fico et al., 2007).

During vertebrate development, glypicans are expressed in a spatiotemporally regulated manner in the nervous system and other tissues (Niu et al., 1996, Saunders et al., 1997, Litwack et al., 1998 and Luxardi et al., 2007). Their expression changes in pathological conditions, such as cancer. GPC3 and/or GPC1 are down-regulated in some ovarian cancer and mesothelioma cell lines (Lin et al., 1999 and Murthy et al., 2000) while upregulated in others (e.g., pancreatic tumors) (Kleeff et al., 1998, Filmus, 2001, Matsuda et al., 2001 and Su et al., 2006). Six glypican (GPC1–6) family members have been identified in mammals, two in *Drosophila melanogaster* (Dally and Dally-like), and two in *Caenorhabditis elegans* (*gpn-1* and *lon-2*) (Fico et al., 2007). Loss-of-function mutations in OCI-5/GPC3 in humans cause Simpson–Golabi–Behmel syndrome (SGBS), characterized by pre- and post-natal overgrowth, visceral and skeletal defects, and an increased risk of tumors (Pilia et al., 1996). A GPC3-deficient mouse model exhibits a similar phenotype (Cano-Gauci et al., 1999). Of the six glypicans in mammals, GPC1 is the most abundantly expressed in the developing brain, in both neuroepithelial precursors

and differentiated neurons (Karthikeyan et al., 1994, Litwack et al., 1994 and Litwack et al., 1998) and functions in neurogenesis of the central nervous system (Jen et al., 2009). However, its potential role in patterning and formation of the peripheral nervous system has yet to be explored.

Here, we show that Glypican-1 is expressed by ectodermal and ingressing chick trigeminal placode cells at the time they differentiate into neurons and assemble into ganglia. Modulation of GPC1 levels by expression of full-length GPC1 or a truncated form that is thought to act in a dominant-negative fashion prevents placodal differentiation or proper ganglion formation, respectively, with particularly strong effects on the ophthalmic lobe. Consistent with studies showing that Wnt signaling is important for differentiation of ophthalmic trigeminal placodes (Lassiter et al., 2007 and Canning et al., 2008), we find that GPC1 regulates Wnt activity in OpV ganglion formation. The results suggest that proper levels of GPC1 are critical for appropriate modulation of canonical Wnt signaling for differentiation and assembly of trigeminal placodes into ganglia.

Results

Expression of Glypican-1 mRNA in the trigeminal placodes and other embryonic tissues during early chick development

As a first step in examining the possible developmental role of Glypican-1 (GPC1), we first characterized its mRNA expression in the chick embryo at stages 9–18 by whole mount in situ hybridization (Fig. 1 and data not shown). This corresponds to the time window of early trigeminal development starting from neural crest migration to ganglion condensation. No expression of GPC1 mRNA was noted in the trigeminal neural crest cells, derived from the midbrain and anterior hindbrain (rhombomeres 1 and 2) levels of the neural tube, from stage 9 through gangliogenesis (Figs. 1A–C, F, L). Interestingly, we find that GPC1 is expressed by the presumptive trigeminal placodal ectoderm starting at approximately stage 12, coincident with the beginning of placodal differentiation and ingression but not earlier (Figs. 1C and D). GPC1 expression persists later as placodal cells assemble and condense into ganglion at stages 14–16 (Figs. 1F and L) and later at stage 18 (data not shown). GPC1 is expressed by both the ophthalmic (OpV) and maxillomandibular (MmV) placodes that form the trigeminal ganglion (Figs. 1F and L). To confirm that these GPC1 expressing cells are in fact placode-derived, we labeled the placodal ectoderm with GFP by in ovo electroporation prior to placodal ingression. Embryos were then collected at later stages after placodal cells had begun to delaminate from the ectoderm. GPC1 expression was detected by in situ hybridization in the GFP-expressing placodal cells that had ingressed into the mesenchyme. Results show that all GFP-expressing placode-derived cells and discrete regions of the placodal ectoderm express GPC1 (Figs. 1G–J), while the interacting HNK-1-positive trigeminal neural crest cells do not. Not all placode-derived cells are GFP-labeled as the transfection of the ectodermal region was mosaic in some cases.

In addition to placodal cells, GPC1 mRNA is expressed in other tissues. In

contrast to the midbrain neural crest, GPC1 is detected in the migrating hindbrain neural crest cells from rhombomeres 4 and 6 during migration at stage 12 (Figs. 1C and E), albeit transiently, being down-regulated by stage 14 (Figs. 1M and N). In the more posterior placodes, GPC1 is expressed in the epibranchial placodal ectoderm at stages 14–16 (Figs. 1F, L, and M). The otic placode expresses GPC1 by stage 12, albeit weakly; by stage 14, its expression is strong in the invaginating and forming otic vesicle (Figs. 1F and M). Furthermore, GPC1 was weakly expressed in the forming cranial neural tube and notochord throughout these stages (Figs. 1A–M). The developing mesoderm and forming limb bud also express GPC1 (Fig. 1K). Expression is particularly dynamic in the developing somites. Through stages 9–18, the GPC1 mRNA appears to be expressed in a gradient in the presomitic mesoderm (PSM) highest at the newly forming somites and decreasing both rostrally toward the more anterior somites and caudally toward the tail (Figs. 1B and O). The expression patterns of GPC1 in the forming neural tube, somite, and limb are consistent with those described previously (Niu et al., 1996). This study analyzed developmental stages at stages 7–12 and 20–25 but not the time window (stages 13–18) or tissues involved in gangliogenesis as demonstrated here.

The multiple tissue-specific expression patterns of GPC1 in the early developing chick embryo are consistent with possible roles for GPC1 patterning several different embryonic regions. The GPC1 expression in the trigeminal placodes at the time of neuronal differentiation and ganglion assembly, after specification, raises the intriguing possibility that GPC1 may have a role in regulating later events of trigeminal development.

Overexpression of Glypican-1 in placodes causes loss of trigeminal ganglia

Glypicans are thought to act as ligand carriers or coreceptors for several major families of signaling molecules (Wnt, FGF, BMP, and Hh) (Lin, 2004 and Fico et al., 2007); some of these have been implicated previously in trigeminal placode formation, most notably Wnts and Fgfs (Stark et al., 2000, Lassiter et al., 2007, Lassiter et al., 2009 and Canning et al., 2008). Since modulation of glypican expression can differentially affect cellular behavior (Qiao et al., 2008) as well as the distribution and signaling of these growth factors (De Cat and David, 2001 and Hufnagel et al., 2006), we asked whether changing levels of GPC1 expression in the trigeminal placodes would also affect the signaling events required for normal gangliogenesis. To test this, we expressed higher levels of GPC1 in the trigeminal placodal tissue at or just prior to its endogenous expression in the placodes. Full-length chick GPC1 expression construct (cytopcig-FL-GPC1), or the empty vector (cytopcig) as control, was introduced into the placodal ectoderm by in ovo electroporation at stages 8+ to 11 (5–14 ss [somites stage]) before placodal ingression and after expression of the earliest known trigeminal placode fate marker Pax3 mRNA which begins by 4 ss (Stark et al., 1997). Embryos with efficient electroporation of OpV and MmV lobes were analyzed at three time points corresponding to early ganglion formation (stages 15–16), after condensation (stages 17–18), and in the mature ganglion (stage 19). Neuronal components of the ganglion were analyzed by immunostaining with the neuronal marker, β -neurotubulin, TuJ1. Since neural crest cells differentiate into neurons much later (beginning at embryonic day 4; ~ stages 22–24) (D'Amico-Martel and Noden, 1980), only placodal cells express this marker at the stages examined, as shown previously by the colabeling of neuronal markers (TuJ1 and Islet1)

with GFP expressed by transfected placodal cells, whereas neural crest cells (Sox10- and HNK-1-positive) lack these markers (Shiau et al., 2008 and Shiau, 2009).

The results show that overexpression of GPC1 in the placodal ectoderm causes a dramatic loss of the trigeminal ganglion, with nearly the entire OpV lobe missing in many cases (Fig. 2). The penetrance of this effect was categorized according to severity: “reduced” ganglia were clearly smaller by overall size in at least one lobe for all stages, whereas “severely reduced” were those that lost all or most of the OpV lobe at stages 15–18 (Figs. 2A–F) or had both lobes markedly reduced at stage 19 (Fig. 2G–L). At stages 15–18, 45% (n = 42) of the cases had markedly “reduced” ganglia, whereas ~ 10% were “severely reduced”. By stage 19, 25% (n = 12) were “reduced” and 8% were “severely reduced,” while no control GFP embryos showed a reduced phenotype (n = 23 at stages 15–18, and n = 7 at stage 19) (Fig. 2M). The slight recovery with time may be caused by dilution of the construct over time, though we cannot rule out the possibility that there also may be some compensation by other mechanisms. The striking loss of trigeminal placodal neurons in the ganglia caused by alteration in GPC1 expression suggests that appropriate regulation of GPC1 expression is essential for gangliogenesis.

GPC1 overexpression blocks proliferation and differentiation of the placodal ectoderm that leads to loss of ganglia

The severely reduced ganglia caused by GPC1 overexpression prompted us to examine whether this is mediated by defects in cell survival and/or proliferation in the placodal tissue. To analyze changes in cell death, stage-matched FL-GPC1 and control

GFP embryos at stage 14 were sectioned and immunostained for active caspase-3 (casp-3), which is a robust marker for apoptotic cells. Given that we can detect a phenotype as early as stages 15–16, embryos were examined at stage 14 which allows analysis of both ingression and coalescence of placodal neurons into ganglion. Only well-transfected FL-GPC1 and control embryos were selected for analysis. We counted transfected GFP+ only and GFP+/casp-3+ double positive cells (apoptotic cells) in the placodal ectoderm as well as in the mesenchyme. The latter correspond to ingressing placode cells and those already in the forming ganglion. The percentage of dying cells was then calculated by dividing the number of GFP+/casp-3+ cells over the total number of GFP+ cells in each region (ectoderm versus mesenchyme). At least 10 serial sections through the trigeminal ganglion anlage were analyzed per n. Using this assay, our data show that there is no significant difference in levels of cell death between FL-GPC1 and control embryos (in the ectoderm, $2.2\% \pm 0.7\%$ cell death in FL-GPC1, $n = 4$ compared with $0.85\% \pm 0.3\%$ cell death in control cases, $n = 4$; p value = 0.22 using a two-tailed Student's t-test, Fig. 3A). No cell death was detected in ingressing placodal cells in the mesenchyme for either control or experimental cases. Taken together, data suggest that increased cell death cannot account for the loss of the OpV lobe. Interestingly, however, we found that transfected FL-GPC1, but not control, placodal ectoderm cells tended to abnormally cluster and formed clumps of cells in the ectoderm instead of forming a normally organized epithelial sheet from which placodes delaminate (Figs. 3B and C).

We next analyzed whether proliferation in the placodal ectoderm is affected, using the same criteria and stages as for analysis of cell death. To determine the percentage of proliferating cells in the placodal tissue at stage 14, we briefly treated

electroporated embryos for 0.5 hour at the time of collection at stage 14 with bromodeoxyuridine (BrdU), an analog of thymidine that gets incorporated into dividing cells during the S phase. The short treatment provided a snapshot of all proliferating cells at the time point of collection, presumably within the 0.5 hour of treatment. At least six serial sections through the trigeminal ganglion anlage were counted and analyzed per n. Interestingly, BrdU analysis shows a significant reduction in proliferation in placodal ectoderm cells of FL-GPC1 embryos ($12.9\% \pm 1.3\%$ proliferation in FL-GPC1 (n = 6) versus $29.7\% \pm 2.7\%$ in control (n = 4) cases; p value = 0.00061), with relatively normal levels of proliferation in the mesenchymally located placodal cells ($8.0\% \pm 2.7\%$ in FL-GPC1 and $11.2\% \pm 3.8\%$ in controls, p value = 0.54 using a two-tailed Student's t-test) (Figs. 3A and C). This difference between ectodermal and mesenchyme-residing cells suggests that GPC1 overexpression predominantly inhibits proliferation in the placodal ectoderm only.

Since proliferation was significantly blocked in the placodal ectoderm and cell death was not significantly higher, the reduced ganglia phenotype may be due to a decrease in generation of placodal neurons in the surface ectoderm, leading to fewer of them ingressing to form ganglion. In support of this, we found significantly less ingression based on the average number of ectoderm-derived GFP+ cells in the mesenchyme of the ganglion region analyzed in FL-GPC1 (36 ± 8 cells, n = 6) compared with controls (95 ± 17 cells, n = 4; p value = 0.015 using a two-tailed Student's t-test) (Fig. 3A). However, there was no significant difference in the average number of GFP+ in the ectoderm (300 ± 36 cells in FL-GPC1 versus 342 ± 5 cells in control GFP cases; p value = 0.38 using a two-tailed Student's t-test) (Fig. 3A). The numbers of

ingressed GFP+ cells and those in the ectoderm between control and experimental cases were counted from the same sections as those used for the BrdU analysis.

The onset of GPC1 expression at the beginning of placodal differentiation in the ectoderm (Fig. 1D) is consistent with its possible role in differentiation of placodal cells. Differentiation of neurons appears to occur in the surface placodal ectoderm prior to ingression. This observation is based on the fact that placodal cells in the ectoderm already express neuronal markers (Islet1 and TuJ1) and all, if not most, of them that have ingressed express Islet1 and TuJ1 (as determined by labeling ingressing placodal cells using ectoderm electroporation with a GFP vector and examining whether all ectoderm-derived GFP+ placodal cells express neuronal markers) (Shiau, 2009 and data not shown). In sections through the ganglion region of experimental and control embryos, we consistently observed fewer placodal neurons in the ectoderm and in the mesenchyme in FL-GPC1 embryos, particularly in the OpV region (Fig. 3D). GPC1 overexpression significantly inhibits proliferation in the ectoderm but not in ingressed placodal cells and we subsequently observed loss of placodal neurons. This suggests that appropriate regulation of cell division in the ectoderm may be crucial for placodal differentiation.

Specification and commitment of the first placode cells to the ophthalmic (OpV) fate occurs by 8 ss (Stark et al., 1997 and Baker et al., 1999). We found no difference in the effect of overexpressing GPC1 on ganglion formation at the different stages of electroporation (5–14 ss), before or after 8 ss, suggesting that the effects of GPC1 overexpression occur after initial fate specification. Furthermore, no changes were noted in expression of the early OpV placode fate marker Pax3 mRNA expression in FL-GPC1

(n = 5/5) embryos compared with controls (n = 2) at stages 12–14 (data not shown).

Taken together, the data suggest that the level of GPC1 expression is critical for the appropriate regulation of cell division in the placodal ectoderm, following their specification but prior to differentiation. GPC1 expression correlates with the onset of neuronal differentiation in the placode and its overexpression causes a specific proliferation defect in the differentiating ectoderm. This in turn leads to loss of placodal neurons, mostly those of the OpV lobe. Thus, problems with placodal differentiation likely explain the phenotype caused by GPC1 overexpression.

Altering GPC1 expression causes ganglion disorganization and both truncated and full-length forms require heparan sulfate modification

Several conserved domains of glypicans are important for their function, including the conserved heparan sulfate (HS) chains (long unbranched disaccharides) near the cell surface that attach to specific serine residues near the carboxyl terminus of the core protein and GPI membrane attachment site (De Cat and David, 2001) (see simplified schematic in Fig. 4A). Although a number of studies have highlighted the importance of HS modification for GPC function in regulation of several signaling pathways (including Wnt, Fgf, Hh, BMP) (Hacker et al., 2005 and Fico et al., 2007), they are not required in all cases (Gonzalez et al., 1998, Capurro et al., 2005, Kirkpatrick et al., 2006 and Williams et al., 2010). GPI anchorage may be important for cell autonomous functions of GPC, such as being coreceptors for stabilizing ligand–receptor interaction or for regulating ligand levels by endocytosis. The GPI linkage also potentially plays a role

in post-translational modifications leading to cleavage of GPC to yield soluble forms of glypican that can affect distribution, spreading, or levels of ligand signaling (Fico et al., 2007 and Gallet et al., 2008).

To better define the mechanism by which full-length GPC1 (FL-GPC1) affects signaling during trigeminal development, we tested the functional requirement of HS modification and membrane anchoring. Three mutant GPC1 expression constructs were designed and tested in the trigeminal placodes: cytopcig-GPC1- Δ GPI which encodes a soluble truncated form of GPC1 where the GPI anchoring domain and remaining C-terminal sequence are removed, cytopcig-GPC1- Δ HS that has a deletion of all three putative HS attachment sites near the carboxyl terminus, and cytopcig-GPC1- Δ GPI- Δ HS which has deletion of both GPI anchoring and glycanation sites (Fig. 4B). We introduced these constructs into the trigeminal placodal ectoderm by *in ovo* electroporation during the same time window and in parallel with FL-GPC1 and control GFP as discussed above. Ganglia were scored at stages 15–19 for the reduced ganglia phenotype with only well-electroporated embryos selected for analysis.

The results show that electroporation of either the mutant with deletion of the GPI anchoring, HS attachment sites or both fail to cause reduced ganglia observed with the wild type construct (Fig. 4C). To determine the size differences, we quantified the area of the ganglion using the ImageJ area function on outlines of TuJ1 stained ganglia. As expected, the size of the ganglion increases as it continues to grow from stage 15–16 to 19 (Supplementary Fig. 1), albeit the area value at stages 15–16 is larger due to the fact that the cells are less condensed and more spread out. Compared with controls, the

ganglion area was, on average, over all stages, decreased by $39.4\% \pm 3.7\%$ after electroporation with FL-GPC1. The area of FL-GPC1 electroporated embryos with phenotype ($0.066 \pm 0.017 \text{ mm}^2$ at stages 15–16, $0.064 \pm 0.006 \text{ mm}^2$ at stage 17–18, $0.11 \pm 0.011 \text{ mm}^2$ at stage 19) was markedly reduced compared with those electroporated with control GFP constructs ($0.10 \pm 0.009 \text{ mm}^2$ at stages 15–16, $0.11 \pm 0.005 \text{ mm}^2$ at stages 17–18, $0.18 \pm 0.012 \text{ mm}^2$ at stage 19) or mutant forms of GPC1-expressing placodal ganglia at all stages (Supplementary Fig. 1). In contrast to that of FL-GPC1 (49%, $n = 53$), expression of mutant GPC1 constructs in the trigeminal placodes resulted in significantly fewer ganglia of reduced size (GPC1- Δ GPI, 8.7% ($n = 23$); GPC1- Δ HS, 9% ($n = 11$); GPC1- Δ GPI -HS, 5.6%, $n = 18$) (Supplementary Fig. 1). Control GFP ganglia exhibited no apparent ganglion reduction ($n = 30$) over all stages.

Previous studies have shown that the truncated soluble form of GPC that lacks GPI membrane anchorage can act as a dominant-negative inhibitor (Zittermann et al., 2009), presumably by competing with endogenous GPC for binding to signaling factors. Consistent with this idea, we found that expression of GPC1- Δ GPI did not cause the same level of reduced ganglia phenotype as that of FL-GPC1. Instead, it caused a distinct phenotype of disrupting ganglion morphology (26.1%, $n = 23$) at a significantly higher frequency than full-length construct (11.3%, $n = 53$); other mutant forms did not cause these effects (Supplementary Fig. 1). Furthermore, the subcellular localization of GPC1- Δ GPI is concentrated at or near the membrane. In contrast, the full-length construct is expressed in both the cytoplasm and on the membrane (Supplementary Fig. 2). This suggests that the GPC1- Δ GPI protein is properly processed for secretion to act in a soluble form. This is consistent with previous reports suggesting that a significant portion

of secreted glypicans lacking the GPI domain remain associated with the cell membrane due to electrostatic interactions (Carey and Evans, 1989 and Gonzalez et al., 1998).

These cumulative results show that both the GPI anchoring and HS GAG chains are required for the effects observed after electroporation of FL-GPC1 into the placodal ectoderm. Furthermore, GPC1 may have a role in ganglion organization as expression of a putative secreted antagonist (GPC1- Δ GPI) leads to aberrant ganglia formation without reducing ganglion size. For either full-length or truncated GPC1 phenotype, we find that HS modification appears to be critical.

Manipulating levels of GPC1 alters endogenous activity of Wnt signaling

Given that glypicans interact with growth factors, it is intriguing to speculate that GPC1 may interact with Wnt signaling in the trigeminal placodes. Blocking canonical Wnt signaling inhibits placodal differentiation and OpV ganglion formation (Lassiter et al., 2007) in a fashion reminiscent of the effects observed with GPC1 overexpression. Furthermore, Wnts have been shown to bind and interact with glypican (De Cat and David, 2001, Ohkawara et al., 2003 and Baeg et al., 2004). Consistent with the possibility that Wnt signaling may be involved in various steps of trigeminal placode development, the trigeminal placode expresses Wnt receptors Frizzled-2 and -7, whereas several different Wnt ligands are expressed in the adjacent chick neural tube (Hollyday et al., 1995, Marcelle et al., 1997 and Stark et al., 2000).

To address if there is a link between GPC1 and Wnt signaling in the trigeminal placodes, we tested whether increasing GPC1 expression or its mutant truncated form (GPC1- Δ GPI) would modulate endogenous levels of canonical Wnt signaling *in vivo*. To assay the activity of Wnt signaling, we used the RFP version of the TOPGAL Wnt reporter (DasGupta and Fuchs, 1999 and Lassiter et al., 2007) which drives RFP expression under the control of LEF/TCF consensus binding sites. Wnt signaling leads to stabilization and nuclear localization of β -catenin, which transactivates LEF/TCF transcription factors that bind to target LEF/TCF sequences to drive the expression of Wnt downstream genes and, in the case of the reporter, to drive RFP expression. The Wnt reporter was co-electroporated with the various glypican constructs: FL-GPC1 to overexpress GPC1 or GPC1- Δ GPI to block GPC1, or with empty GFP vector as control at stages 9–11. Electroporated embryos with broad transfection in the trigeminal region were collected at stages 14–16 for analysis.

In control GFP embryos in which there is broad transfection of the entire trigeminal ganglia, we found Wnt signaling activity restricted to the OpV region. In general, few to no ganglion cells were RFP⁺ in the MmV (Fig. 5A). At early stage 14, Wnt reporter expression was observed in the dorsal ectoderm (including ectoderm overlying the dorsal neural tube) and OpV placodes at stage 14 (data not shown; Lassiter et al., 2007). RFP expression was restricted to the OpV lobe of the ganglion at stages 15–16 and surrounding dorsal ectoderm (generally near the neural tube and above the OpV branch) (Fig. 5A). The area of cells in the OpV ganglion that expressed the RFP Wnt reporter appeared to increase over time, suggesting that the RFP expression is reflective of continuing addition of OpV placodal neurons to the ganglion and not merely from

residual RFP expression of placodal cells from earlier stages (Fig. 5A).

Overexpression of GPC1 in the trigeminal placodal ectoderm caused a reduction in Wnt signaling activity in the OpV ganglion cells but not in the dorsal ectoderm cells external to the ganglion (22.2%, n = 18, Figs. 5A and B). The knockdown of Wnt signaling by GPC1 overexpression suggests that GPC1 may negatively modulate Wnt signaling. Further support for this idea stems from the finding that GPC1 gain-of-function caused loss of OpV ganglion, which is the same phenotype previously reported for inhibition of Wnt signaling (Lassiter et al., 2007).

Consistent with the possibility that GPC1 modulates Wnt signaling, the truncated GPC1 construct (GPC1- Δ GPI) has the reciprocal effect of causing some expansion of the RFP Wnt reporter expression domain in the trigeminal ganglia (36%, n = 25, Figs. 5A and B). Not only was there an apparent increase in RFP expression in the OpV placodal ganglion, but, strikingly, there also was an expansion of RFP expression to the MmV domain near the border of the OpV lobe, as well as in sporadic placodal cells in the MmV ganglion distinct from controls (Fig. 5A).

These results show that manipulating GPC1 expression or function causes a change in endogenous Wnt signaling levels, suggesting a potential role for Glypican-1 as a regulator of canonical Wnt signaling in trigeminal placodes.

Activation of Wnt signaling reverses the effects of GPC1 overexpression but phenocopies effects of truncated GPC1

If the effects of GPC1 overexpression are mediated by reduced Wnt signaling, we predict that activation of Wnt signaling should rescue the ganglion loss. To test this, we used a dominant-active form of β -catenin (DA- β cat) in which the phosphorylation sites required for APC-mediated degradation are mutated, thus allowing β -catenin to constitutively activate Wnt target genes (Tetsu and McCormick, 1999 and Lassiter et al., 2007). We co-electroporated DA- β cat with FL-GPC1 or control GFP in the trigeminal placodal ectoderm at stages 9–11 and examined formation of trigeminal placodal ganglion at stages 15–18 using TuJ1 antibody staining. The results show that activation of canonical Wnt signaling in these FL-GPC1 electroporated embryos eliminated the reduced ganglia phenotype observed after GPC1 overexpression (Fig. 6A). Furthermore, constitutive activation of Wnt-signaling alone (by DA- β cat plus GFP expression) in the placodal tissue produced disorganized ganglia (42.9%, n = 7) (Figs. 6A and B), similar to the effects of expressing the GPC1- Δ GPI construct. In addition, DA- β cat and FL-GPC1 caused ganglion disorganization (33.3%, n = 6), perhaps due to abnormally high levels of Wnt signaling which not only reversed the inhibitory effects of GPC1 on Wnt signaling but also induced a gain-of-function phenotype. This effect is similar to expression of DA- β cat alone. Thus, increased Wnt signaling through DA- β cat expression reversed the reduced ganglia phenotype of FL-GPC1, and the effects of constitutively activated Wnt signaling phenocopied that of the truncated GPC1 that may act in a dominant-negative manner. Taken together, these data suggest a potential negative regulation of Wnt signaling by GPC1 in the trigeminal placodes. GPCs are also known to interact with other signaling pathways (Fico et al., 2007 and Filmus et al., 2008), raising the possibility that

GPC1 not only interact with Wnts but perhaps also with other signaling pathways functioning during placode differentiation.

Discussion

Our data provide novel insights into the expression and function of Glypican-1 as a potential modulator of Wnt signaling in the trigeminal placodes during neuronal differentiation and ganglion assembly. Wnt–glypican interactions in vivo have been best-studied in the *Drosophila* wing imaginal disc (Baeg and Perrimon, 2000, Franch-Marro et al., 2005, Gallet et al., 2008 and Yan et al., 2009) but are poorly understood in vertebrate development. Dally (division abnormally delayed), orthologue of vertebrate glypican 3/5, was found in a screen for defects in cell division patterning in the forming *Drosophila* CNS (Nakato et al., 1995 and Filmus and Song, 2000). Dally mutants have delayed G₂–M transition in dividing cells in the eye disc and lamina as well as defects in morphogenesis of adult tissues (i.e., the eye, antenna, wing, and genitalia) and in viability. Dally appears to act as a classical coreceptor that facilitates or enhances Wingless (Wg) signaling (Franch-Marro et al., 2005). In contrast, Dally-like (Dlp), the *Drosophila* orthologue of vertebrate GPC 1/2/4/6 (Filmus et al., 2008), has the opposite effect to Dally. It inhibits local but facilitates long-range Wnt/Wingless (Wg) signaling by transporting the signal to neighboring cells (Franch-Marro et al., 2005, Gallet et al., 2008 and Yan et al., 2009). Overexpression of GPC1 homologue Dlp causes reduced local Wg signaling and loss of imaginal disc tissue in a cell autonomous manner, whereas Dlp knockdown causes increased local Wg signaling (Baeg and Perrimon,

2000 and Franch-Marro et al., 2005).

Similar to the effects of Dlp, we observed a decrease in Wnt signaling with GPC1 overexpression and an increase with the expression of a putative dominant-negative form of GPC1, GPC1-ΔGPI, which lacks the GPI anchorage, in the trigeminal placodal tissue. Our data show that the mutant GPC1-ΔGPI has the reciprocal effect to full-length GPC1 by causing 1) an increase in Wnt signaling and 2) ganglion disorganization instead of a decrease in Wnt signaling and ganglion reduction as is the case after FL-GPC1 transfection. This suggests that the truncated GPC1 form acts in a dominant-negative manner to disrupt normal GPC1 function or at least in a way that is distinct from the function of the full-length glycoprotein. In light of the alteration of endogenous Wnt signaling by manipulating GPC1 expression in the trigeminal placodes, the results suggest that GPC1 acts similarly to Dlp in that it can negatively regulate Wnt signaling. Similar negative regulation by GPC3 on canonical Wnt signaling has also been shown in mouse and culture studies (Song et al., 2005).

The effects of altering GPC1 expression on endogenous Wnt signaling in trigeminal placodes appear to occur at later times during differentiation and assembly of placodal ganglia and not during Wnt's role in early ophthalmic (OpV) fate specification (Lassiter et al., 2007 and Canning et al., 2008). We found that GPC1 expression begins at ~ stage 12 which is well after placode induction and that GPC1 overexpression does not affect expression of the early placode marker Pax3 but rather blocks later steps in neuronal differentiation.

Interestingly, the most severe effect of GPC1 overexpression was the loss of OpV

placodal neurons, whereas MmV neurons were less affected. The OpV neurons are the same cells in which endogenous Wnt signaling is detected. We found that expression of the TOPGAL Wnt reporter was largely restricted to the OpV area and mostly absent from the MmV. These findings are consistent with the possibility that GPC1 regulates Wnt signaling in the forming OpV lobe of the trigeminal ganglion.

How might GPC1 regulate Wnt signaling? In *Drosophila*, genetic evidence on Dally mutants clearly shows that Dally has a positive influence on Wg signaling (Lin and Perrimon, 1999, Fujise et al., 2001, Franch-Marro et al., 2005 and Han et al., 2005). However, the mechanism of Dlp is more complicated and several models have been proposed to explain its negative regulation. This includes cleavage of Dlp at the GPI anchor to create a secreted antagonist for Wg ligands (Kreuger et al., 2004), endocytosis of Dlp through its GPI anchor with Wg (as exchange of GPI anchor for a transmembrane domain blocks this function) (Gallet et al., 2008), functioning of Dlp as a competitor for ligand binding, and positive or negative action of Dlp based on the ratio of Wg, Wg receptor, and Dlp (Yan et al., 2009) or based on the modification of Dlp by cleavage (Kreuger et al., 2004).

Here, we find that excess GPC1 expression inhibited Wnt signaling, similar to that of the Dlp, and expression of a mutant truncated GPC1 enhanced Wnt signaling. Distinct phenotypes, either loss or disorganization of the ganglion, were observed for the two types of perturbations respectively. One possibility is that GPC1 may act as a negative regulator of Wnt signaling in trigeminal placodes. Alternatively, GPC1 may act as both a negative and a positive regulator of Wnt such that different modes of GPC1

function (e.g., either as full-length or cleaved soluble form) or different levels of GPC1 expression might differentially influence Wnt signaling. For example, full-length GPC1 is capable of negatively regulating Wnt by reducing ligand levels by endocytosis via its GPI anchor, whereas truncated soluble GPC1 competes with full-length for ligand binding and therefore blocks endocytosis but promotes ligand distribution. Although the detailed mechanism is not yet known, it is clear from our findings that an appropriate level of GPC1 expression is required for normal formation of trigeminal placode-derived neurons, such that elevated GPC1 levels cause dramatic ganglion loss and lead to changes to endogenous Wnt activity.

GPCs interact with several major signaling pathways in addition to Wnts. We have previously shown that the interaction between Slit1 from neural crest cells and its cognate receptor Robo2 on trigeminal placodes mediates proper assembly of the trigeminal ganglion in part through regulation of N-cadherin protein distribution on placodal neurons for ganglion aggregation (Shiau et al., 2008 and Shiau and Bronner-Fraser, 2009). Direct interactions of heparan sulfate proteoglycans (HSPGs) with Slit have been suggested to be important for its function (Hussain et al., 2006, Fukuhara et al., 2008 and Hohenester, 2008). Consistent with this, recombinant vertebrate Glypican-1 has been shown to bind specifically to Slit1 and Slit2 in rat brain extracts (Liang et al., 1999 and Ronca et al., 2001). In light of this and the effect of disorganized ganglia caused by GPC1 inhibition using the soluble truncated form of GPC1, we cannot rule out the possibility that GPC1 may also regulate aspects of Slit-Robo signaling during trigeminal gangliogenesis. Similarly, GPC1 may affect Fgf signaling, which has been implicated in differentiation and ingression of trigeminal placodes (Canning et al.,

2008 and Lassiter et al., 2009). Loss of Fgf signaling leads to failure of placodes to delaminate from the ectoderm and contribute to ganglion formation in the mesenchyme (Lassiter et al., 2009) similar to the effects we have shown of GPC1 overexpression. Regulation of Fgf signaling by glypicans has been demonstrated previously in other systems, including the mammalian brain and *Drosophila* tracheal morphogenesis (Su et al., 2006, Yan and Lin, 2007 and Jen et al., 2009).

In summary, we identify the heparan sulfate proteoglycan, GPC1, as a novel molecular player in trigeminal gangliogenesis. It is distinctively expressed by the trigeminal placodal ectoderm and placode-derived sensory neurons. Importantly, we show that it can act as a regulator of Wnt signaling during placodal differentiation and ganglion formation and that proper levels of GPC1 expression are essential for these processes in vivo. Our results represent an important entry point into dissecting the regulation of signaling mechanisms involved in early formation of the trigeminal sensory system in chick, potentially revealing how signaling is modulated at proper levels.

Acknowledgments

We thank Andy Groves for the pTOP-nDSRed2 plasmid and members of M.B.-F. lab for discussions and technical advice, in particular Meyer Barembaum, Tatjana Sauka-Spengler, and Pablo Strobl. This work was supported by US National Institutes of Health (NIH) National Research Service Award5T32 GM07616 to C. E. S. and N.H. and NIH grant DE16459 to M.B.-F

Materials and methods

Embryos

Fertilized chicken (*Gallus gallus domesticus*) eggs were obtained from local commercial sources and incubated at 37 °C to the desired stages.

In situ hybridization

cDNA plasmid obtained from BBSRC (ChickEST clone 418p2) was used to transcribe antisense riboprobe against chick Glypican-1. The plasmid was sequenced and found to contain the coding sequence of the chick Glypican-1 gene (NCBI accession number: XM_422590.1) corresponding to nucleotides 1233–2107. Whole-mount chick in situ hybridization was performed as described (Shiau et al., 2008). Embryos were imaged and subsequently sectioned at 12 µm.

Immunohistochemistry

Primary antibodies used were: anti-TuJ1 (Covance; 1:250), anti-HNK-1 (American Type Culture; 1:3–1:5), anti-GFP to recognize GFP signal after in situ hybridization (Molecular Probes; 1:150–1:250), anti-Islet1 (DSHB, clone 40.2D6; 1:150–1:250), and anti-active-caspase-3 (Promega; 1:150–250). Appropriate secondary antibodies against the subtype of the primary antibodies were conjugated to Alexa Fluor 488, 568, or 350 dyes (Molecular Probes). Images were taken on a Zeiss Axioskop2 plus fluorescence

microscope, and processed using Adobe Photoshop CS3.

In ovo electroporation of the trigeminal ectoderm

Plasmid constructs were targeted to the presumptive trigeminal placodal ectoderm at the approximate axial level between the posterior forebrain and anterior hindbrain at 5 somites stage (stage 8+) up to stage 11. Immediately after injection, platinum electrodes were placed vertically across the chick embryo delivering current pulses of 5×8 V in 50 ms at 100 ms intervals as described (Shiau et al., 2008). Targeting DNA to the ectoderm resulted in transfection of the trigeminal placodes in the ectoderm and subsequently placode-derived cells that detach from the ectoderm and migrate into the ganglion anlage. The operated eggs were sealed and incubated at 37 °C for later analysis. Incubation times were ~ 16–24 hours to reach stages 13–14, ~ 24–36 hours to reach stages 15–16, ~ 40–48 hours to reach stages 17–18, and ~ 50–60 hours to reach stage 19.

Plasmid constructs

Full-length chick Glypican-1 cDNA (clone CS5) was isolated from a 4- to 12-somite stage chick macroarray library (Gammill and Bronner-Fraser, 2002). To create cytopcig-FL-GPC1, the full-length coding sequence (1.65 kb) was amplified from the library clone CS5 by PCR using forward and reverse primers corresponding to the coding sequence with flanking XhoI and ClaI site, respectively. Gene fragment was directionally inserted into the cytopcig vector (Shiau et al., 2008) at the XhoI/ClaI sites. Three mutant GPC1

constructs were made by a single-step or fusion PCR amplification off the full-length sequence, and a modified gene fragment was directionally cloned into the XhoI and ClaI sites in the cytopcig vector. These are 1) cytopcig–GPC1–GPI, which encodes the first 517 amino acids (1.55 kb) with a premature stop codon which eliminates the GPI-anchoring domain, 2) cytopcig–GPC1– Δ HS, which has a 18-bp deletion that spans a coding region of six residues, SGS GSG (483–488 aa), containing three tandemly positioned putative glycosaminoglycan (GAG) attachment sites (serine residues 483, 485, 487) based on sequence annotation in UniProtKB for chick GPC1 protein (accession P50593), and 3) cytopcig–GPC1– Δ GPI– Δ HS, which has deletions of both the GPI-anchor domain and the putative HS sites. Two versions of full-length and mutant constructs were made: one without myc–tag fusion and one with a 6 \times myc–tag inserted at ClaI/EcoRV sites in frame with the coding sequence at the C-terminus, which was used to validate protein expression of the constructs. Both versions were tested and determined to give the same effects on ganglion development, albeit FL-GPC1 was more potent without the myc–tag. Thus, most experiments with the full-length and mutant expressions were conducted with the construct lacking the myc–tag. Dominant-active β -catenin construct was made in the pCIG vector with IRES nuclear localized GFP as previously described (Megason and McMahon, 2002 and Lassiter et al., 2007), and RFP-Wnt reporter (also named pTOP-nDSRed2) (gift from Dr. Andy Groves [Lassiter et al., 2007]) was a modified version of the TOPGAL construct (DasGupta and Fuchs, 1999) where the reporter gene was replaced with RFP.

BrdU treatment

Electroporated embryos were screened and selected for broad GFP expression in the trigeminal region at stage 14 for both control and experimental cases. Each embryo was explanted into an individual well and treated with 0.1 mM BrdU in Ringer's solution at 37 °C for 30 minutes. Embryos were then fixed in 4% paraformaldehyde overnight at 4 °C, washed in PBS, incubated in 2N HCl in PBS for 30 minutes, followed by 0.1 M perboric acid (H₃BO₄) for 10 minutes, washed in PBS several times, and processed for cryosectioning and immunostaining with the mouse anti-BrdU (Sigma, B2531; 1:150–1:250).

Quantification of the area of trigeminal ganglion

An outline of the ganglion as marked by TuJ1 staining was made by the freehand selection tool on whole mount grayscale fluorescent images in the ImageJ software. All images were taken with the same setup using a 5× objective on the Zeiss Axioskop2 plus microscope and at the same image size, with the entire ganglion in focus. The area of the ganglion outline was determined by the area measurement function in ImageJ with the scale calibrated to the actual length.

Figures and Figure Legends

Figure 1

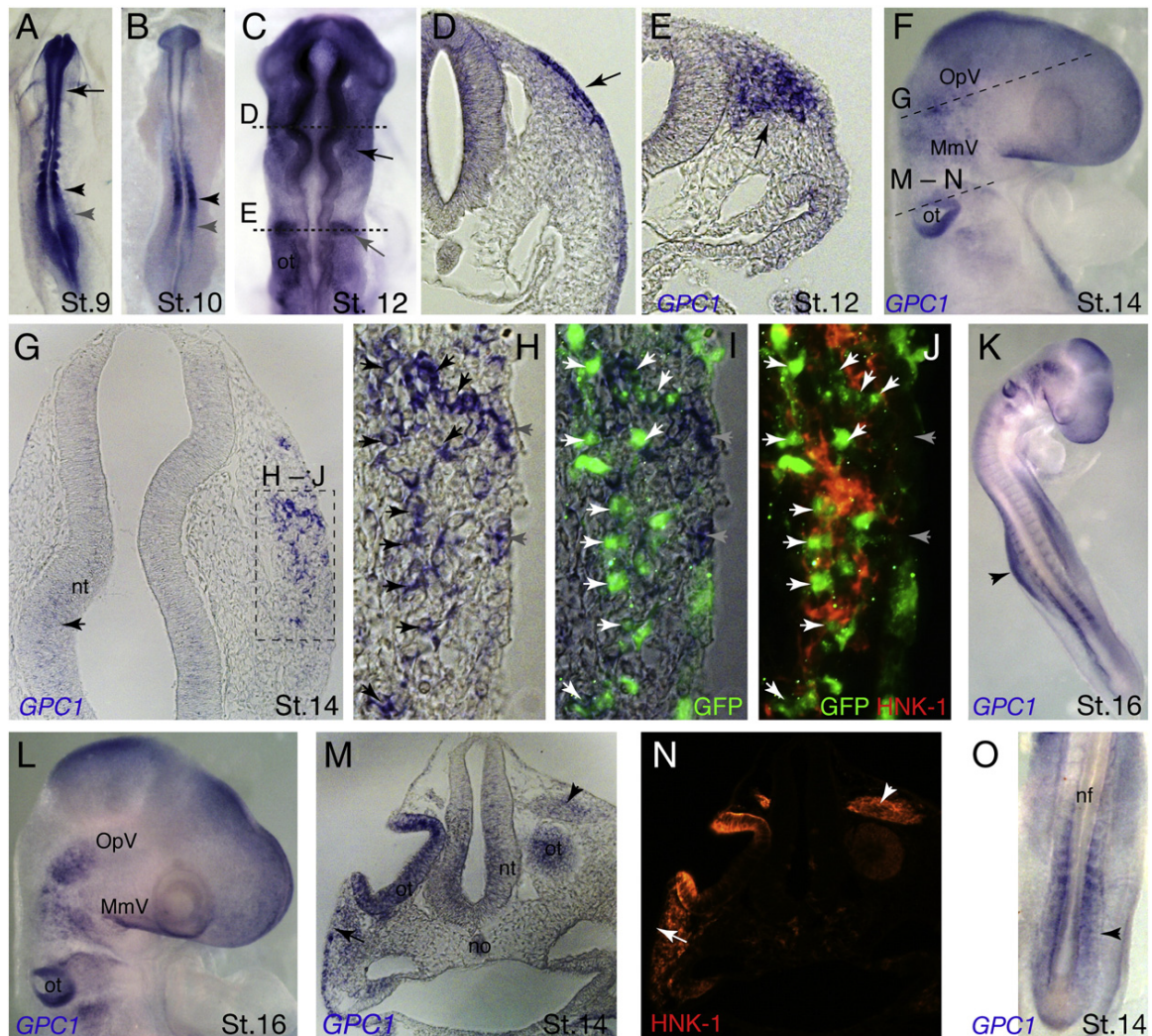


Fig. 1. Expression of Glypican-1 mRNA in the early chick embryo. (A) Stage 9 and (B) stage 10 embryos showing GPC1 mRNA expression in the neural tube (arrow) but not in the migrating midbrain neural crest cells, and in the presomitic mesoderm (PSM) and the most caudal somites in a gradient fashion, high (black arrowhead) to low (gray arrowhead) expression. (C) Stage 12 embryo showing onset of GPC1 expression in the

forming trigeminal placodes (arrow) and migrating hindbrain neural crest cells at rhombomere 4 (r4) (gray arrow). Cross sections as indicated in C showing GPC1 expression in (D) placodal ectoderm and spurs of ingressing placodal cells (arrow) (E) and hindbrain migratory neural crest cells (arrow). (F) GPC1 expression in the ophthalmic (OpV) and maxillo-mandibular (MmV) placodes of the forming trigeminal ganglion and in the otic vesicle at stage 14. (G) Cross section through the OpV region of F showing GPC1 expression in the placodal ectoderm and ingressing placodes (dotted box) and weakly in the neural tube. (H–J) Higher magnification of the dotted box in G showing GFP-labeled ingressing trigeminal placodal cells express GPC1 (arrows) but HNK-1 expressing neural crest cells do not. (K) Stage 16 embryo showing expression in the forming limb bud (arrowhead). (L) GPC1 expression persists in the OpV and MmV placodes and the otic vesicle. (M–N) Cross section of F showing GPC1 expression in the otic placode, epibranchial ectoderm (arrow), and r4 HNK-1-expressing hindbrain neural crest cells (arrowhead). (O) GPC1 expression persists in the PSM (arrowhead) and newly formed somites at stage 14. OpV, ophthalmic; MmV, maxillo-mandibular; nt, neural tube; ot, otic; no, notochord; nf, neural folds.

Figure2

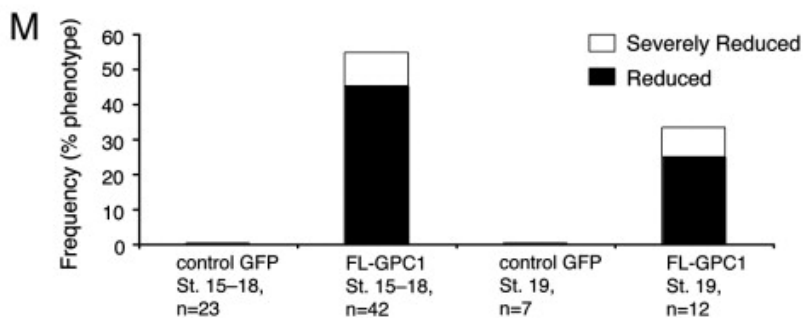
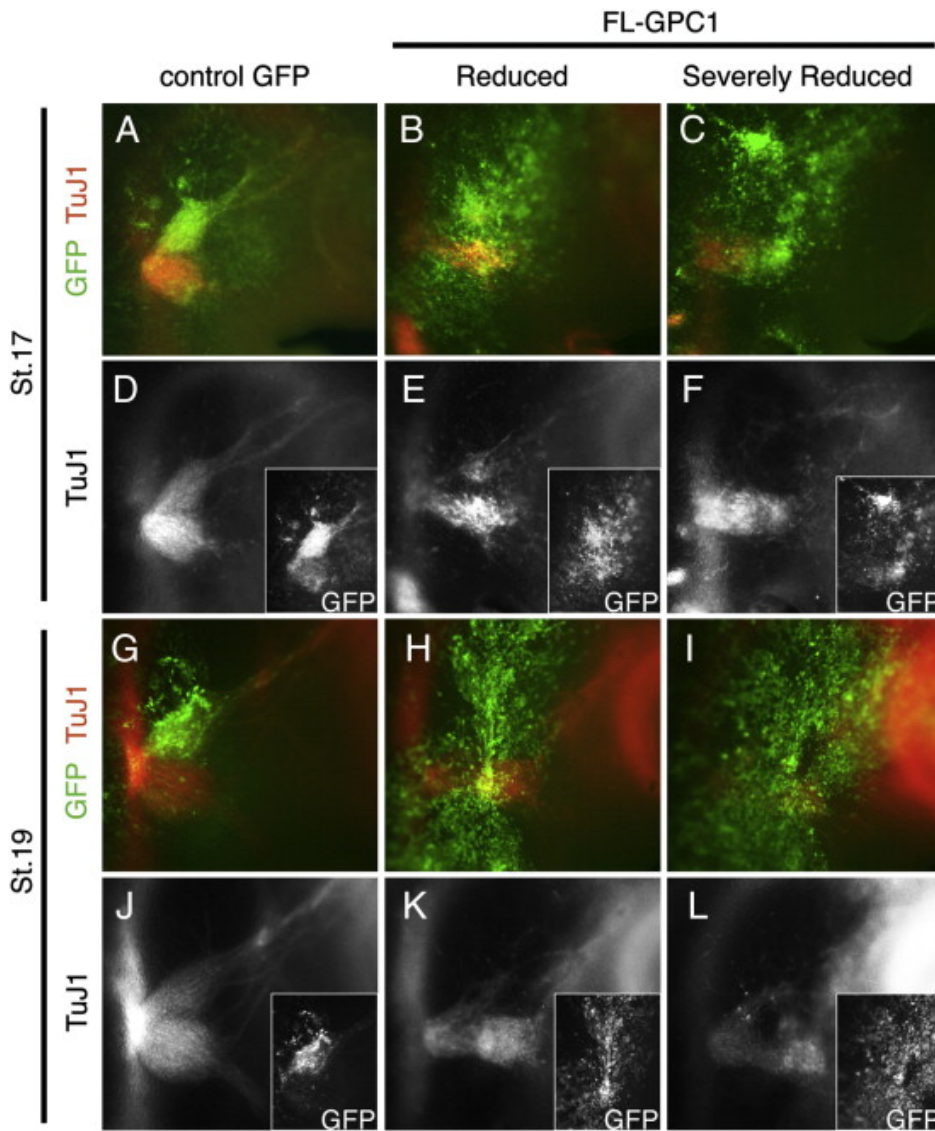


Fig. 2. Increased Glypican-1 expression in the placodal ectoderm leads to significant loss of placodal ganglia. Ectoderm-electroporated embryos analyzed at stage 17 showing (A) normal trigeminal ganglion formation with control GFP and (B and C) reduced or severely reduced ganglia with full-length GPC1 (FL-GPC1). Color overlay images show area of transfection by GFP expression in green and placodal neurons by TuJ1 antibody staining in red. (D–F) Single-channel images of TuJ1 of the above overlay images in A–C; insets, GFP expression only. Ganglia assessed at stage 19 showing (G) normal ganglion in controls but (H and I) markedly reduced ganglia in FL-GPC1 embryos. (J–L) Single channel images of TuJ1 of G-I and insets show GFP expression of the color overlay. (M) Histogram showing frequency of reduced and severely reduced ganglia phenotypes. n = number of ganglia analyzed.

Figure 3

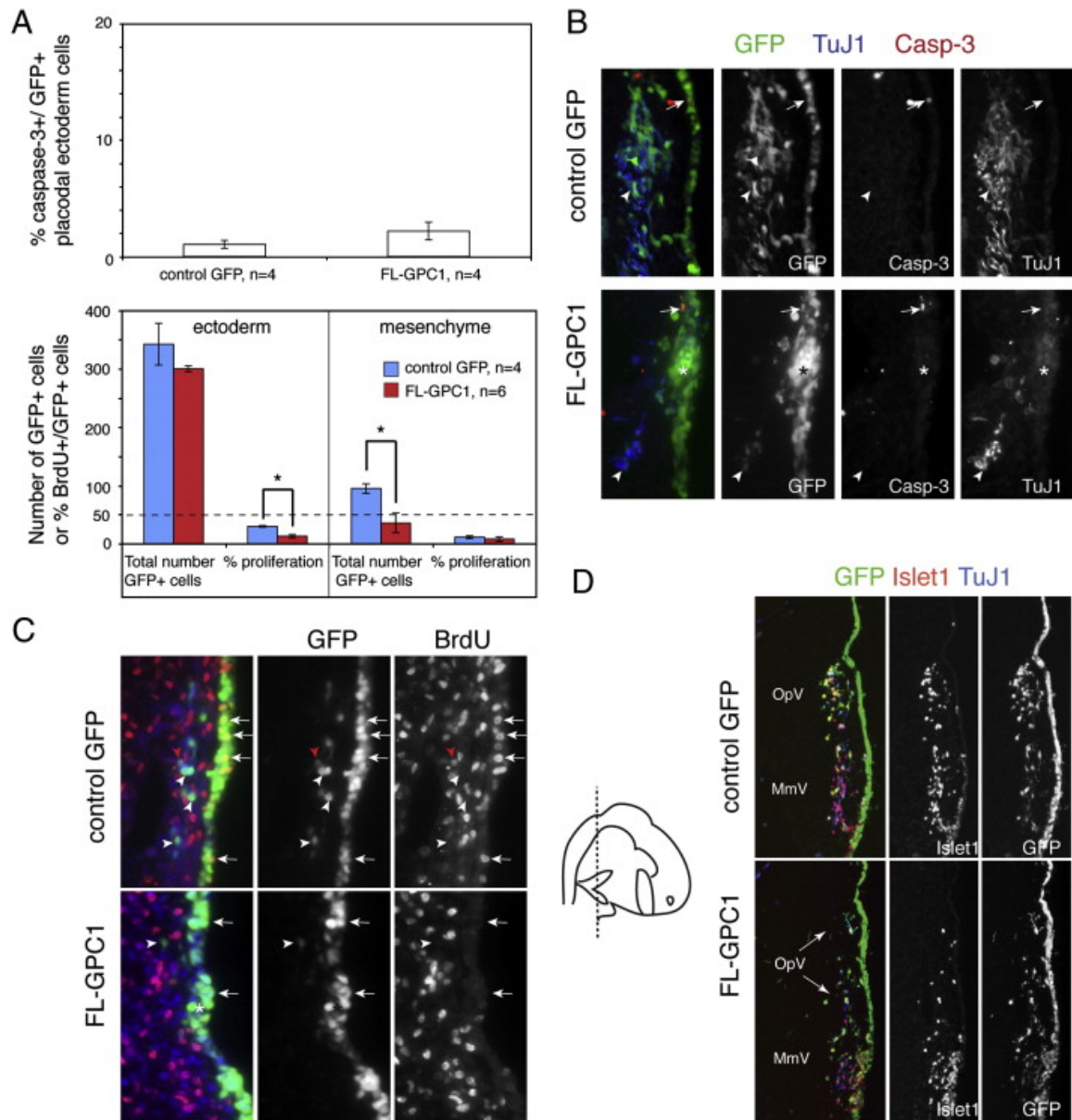


Fig. 3. GPC1 overexpression blocks cell proliferation and differentiation of the placodal ectoderm, but does not induce significant cell death. (A) Top, histogram showing no significant difference in cell death level between control GFP and FL-GPC1 in the ectoderm. Bottom, graph showing that, compared with controls, FL-GPC1 embryos had

significantly reduced percentage of proliferation in the placodal ectoderm and decreased total number of ingressing placodal cells. Dotted line marks the 50% level. Bars indicate s.e.m. n = the number of forming ganglia analyzed. (B) Cross sections through the OpV region at stage 15 showing few caspase-3 positive transfected cells in the ectoderm (arrow) and none in the mesenchyme (arrowhead, which are ingressed placodal cells) in both control GFP and FL-GPC1 embryos. FL-GPC1 transfected ganglia had regions of strikingly aberrant clustering of cells in the ectoderm distinct from controls (asterisk). (C) Electroporated embryos collected at stage 14 were treated with a short half hour pulse of BrdU to detect S-phase mitotic cells at the time of analysis. Frontal plane sections at stage 14 showing (top panels) many proliferating cells in the ectoderm in control (BrdU+, arrows). By contrast, (bottom panels) most FL-GPC1 transfected ectodermal cells are non-mitotic (BrdU- and GFP +, arrows) and tend to cluster (asterisk). Most ingressed placodal cells in both control and FL-GPC1 transfections were not mitotic (BrdU-, arrowheads) though occasionally a very small number of them are (red arrowhead, top panel). (D) Frontal plane sections through the ganglion as shown by the dotted line in the schematic (left) showing strikingly less placodal neurons (Islet1+/TuJ1+) particularly in the OpV region in FL-GPC1 embryo (arrows) compared with control. OpV, ophthalmic; MmV, maxillo-mandibular.

Figure 4

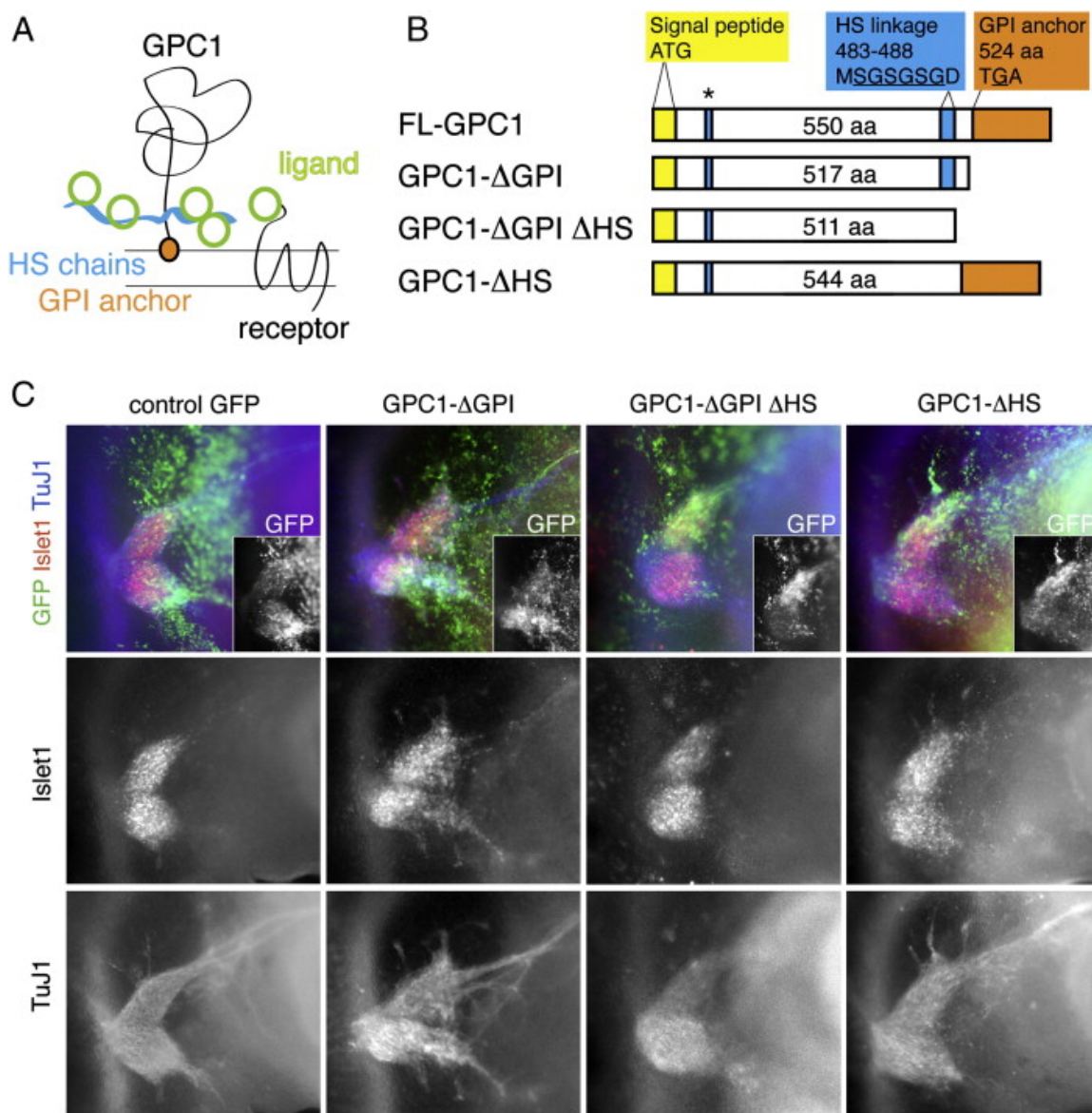


Fig. 4. Truncated form of GPC1 causes disorganization of ganglion distinct from full-length, and both full-length and truncated forms require the putative heparan sulfate glycosaminoglycan (GAG) attachment sites for function. (A) Simplified schematic of glypican shows its heparan sulfate (HS) side chains near the cell surface and GPI membrane anchor acting as a potential coreceptor or ligand carrier for signaling receptors.

(B) Diagram showing the domains of the full-length GPC1 (FL-GPC1) and the modifications made on the mutant forms of GPC1. Since HS attachment sites are known to localize near the membrane anchor of glypicans, all predicted HS attachment sites at the C-terminus for chick GPC1 in the UniProtKB database were excised in HS deletion constructs; there remains only one predicted site located near the N-terminus (asterisk).

(C) Representative images showing stage 18 placodal ganglia (Islet1+/TuJ1+) electroporated with mutant GPC1 constructs with deletions of HS or both GPI and HS domains that were generally normal and similar to controls. By contrast, GPC1- Δ GPI transfected placodal ganglia were normally sized but disorganized.

Figure 5

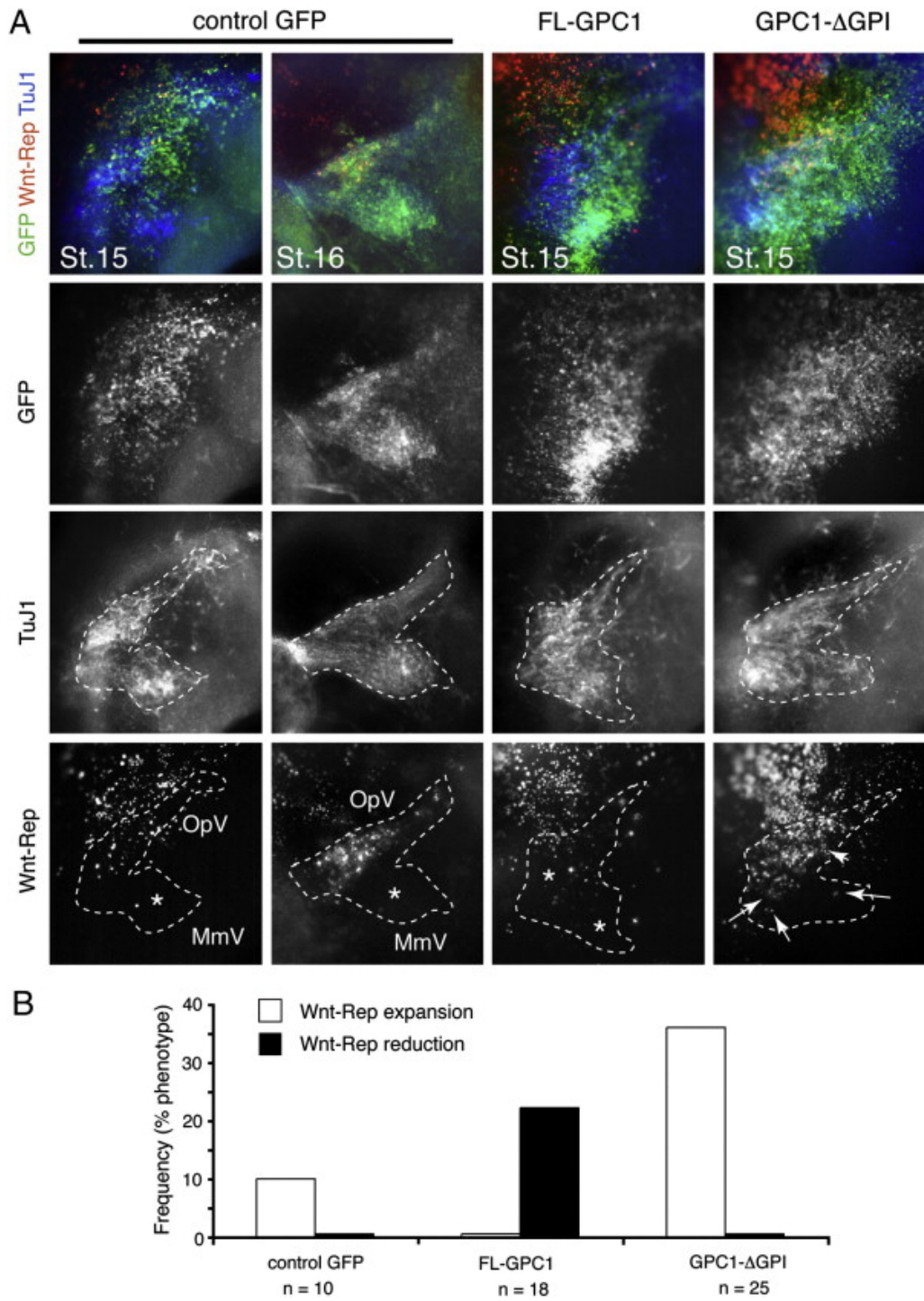


Fig. 5. Changes to GPC1 expression alters endogenous Wnt signaling activity. (A)

Top row, color overlay images showing trigeminal ganglia in whole mount chick embryos at stages 15–16 after electroporation with control GFP, FL-GPC1, or GPC1- Δ GPI constructs. GFP in green showing area of transfection (also shown in second row panels). TuJ1 in blue showing placodal neurons (also shown in third row panels). RFP version of TOPGAL Wnt reporter expression in red showing endogenous activity of Wnt signaling (also shown in fourth row panels). Outline of the trigeminal ganglion is demarcated by the dotted lines. Fourth row panels, controls show Wnt reporter expression restricted to the OpV region at stages 15 and 16 with generally absence of reporter in the MmV region (asterisk), albeit occasionally one or a few cells were Wnt-Rep⁺. Reporter expression in the OpV appears to increase over time. By contrast, FL-GPC1 expressing placodal ganglia had markedly reduced Wnt reporter expression in the OpV region, and similar to controls, had generally little to no reporter expression in the MmV region (lower asterisk). Conversely, expression of GPC1- Δ GPI led to more expression of Wnt reporter in the OpV (arrowhead) and expansion of reporter expression into the MmV region in more cells, though sparsely (arrows). (B) Histogram showing percentages of cases of reduction of Wnt reporter expression in the OpV and of expansion of Wnt reporter expression, which means an increase in reporter expression in OpV as well as expression in greater number of cells in MmV, after electroporation with control GFP, FL-GPC1, or GPC1- Δ GPI. n = number of ganglia analyzed. Wnt-Rep, Wnt reporter; OpV, ophthalmic; MmV, maxillo-mandibular.

Figure 6

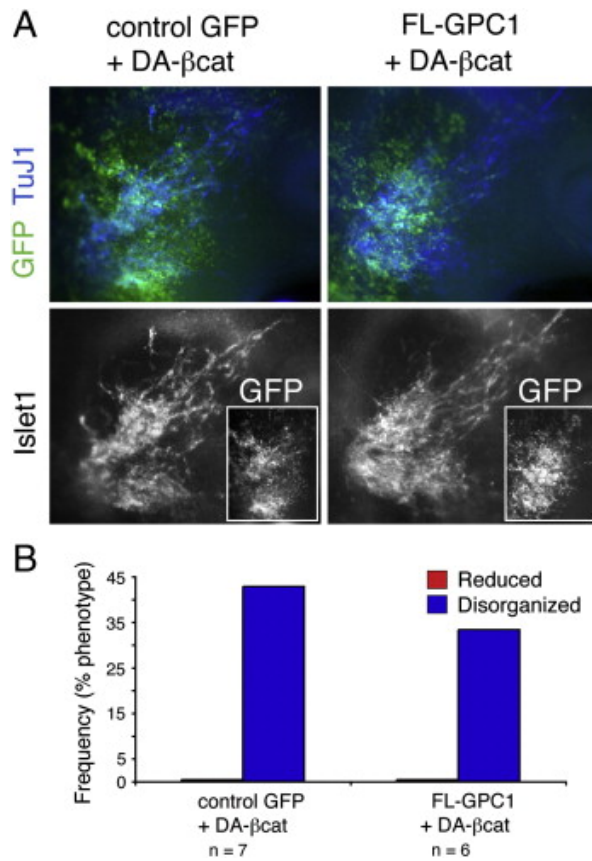
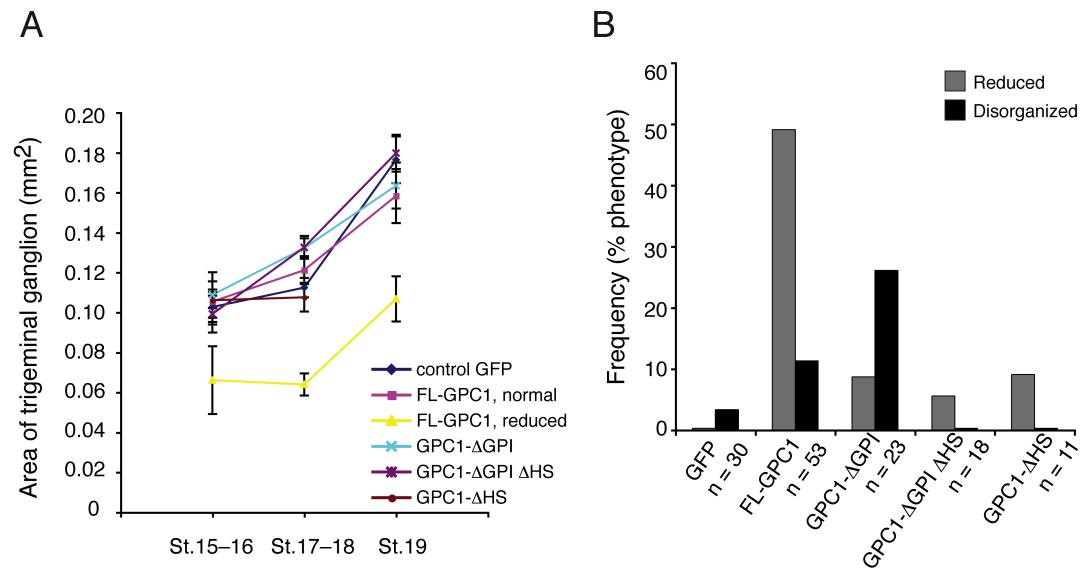


Fig. 6. Induced activation of Wnt signaling phenocopies the effects of truncated GPC1 and reverses the effects of GPC1 overexpression. (A) Coexpression of a dominant-active form of β -catenin (DA- β cat) with FL-GPC1 in the placodal tissue suppresses the reduced ganglia phenotype. Both control and experimental expressions of DA- β cat with control GFP or FL-GPC1, respectively, led to some disorganized integration of placodal cells into ganglia. GFP in green showing area of transfection and TuJ1 in blue showing placodal neurons. (B) Histogram showing frequency of phenotypes: “reduced” means decreased in overall ganglion size and “disorganized” means aberrant integration of placodal cells. n represents number of ganglia analyzed.

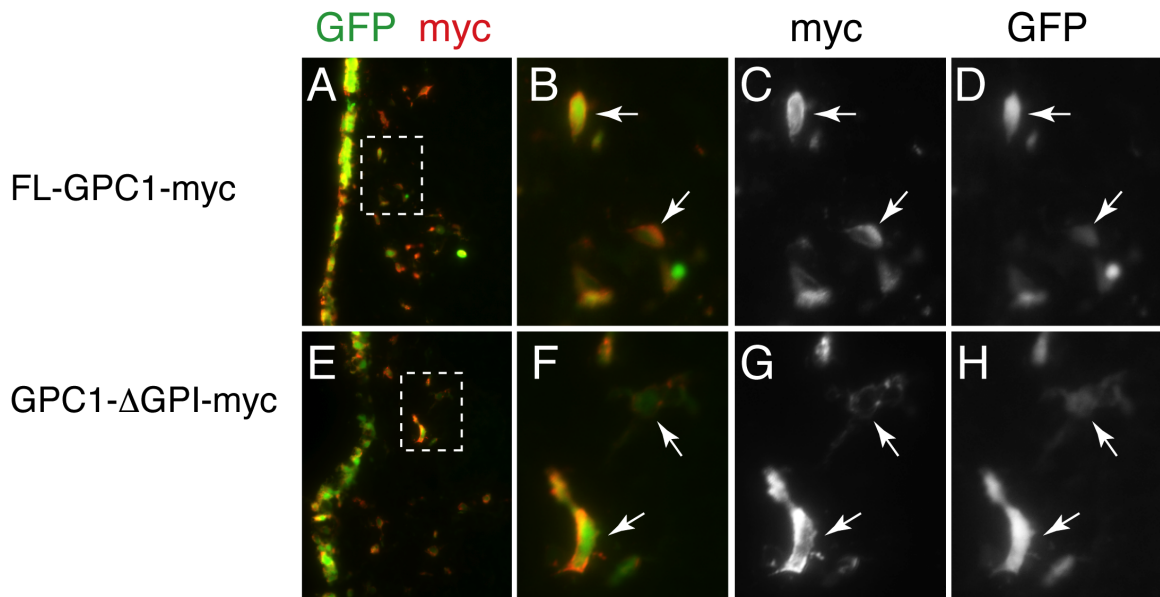
Supplementary Figure 1



Supplementary Figure 1 Measurement of ganglia sizes shows dramatic reduction after expression of full-length but not mutant forms of GPC1. (A) Graph showing the area of trigeminal ganglia does not show significant differences between control and mutant GPC1 electroporated embryos through the different stages of analysis (stages 15 – 19). Separate plots were made for FL-GPC1 electroporated ganglia, also shown in Fig. 2, that were either normally or reduced sized in order to show the dramatic area reduction in “reduced” phenotype cases. Bars show s.e.m. (B) Histogram showing frequency of the two types of phenotypes detected over all analyzed stages 15–19: “reduction” means overall ganglion size is reduced and “disorganized” means aberrant integration of placodal cells but with generally normal ganglion size. GPC1 over-expression by FL-GPC1 caused a significant percentage of reduced ganglia (accounting for both “reduced” and “severely reduced” phenotypes as shown in Fig. 2), while GPC1 inhibition by GPC1-

Δ GPI led to a high percentage of disorganized ganglia. The reduced ganglia phenotype is largely not detected with expression of any mutant GPC1 construct.

Supplementary Figure 2



Supplementary Figure 2 Subcellular localization of FL-GPC1 and GPC1- Δ GPI proteins by myc-tag detection. Chick embryos transfected by in ovo electroporation targeting the trigeminal placodal tissue with either the cytopcig-FL-GPC1-6xmyc or cytopcig- GPC1- Δ GPI-6xmyc construct were selected for high cytoplasmic GFP reporter expression and collected for section analysis at stage 14. Sections through the trigeminal region show (A-D) GFP positive transfected ectodermal and placodal cells expressing FL-GPC1-6xmyc protein as shown by the myc tag in red. (B-D) Higher magnification of the dotted box region in A showing expression of FL-GPC1 myc fusion protein localized to both the cytoplasm and the cell membrane (arrows). (E-H) By contrast, GPC1- Δ GPI-6xmyc protein expression is more highly concentrated at or near the placodal cell membrane than FL-GPC1 (arrows), and in some cells is undetectable in the cytoplasm (top arrow).

References

- Baeg, G.H., Perrimon, N., 2000. Functional binding of secreted molecules to heparin sulfate proteoglycans in *Drosophila*. *Curr. Opin. Cell Biol.* **12**: 575–580.
- Baeg, G.H., Selva, E.M., Goodman, R.M., Dasgupta, R., Perrimon, N., 2004. The wingless morphogen gradient is established by the cooperative action of Frizzled and heparan sulfate proteoglycan receptors. *Dev. Biol.* **276**: 89–100.
- Baker, C.V., Stark, M.R., Marcelle, C., Bronner-Fraser, M., 1999. Competence, specification and induction of Pax-3 in the trigeminal placode. *Development* **126**: 147–156.
- Canning, C.A., Lee, L., Luo, S.X., Graham, A., Jones, C.M., 2008. Neural tube derived Wnt signals cooperate with FGF signaling in the formation and differentiation of the trigeminal placodes. *Neural Dev.* **3**: 35.
- Cano-Gauci, D.F., Song, H.H., Yang, H., McKerlie, C., Choo, B., Shi, W., Pullano, R., Piscione, T.D., Grisaru, S., Soon, S., Sedlackova, L., Tanswell, A.K., Mak, T.W., Yeger, H., Lockwood, G.A., Rosenblum, N.D., Filmus, J., 1999. Glypican-3-deficient mice exhibit developmental overgrowth and some of the abnormalities typical of Simpson–Golabi–Behmel syndrome. *J. Cell Biol.* **146**: 255–264.
- Capurro, M.I., Xiang, Y.Y., Lobe, C., Filmus, J., 2005. Glypican-3 promotes the growth of hepatocellular carcinoma by stimulating canonical Wnt signaling. *Cancer Res.* **65**: 6245–6254.
- Carey, D.J., Evans, D.M., 1989. Membrane anchoring of heparan sulfate proteoglycans by phosphatidylinositol and kinetics of synthesis of peripheral and detergent-solubilized proteoglycans in Schwann cells. *J. Cell Biol.* **108**: 1891–1897.
- D'Amico-Martel, A., Noden, D.M., 1980. An autoradiographic analysis of the development of the chick trigeminal ganglion. *J. Embryol. Exp. Morphol.* **55**: 167–182.
- DasGupta, R., Fuchs, E., 1999. Multiple roles for activated LEF/TCF transcription complexes during hair follicle development and differentiation. *Development* **126**: 4557–4568.
- De Cat, B., David, G., 2001. Developmental roles of the glypicans. *Semin. Cell Dev. Biol.* **12**: 117–125.
- Fico, A., Maina, F., Dono, R., 2007. Fine-tuning of cell signalling by glypicans. *Cell. Mol. Life Sci.* doi:10.1007/S00018-007-7471-6.
- Filmus, J., 2001. Glypicans in growth control and cancer. *Glycobiology* **11**: 19R–23R.
- Filmus, J., Song, H.H., 2000. Glypicans. In: Iozzo, R.V. (Ed.), *Proteoglycans: Structure, Biology, and Molecular Interactions*. CRC Press, pp. 161–176.
- Filmus, J., Capurro, M., Rast, J., 2008. Glypicans. *Genome Biol.* **9**: 224.
- Franch-Marro, X., Marchand, O., Piddini, E., Ricardo, S., Alexandre, C., Vincent, J.P., 2005. Glypicans shunt the Wingless signal between local signalling and further transport. *Development* **132**: 659–666.
- Fujise, M., Izumi, S., Selleck, S.B., Nakato, H., 2001. Regulation of dally, an integral membrane proteoglycan, and its function during adult sensory organ formation of *Drosophila*. *Dev. Biol.* **235**: 433–448.
- Fukuhara, N., Howitt, J.A., Hussain, S.A., Hohenester, E., 2008. Structural and functional

- analysis of slit and heparin binding to immunoglobulin-like domains 1 and 2 of *Drosophila* Robo. *J. Biol. Chem.* **283**: 16226–16234.
- Gallet, A., Staccini-Lavenant, L., Therond, P.P., 2008. Cellular trafficking of the glypican Dally-like is required for full-strength Hedgehog signaling and wingless transcytosis. *Dev. Cell* **14**: 712–725.
- Gammill, L.S., Bronner-Fraser, M., 2002. Genomic analysis of neural crest induction. *Development* **129**: 5731–5741.
- Gonzalez, A.D., Kaya, M., Shi, W., Song, H., Testa, J.R., Penn, L.Z., Filmus, J., 1998. OCI-5/GPC3, a glypican encoded by a gene that is mutated in the Simpson–Golabi–Behmel overgrowth syndrome, induces apoptosis in a cell line-specific manner. *J. Cell Biol.* **141**: 1407–1414.
- Hacker, U., Nybakken, K., Perrimon, N., 2005. Heparan sulphate proteoglycans: the sweet side of development. *Nat. Rev. Mol. Cell Biol.* **6**: 530–541.
- Han, C., Yan, D., Belenkaya, T.Y., Lin, X., 2005. *Drosophila* glypicans Dally and Dally-like shape the extracellular Wingless morphogen gradient in the wing disc. *Development* **132**: 667–679.
- Hohenester, E., 2008. Structural insight into Slit–Robo signalling. *Biochem. Soc. Trans.* **36**: 251–256.
- Hollyday, M., McMahon, J.A., McMahon, A.P., 1995. Wnt expression patterns in chick embryo nervous system. *Mech. Dev.* **52**: 9–25.
- Hufnagel, L., Kreuger, J., Cohen, S.M., Shraiman, B.I., 2006. On the role of glypicans in the process of morphogen gradient formation. *Dev. Biol.* **300**: 512–522.
- Hussain, S.A., Piper, M., Fukuhara, N., Strohlic, L., Cho, G., Howitt, J.A., Ahmed, Y., Powell, A.K., Turnbull, J.E., Holt, C.E., Hohenester, E., 2006. A molecular mechanism for the heparin sulfate dependence of slit–robo signaling. *J. Biol. Chem.* **281**: 39693–39698.
- Jen, Y.H., Musacchio, M., Lander, A.D., 2009. Glypican-1 controls brain size through regulation of fibroblast growth factor signaling in early neurogenesis. *Neural Dev.* **4**: 33.
- Karthikeyan, L., Flad, M., Engel, M., Meyer-Puttitz, B., Margolis, R.U., Margolis, R.K., 1994. Immunocytochemical and in situ hybridization studies of the heparan sulfate proteoglycan, glypican, in nervous tissue. *J. Cell Sci.* **107** (Pt 11): 3213–3222.
- Kirkpatrick, C.A., Knox, S.M., Staatz, W.D., Fox, B., Lercher, D.M., Selleck, S.B., 2006. The function of a *Drosophila* glypican does not depend entirely on heparan sulfate modification. *Dev. Biol.* **300**: 570–582.
- Kleeff, J., Ishiwata, T., Kumbasar, A., Friess, H., Buchler, M.W., Lander, A.D., Korc, M., 1998. The cell-surface heparan sulfate proteoglycan glypican-1 regulates growth factor action in pancreatic carcinoma cells and is overexpressed in human pancreatic cancer. *J. Clin. Invest.* **102**: 1662–1673.
- Kreuger, J., Perez, L., Giraldez, A.J., Cohen, S.M., 2004. Opposing activities of Dally-like glypican at high and low levels of Wingless morphogen activity. *Dev. Cell.* **7**: 503–512.
- Lassiter, R.N., Dude, C.M., Reynolds, S.B., Winters, N.I., Baker, C.V., Stark, M.R., 2007. Canonical Wnt signaling is required for ophthalmic trigeminal placode cell fate

- determination and maintenance. *Dev. Biol.* **308**: 392–406.
- Lassiter, R.N., Reynolds, S.B., Marin, K.D., Mayo, T.F., Stark, M.R., 2009. FGF signaling is essential for ophthalmic trigeminal placode cell delamination and differentiation. *Dev. Dyn.* **238**: 1073–1082.
- Liang, Y., Annan, R.S., Carr, S.A., Popp, S., Mevissen, M., Margolis, R.K., Margolis, R.U., 1999. Mammalian homologues of the *Drosophila* slit protein are ligands of the heparan sulfate proteoglycan glypican-1 in brain. *J. Biol. Chem.* **274**: 17885–17892.
- Lin, X., 2004. Functions of heparan sulfate proteoglycans in cell signaling during development. *Development.* **131**: 6009–6021.
- Lin, X., Perrimon, N., 1999. Dally cooperates with *Drosophila* Frizzled 2 to transduce Wingless signaling. *Nature.* **400**: 281–284.
- Lin, H., Huber, R., Schlessinger, D., Morin, P.J., 1999. Frequent silencing of the GPC3 gene in ovarian cancer cell lines. *Cancer Res.* **59**: 807–810.
- Litwack, E.D., Stipp, C.S., Kumbasar, A., Lander, A.D., 1994. Neuronal expression of glypican, a cell-surface glycosylphosphatidylinositol-anchored heparan sulfate proteoglycan, in the adult rat nervous system. *J. Neurosci.* **14**: 3713–3724.
- Litwack, E.D., Ivins, J.K., Kumbasar, A., Paine-Saunders, S., Stipp, C.S., Lander, A.D., 1998. Expression of the heparan sulfate proteoglycan glypican-1 in the developing rodent. *Dev. Dyn.* **211**: 72–87.
- Luxardi, G., Galli, A., Forlani, S., Lawson, K., Maina, F., Dono, R., 2007. Glypicans are differentially expressed during patterning and neurogenesis of early mouse brain. *Biochem. Biophys. Res. Commun.* **352**: 55–60.
- Marcelle, C., Stark, M.R., Bronner-Fraser, M., 1997. Coordinate actions of BMPs, Wnts, Shh and noggin mediate patterning of the dorsal somite. *Development* **124**: 3955–3963.
- Matsuda, K., Maruyama, H., Guo, F., Kleeff, J., Itakura, J., Matsumoto, Y., Lander, A.D., Korc, M., 2001. Glypican-1 is overexpressed in human breast cancer and modulates the mitogenic effects of multiple heparin-binding growth factors in breast cancer cells. *Cancer Res.* **61**: 5562–5569.
- Megason, S.G., McMahon, A.P., 2002. A mitogen gradient of dorsal midline Wnts organizes growth in the CNS. *Development* **129**: 2087–2098.
- Murthy, S.S., Shen, T., De Rienzo, A., Lee, W.C., Ferriola, P.C., Jhanwar, S.C., Mossman, B.T., Filmus, J., Testa, J.R., 2000. Expression of GPC3, an X-linked recessive overgrowth gene, is silenced in malignant mesothelioma. *Oncogene* **19**: 410–416.
- Nakato, H., Futch, T.A., Selleck, S.B., 1995. The division abnormally delayed (dally) gene: a putative integral membrane proteoglycan required for cell division patterning during postembryonic development of the nervous system in *Drosophila*. *Development* **121**: 3687–3702.
- Niu, S., Antin, P.B., Akimoto, K., Morkin, E., 1996. Expression of avian glypican is developmentally regulated. *Dev. Dyn.* **207**: 25–34.
- Ohkawara, B., Yamamoto, T.S., Tada, M., Ueno, N., 2003. Role of glypican 4 in the regulation of convergent extension movements during gastrulation in *Xenopus laevis*. *Development* **130**: 2129–2138.

- Pilia, G., Hughes-Benzie, R.M., MacKenzie, A., Baybayan, P., Chen, E.Y., Huber, R., Neri, G., Cao, A., Forabosco, A., Schlessinger, D., 1996. Mutations in GPC3, a glypican gene, cause the Simpson–Golabi–Behmel overgrowth syndrome. *Nat. Genet.* **12**: 241–247.
- Qiao, D., Yang, X., Meyer, K., Friedl, A., 2008. Glypican-1 regulates anaphase promoting complex/cyclosome substrates and cell cycle progression in endothelial cells. *Mol. Biol. Cell* **19**: 2789–2801.
- Ronca, F., Andersen, J.S., Paech, V., Margolis, R.U., 2001. Characterization of Slit protein interactions with glypican-1. *J. Biol. Chem.* **276**: 29141–29147
- Saunders, S., Paine-Saunders, S., Lander, A.D., 1997. Expression of the cell surface proteoglycan glypican-5 is developmentally regulated in kidney, limb, and brain. *Dev. Biol.* **190**: 78–93.
- Shiau, C.E., 2009. Formation of cranial sensory ganglia: role of neural crest–placode interactions, Slit–Robo, and Cadherins. Biology. Caltech, Pasadena.
- Shiau, C.E., Bronner-Fraser, M., 2009. N-cadherin acts in concert with Slit1–Robo2 signaling in regulating aggregation of placode-derived cranial sensory neurons. *Development* **136**: 4155–4164.
- Shiau, C.E., Lwigale, P.Y., Das, R.M., Wilson, S.A., Bronner-Fraser, M., 2008. Robo2–Slit1 dependent cell–cell interactions mediate assembly of the trigeminal ganglion. *Nat. Neurosci.* **11**: 269–276.
- Song, H.H., Shi, W., Xiang, Y.Y., Filmus, J., 2005. The loss of glypican-3 induces alterations in Wnt signaling. *J. Biol. Chem.* **280**: 2116–2125.
- Stark, M.R., Sechrist, J., Bronner-Fraser, M., Marcelle, C., 1997. Neural tube–ectoderm interactions are required for trigeminal placode formation. *Development* **124**: 4287–4295.
- Stark, M.R., Biggs, J.J., Schoenwolf, G.C., Rao, M.S., 2000. Characterization of avian frizzled genes in cranial placode development. *Mech. Dev.* **93**: 195–200.
- Su, G., Meyer, K., Nandini, C.D., Qiao, D., Salamat, S., Friedl, A., 2006. Glypican-1 is frequently overexpressed in human gliomas and enhances FGF-2 signaling in glioma cells. *Am. J. Pathol.* **168**: 2014–2026.
- Tetsu, O., McCormick, F., 1999. beta-Catenin regulates expression of cyclin D1 in colon carcinoma cells. *Nature* **398**: 422–426.
- Williams, E.H., Pappano, W.N., Saunders, A.M., Kim, M.S., Leahy, D.J., Beachy, P.A., 2010. Dally-like core protein and its mammalian homologues mediate stimulatory and inhibitory effects on Hedgehog signal response. *Proc. Natl Acad. Sci. USA* **107**: 5869–5874.
- Yan, D., Lin, X., 2007. Drosophila glypican Dally-like acts in FGF-receiving cells to modulate FGF signaling during tracheal morphogenesis. *Dev. Biol.* **312**: 203–216.
- Yan, D., Wu, Y., Feng, Y., Lin, S.C., Lin, X., 2009. The core protein of glypican Dally-like determines its biphasic activity in wingless morphogen signaling. *Dev. Cell.* **17**: 470–481.
- Zittermann, S.I., Capurro, M.I., Shi, W., Filmus, J., 2009. Soluble glypican 3 inhibits the growth of hepatocellular carcinoma in vitro and in vivo. *Int. J. Cancer* **126**: 1291–1301.